The Journal of Gemmology

Volume 35 / No. 1 / 2016

The Gemmological Association of Great Britain

Gem-A

THE GEMMOLOGICAL ASSOCIATION
OF GREAT BRITAIN

Save the date

Gem-A Conference

Saturday 5 and
Sunday 6 November 2016

Visit www.gem-a.com for the latest information

Creating gemmologists since 1908

Join us.

The Gemmological Association of Great Britain, 21 Ely Place, London, EC1N 6TD, UK. T: +44 (0)20 7404 3334 F: +44 (0)20 7404 8843.
Registered charity no. 1109555. A company limited by guarantee and registered in England No. 1945780. Registered Office: 3rd Floor, 1-4 Argyll Street, London W1F 7LD.

The Journal of Gemmology
Volume 35 / No. 1 / 2016

COLUMNS

Cover Photo: Cat's-eye chrysoberyls are shown here in a gold ring (11.71 ct oval), as loose round cabochons (11.00 and 14.09 ct) and mounted in gold cufflinks (6.48–8.89 ct). Courtesy of The Edward Arthur Metzger Gem Collection at the Heasley Museum, Cornell University, Ithaca, New York, USA; composite photo by Jeff Scovil.


p. 22


p. 64

ARTICLES

Feature Articles

Gemmological Brief

The Journal is published by Gem-A in collaboration with SSEF and with the support of AGL and GIT.

Gem-A THE GEMMOLOGICAL ASSOCIATION OF GREAT BRITAIN
SSEF SCHWEIZERISCHES GEMMOLOGISCHES INSTITUT SWISS GEMMOLOGICAL INSTITUTE INSTITUT SUISSE DE GEMMOLOGIE
AGL AMERICAN GEMOLOGICAL LABORATORIES
The Gem and Jewelry Institute of Thailand (Public Organization)

ISSN: 1355-4565, http://dx.doi.org/10.15506/JoG.2016.35.1

The Journal of Gemmology

Content Submission

The Editor-in-Chief is glad to consider original articles, news items, conference/excursion reports, announcements and calendar entries on subjects of gemmological interest for publication in *The Journal of Gemmology*. A guide to the various sections and the preparation of manuscripts is given at www.gem-a.com/publications/journal-of-gemmology/submit-an-article.aspx, or contact the Production Editor.

Subscriptions

Gem-A members receive *The Journal* as part of their membership package, full details of which are given at www.gem-a.com/membership.aspx. Laboratories, libraries, museums and similar institutions may become Direct Subscribers to *The Journal* (see www.gem-a.com/publications/subscribe.aspx).

Advertising

Enquiries about advertising in *The Journal* should be directed to the Marketing Consultant. For more information, see www.gem-a.com/publications/journal-of-gemmology/advertising-in-the-journal.aspx.

Database Coverage

The Journal of Gemmology is covered by the following abstracting and indexing services: Australian Research Council academic journal list, British Library Document Supply Service, Chemical Abstracts (CA Plus), Copyright Clearance Center's RightFind application, CrossRef, EBSCO (Academic Search International, Discovery Service and TOC Premier), Gale/Cengage Learning Academic OneFile, GeoRef, Mineralogical Abstracts, ProQuest, Scopus and the Thomson Reuters' Emerging Sources Citation Index (in the Web of Science).

Copyright and Reprint Permission

The Journal of Gemmology is published quarterly by Gem-A, The Gemmological Association of Great Britain. Any opinions expressed in *The Journal* are understood to be the views of the contributors and not necessarily of the publisher.

Printed by DG3 (Europe) Ltd.

ISSN: 1355-4565

Gem-A
THE GEMMOLOGICAL ASSOCIATION OF GREAT BRITAIN

21 Ely Place
London EC1N 6TD
UK

t: +44 (0)20 7404 3334
f: +44 (0)20 7404 8843
e: information@gem-a.com
w: www.gem-a.com

Registered Charity No. 1109555
Registered office: Palladium House, 1–4 Argyll Street, London W1F 7LD

What's New

INSTRUMENTS AND TECHNIQUES

DiamondDect Diamond Identification Instrument

TaiDiam Technology Co. Ltd. (Zhengzhou, China) announced in September 2015 the availability of the DiamondDect portable diamond identification instrument from its associated company Krisdiam. Weighing approximately 8 kg, the instrument includes a polariscope, microscope, fibre-optic illuminator and more, plus a Windows-based computer tablet equipped with identification software to separate CVD and HPHT synthetics from natural diamonds. According to TaiDiam, the instrument can analyse colourless to near-colourless diamonds from 0.01 ct (loose) or 0.03 ct (mounted) up to 10 ct. For additional information, visit http://en.taidiam.com/news_detail/newsId=61.html. A user manual with helpful information on separating natural from synthetic diamonds is available at http://en.taidiam.com/download_detail/&downloadsId=19.html.

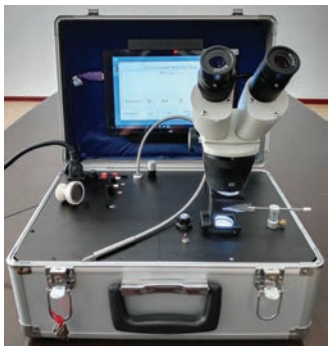

CMS

Triple D Photo Kit

In February 2015, Triple D Experience Ltd. in Israel launched a Photo Kit for gem photography that works with a smartphone. The kit consists of a portable, compact unit that includes a stone holder, light source, background and magnifier that cradles a smartphone, enabling the user to take a high-quality photo or video of a gemstone. The accompanying free smartphone app (for iPhone and Android) enables the user to enter stone data and an identification report, send information to clients, communicate via live chat, and store information for ease of access. To learn more, visit http://tripled-experience.com.

CMS

Upgraded DiamondView Instrument

In June 2015, the De Beers Group of Companies released through its International Institute of Diamond Grading & Research an enhanced version of the DiamondView. The upgraded instrument produces a surface fluorescence image that provides information on a sample's growth history that is useful for separating natural from synthetic diamonds. The upgraded model has changeable filters that are useful for enhancing features shown by some synthetic diamonds, particularly the latest-generation CVD products that show blue fluorescence. The instrument is available in a standard magnification model for stones weighing 0.05–10 ct, and in a high-magnification version for melee-sized goods of 0.01–0.20 ct. A new adapter for the vacuum stone holder allows for the examination of some jewellery items such as stud earrings and simple rings. For more information, visit www.iidgr.com/en/instruments/diamondview.

BML

Variofoc LED Lighting System

In March 2015, System Eickhorst released the Variofoc LED incident lighting system, which features a series of interchangeable LED heads designed for use in a double-gooseneck lamp unit. Three types of LED heads are available: spot, flood and diffuse, each in colour temperatures of neutral white (6,000 K) or daylight (4,000 K). Another interchangeable LED head provides long-wave UV illumination (366 nm). A variety of mountings are available, including a foot plate that allows the unit to be used in conjunction with a gemmological microscope. Visit www.eickhorst.com/en/lamps-lighting/desktop-lights/variofoc-led/merkmale.

BML

NEWS AND PUBLICATIONS

AGTA GemFair Tucson Seminars

The American Gem Trade Association hosted an array of seminars 3–6 February 2016 in Tucson, Arizona, USA. The seminars covered various aspects of gem mining, marketing, industry, identification and jewellery by presenters from around the world. A flash drive containing recordings of 27 of the seminars can be purchased for US$50.00 for non-AGTA members (AGTA members have access through the AGTA eLearning online program). Visit www.agta.org/education/seminars.html for the order form, as well as a summary of the presentations and speakers. *CMS*

Environmental and Social Responsibility for Coloured Stones

The Responsible Ecosystems Sourcing Platform released an International Working Group report on 29 January 2016 titled 'Challenges to Advancing Environmental and Social Responsibility in the Coloured Gems Industry'. Among the 10 major challenges discussed are the importance of tailoring socioeconomic solutions to the unique needs of each geopolitical venue and the lack of basic awareness of environmental principles. For a summary description and a link to the full report, visit http://tinyurl.com/gopvosp. *CMS*

Gold Demand Trends 2015

The World Gold Council released its annual report in February 2016, with a summary web page at www.gold.org/supply-and-demand/gold-demand-trends, where the full report, press report and statistics can be downloaded. Gold demand in the fourth quarter increased to a 10-quarter high of 1,117.7 tonnes. Full-year demand was virtually unchanged, with weakness in the first half offset by strength in the second half. Fourth-quarter growth was driven by central banks and investment, offset by a marginal contraction in jewellery and continued declines in technology. Supply remained constrained: Annual mine production increased by the slowest rate since 2008 (+1%) and recycling dropped to multi-year lows. Total supply declined 4% to 4,258 tonnes, the lowest since 2009. *CMS*

GSJ 2015 Annual Meeting Abstracts

Abstracts of papers presented at the 2015 Annual Meeting of the Gemmological Society of Japan are available at www.jstage.jst.go.jp/browse/gsj. The abstracts are written in Japanese with a brief English summary provided. Abstracts from prior GSJ conferences dating back to 2001 are also available.

CMS

ICGL *Newsletter*

The Winter 2015 issue of the International Consortium of Gem-Testing Laboratories *Newsletter* is now available at http://icglabs.org. Topics include use of a multi-spectral induced luminescence imaging system for screening of near-colourless HPHT synthetic diamond melee in China, identification of dyed golden South Sea cultured pearls and examination of a treated blue diamond. *CMS*

Large CVD synthetic diamond seen by HRD Antwerp

On 28 September 2015, HRD Antwerp posted an article by Ellen Barrie and Ellen Biermans titled

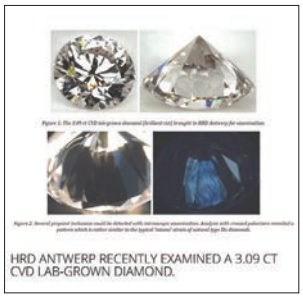

'HRD Antwerp Recently Examined a 3.09 ct CVD Lab-Grown Diamond' at www.hrdantwerp.com/en/news/hrd-antwerp-recently-examined-a-309-ct-cvd-lab-grown-diamon. The report contains a thorough description of the large CVD synthetic, including photomicrographs, DiamondView images, and both UV-Vis and photoluminescence spectra. *CMS*

MAGI Application Note on Diamond Type

The M&A Gemological Instruments website posted 'Application Note: Diamond classification – the diamond types', by Alberto Scarani and Mikko Astrom, on 29 January 2016. It provides a summary of diamond types and impurities as background to a discussion of FTIR spectroscopy and MAGI's GemmoFtir Diamond Type Analysis software. To download the report, visit www.gemmoraman.com/Articles//DiamondTyping.aspx. *CMS*

SSEF *Facette*

The Swiss Gemmological Institute SSEF has released the latest issue of *Facette Magazine* (No. 22, February 2016), which is available at www.ssef.ch/research-publications/facette. It describes: SSEF's new laboratory in Basel; SSEF's criteria for colour terms 'pigeon blood red' and 'royal blue'; rubies from Mozambique (including their low-temperature treatment) and Madagascar (Andilamena); sapphires from Madagascar (Andranondambo), Nigeria and Thailand (Kanchanaburi); REE in danburite; heat treatment of spinel from Mahenge, Tanzania; cobalt diffusion-treated spinel; a challenging Ramaura synthetic ruby; natural diamonds found in a parcel of HPHT synthetic diamonds; analysis of melee-size diamonds and small baguettes with the Lumos micro-FTIR spectrometer; updates concerning the ASDI instrument for analysing melee-size diamonds; pearl analysis with X-ray phase contrast and scattering imaging; pearl structures visualized by neutron scattering; 'ageing' treatment of pearls; a 'historic' necklace containing cultured pearls; carbon-14 dating of pearls from a shipwreck; several exceptional items sold at auction by Christie's and Sotheby's in 2014–2015; examination of iconic rubies from Mozambique; conference reports; recaps of SSEF courses, instrumentation and published research; and more. *BML*

Updated Cumulative Index for *The Journal of Gemmology*

In February 2016, Gem-A released the first update of *The Journal*'s cumulative index, covering all issues from 1947 to 2015 (Volumes 1–34). The contents are listed by subject, but the PDF file also can be searched for specific authors as well as topics. The cumulative index is available only in electronic format for free download from *The Journal*'s website at www.gem-a.com/publications/journal-of-gemmology/indexes.aspx. *CMS*

Wyoming Jades Revisited

In mid-December 2015, Palagems.com posted an article by the late Roger Merk FGA, titled 'Wyoming jades revisited' at http://m.palagems.com/wyoming-jades-revisited. The article is a personal look at the history and types of nephrite from Wyoming, USA, with photos of some exceptional examples of rough, sliced and fashioned specimens that illustrate the range of colours, textures and exterior appearances. *CMS*

OTHER RESOURCES

GemeSquare App and GemePrice5.0

Released in January 2016 by GemeWizard Inc. (Ramat Gan, Israel), the GemeSquare smartphone app is a free colour communication system that allows users to precisely define and describe a particular colour; both iOS and Android devices are supported. In February 2016, GemeWizard released GemePrice5.0, the most recent edition of this online wholesale pricing system for diamonds, coloured stones and jewellery. New to this version are 10 gem varieties that display different textures or optical effects, including turquoise, lapis lazuli, agate and moonstone. The system is available only to gem-industry professionals through subscription at www.gemewizard.com/store-price.php. *CMS*

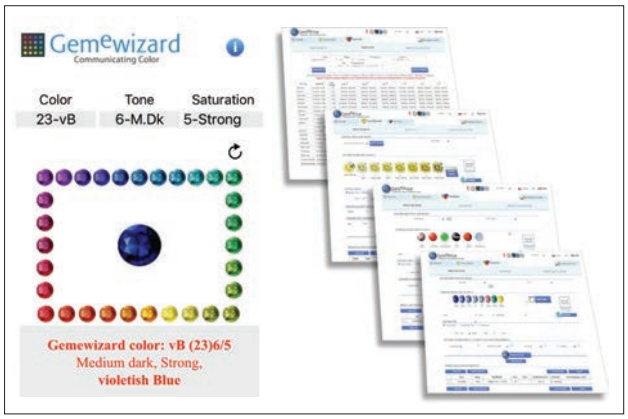

Historical Reading Lists from the GIA Library

The Richard T. Liddicoat Gemological Library at the Gemological Institute of America (Carlsbad, California, USA) recently posted four Historical Reading lists online: 'Diamonds in Arkansas', 'The Koh-i-noor Diamond', 'Pearls from India' and 'Ruby Mines of Burma'. Prepared by Dr James Shigley, each list includes brief descriptions of the references cited, along with information about where to locate the articles. To peruse these lists, visit www.gia.edu/library and click on the links under 'Recommended Reading & Bibliographies'. *CMS*

Hyperion Inclusion Search Engine

In December 2015, Lotus Gemology Co. Ltd. (Bangkok, Thailand) launched Hyperion, an online photographic library of gem inclusions. It includes a search feature that enables the user to look for images based on gem type, origin, enhancement and/or keyword. Gem types include natural and synthetic ruby, sapphire and spinel. Origins include 31 countries and five types of synthetics. Under enhancement, the options are 'none' plus 10 treatment choices. Also available is a useful listing of selected literature on gem inclusions. Use of the service is free at www.lotusgemology.com/index.php/library/inclusion-gallery, but note that the images are copyrighted. *CMS*

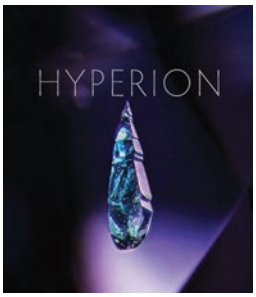

MISCELLANEOUS

Gems from the French Crown Jewels

The MINES ParisTech Mineralogy Museum opened a new permanent exhibit on 5 January 2016 featuring emerald, pink topaz and amethyst from the French Crown Jewels, including gems from the ornaments of Empress Marie-Louise (1791–1847) and the Imperial Crown of Napoléon III (1808–1873). Details are posted at www.musee.mines-paristech.fr/Our-Collections/Exhibits/CrownJewels. *CMS*

What's New provides announcements of new instruments/technology, publications, online resources and more. Inclusion in What's New does not imply recommendation or endorsement by Gem-A. Entries are prepared by Carol M. Stockton (CMS) or Brendan M. Laurs (BML), unless otherwise noted.


Pink Apatite with
Muscovite on Albite
Shah Nassir Peak,
Gilgit, Pakistan
Coming Soon:
The Sisk Gemology Reference
by Jerry Sisk
jtv jewelry love • jtv.com

Gem Notes

COLOURED STONES

Apatite from Hormuz Island, Iran

During the past two decades, small quantities of gem-quality apatite have been gathered by local mineral enthusiasts on Iran's Hormuz Island in the Persian Gulf. The gems are formed in joints and fractures contained within hematite-goethite iron ores that are associated with deeply altered igneous rocks of variable composition ranging from dacite-trachyte to quartz diorite (Elyasi et al., 1977). The apatite is thought to have a hydrothermal or igin (Padyar et al., 2012). Weathering of the host rocks has dispersed the apatite in areas associated with ochre-coloured soil and salt deposits (Figure 1). The apatite is found as broken pieces and euhedral crystals, typically up to 2–3 cm long, that are somewhat fractured. The gem-quality material is transparent to translucent, and generally ranges from yellow to greenish yellow (Figure 2); less commonly it is green or orangey yellow. It shows various degrees of colour saturation, from very pale to strong. Some samples show colour zoning, with yellower cores and greener outer portions.

Figure 2: These broken pieces and crystal fragments of apatite from Hormuz Island show a light yellow colour with various degrees of iron staining. The coin is 3 cm in diameter. Photo by B. Rahimzadeh.

Figure 1: Apatite from Hormuz Island, Iran, is found dispersed over the ground from weathering of associated iron-rich ores. Photo by B. Rahimzadeh.

Recently, apatite from Hormuz Island was characterized by these authors for this report. The samples consisted of one cabochon, three faceted stones and two freeform carvings weighing 2–4 ct (e.g. Figure 3). They were greenish yellow to green, and RI readings ranged from 1.625 to 1.640 (with small birefringence values) for the faceted stones and were 1.64 (spot readings) for the other samples. An RI of 1.625 is somewhat low for apatite, but the higher measurements were consistent with reported values (1.63–1.64, cf. O'Donoghue, 2006). The hydrostatic SG values were 3.13–3.17, which is somewhat low for apatite (3.17–3.23, cf. O'Donoghue, 2006). The greener samples showed higher SG and lower RI measurements. All of the stones were inert to long- and short-wave UV radiation. Microscopic examination revealed small euhedral hematite inclusions and conchoidal fractures in some samples that were locally iron stained.

Hormuz Island apatite may have significant potential for the gem industry if systematic exploration is undertaken and appropriate methods for cutting and polishing the stone are introduced into the local market. Another source

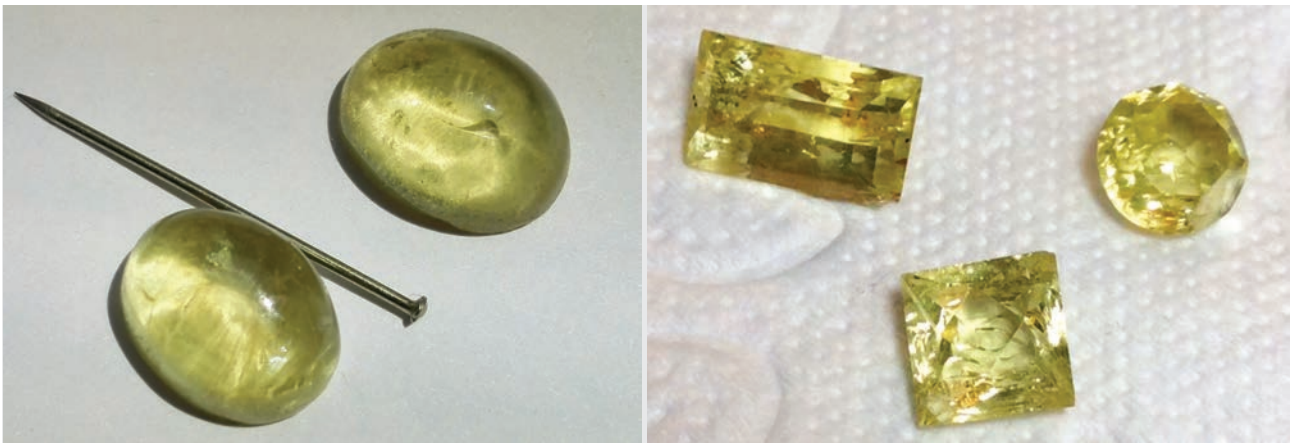

Figure 3: The Hormuz Island apatite samples studied for this report included these slightly greenish yellow cabochons (left, ~4 ct each) and yellow faceted stones (right, ~2–4 ct). Photos by B. Rahimzadeh.

of apatite (some of which is gem quality) is the Sfordi mine in central Iran, where the crystals are hosted by iron-oxide deposits related to alkaline igneous rocks (syenite).

Dr Bahman Rahimzadeh (b_rahimzadeh@sbu.ac.ir)
and Rasoul Sheakhy Qeshlaqi
Shahid Beheshti University, Tehran, Iran

References

Elyasi J., Aminsobhani E., Behzad A., Moiinvaziri H. and Meisami A., 1977. Geology of Hormuz Island. *Proceedings of the Second Geological Symposium of Iran*, The Iranian Petroleum Institute, Tehran, Iran, 31–72 [in Persian].

O'Donoghue M., Ed., 2006. *Gems: Their Sources, Descriptions and Identification*, 6th edn. Butterworth-Heinemann, Oxford, 873 pp.

Padyar F., Borna B., Qurbani V., Alizadeh V. and Jafarzadeh N., 2012. Study of fluid inclusions and Raman microspectrometry of Hormuz Island apatites. *The 13th Conference of Geosciences,* Geological Survey and Mineral Exploration of Iran, Tehran, 13–16 February, 6 pp.

Purple Apatite from Namibia

Gem-quality apatite is rarely produced from Namibia, and an interesting yellow chatoyant stone was documented fairly recently by one of these authors (Johnston, 2014). During the past few years, apatite in various other colours—including deep purple—also was produced in Namibia. From late 2012 to 2014, one of the authors' (CLJ) suppliers reported finding small amounts of purple apatite on Farm Okatjimukuju, located approximately 20 km south-east of Karibib. The apatite-bearing pockets were associated with quartz, albite and muscovite. The initial finds consisted of moderately purple apatite crystals with a white/green core, but unfortunately the vast majority of the material was recovered as broken pieces that were not transparent. Additional mining produced a few dark purple apatites consisting of well-formed doubly terminated hexagonal prisms (some on matrix). Shortly before mining ceased, approximately 20–30 much better specimens were found that showed a superb deep purple colour (e.g. Figure 4) and relatively good lustre. Individual crystals measured from 1 × ½ cm up to 8 × 6 cm, and some were found on a matrix of transparent quartz crystals. In addition to purple, the apatite colours included white, colourless, pink, green-grey and dark green. The area was reclaimed in 2014, and no additional apatite mining has been allowed by the property owner.

Some of this purple apatite appeared at the September 2015 Hong Kong gem show, and additional material was brought to the October 2015 Munich show. One of these authors (JJB) acquired 500 g of the rough material, which proved challenging to work with due to abundant fractures that required clipping with pliers and some grinding on the cutting wheel to see inside. After this process, only ~100 g of preformed pieces remained that were somewhat clean. Author JJB faceted ~20 stones that ranged from light lavender

Figure 4: Deep purple apatite is associated with quartz and albite on this specimen (14 × 13 cm) from the Karibib area of Namibia. Specimen and photo courtesy of Hans Soltau.

to deep purple; some of them had a slight grey overtone. So far, most of the gems weigh <2 ct (eye clean to very slightly included), and only four eye-clean stones weighing >3 ct have been cut, including a top-colour 3.51 ct oval and a 7.27 ct

Figure 5: Weighing 7.27 ct, this eye-clean cushion brilliant is unusually large for purple apatite from Namibia. Photo by Jeff Scovil.

cushion (Figure 5). In addition, a parcel of small-sized material is being cut overseas.

The purple colour of this apatite is reminiscent of the classic material produced from the Pulsifer Quarry in Maine, USA (e.g. Manchester and Bather, 1918).

Christopher L. Johnston
(chris@johnstonnamibia.com)
Omaruru, Namibia

John J. Bradshaw
Coast-to-Coast Rare Stones
Nashua, New Hampshire, USA

References

Johnston C.L., 2014. Gem Notes: Cat's-eye apatite from Namibia. *Journal of Gemmology*, **34**(3), 191.

Manchester J.G. and Bather W.T., 1918. Famous mineral localities: Mt. Mica, Mt. Apatite and other localities in Maine. *American Mineralogist*, **3**, 169–174.

Orange-Red to Yellowish Brown Cordierite from Madagascar

Gem-quality cordierite is typically seen as blue material (iolite), showing strong pleochroism in yellow, light blue and dark violet-blue. However, in late 2014 one of the authors (FP) learned about a new occurrence of a much different cordierite, which typically ranged from dark orange-red to yellowish brown. The material is recovered by local miners from weathered residual deposits in southern Madagascar, probably in the Gogogogo area, north of Ampanihy in Tuléar Province. One of the authors (FP) obtained about 120 kg of rough material of mixed quality from the miners over a period of a few months, from which only a few kilograms were suitable for cutting cabochons and faceted stones (e.g. Figures 6 and 7).

Three faceted stones weighing 2.55, 3.17 and 3.63 ct were characterized for this report (Figure 7). They displayed strong pleochroism, in (1) strong orange, (2) greyish purplish (red-) pink and (3) slightly brownish ('straw') yellow. The pleochroism

Figure 6: Cabochons cut from the new Madagascar cordierite show unusual orange-red to yellowish brown coloration. The total weight of the stones shown here is 45.18 ct. Photo by F. Pezzotta.

could clearly be observed with the naked eye, resulting in an overall dark, slightly brownish orange-red or yellowish brown depending on the viewing angle. RI values varied between 1.530 and 1.540, with n_α = 1.530, n_β = 1.533–1.534 and n_γ = 1.540, yielding a birefringence of 0.010. The optic sign was consistently biaxial positive, which differs from the common blue iolite (biaxial negative). Hydrostatic SG values were 2.53–2.55; these are at the low end of the known range for cordierite (2.53–2.78, cf. Deer et al., 1986). All samples were inert to long- and short-wave UV radiation. The stones were moderately included, mostly with partially healed fissures but also with irregularly shaped, breadcrumb-like inclusions and various mineral inclusions. Raman microspectroscopy using a Thermo DXR Raman microscope with 532 nm laser excitation identified the inclusions as follows: rounded and elongated—or thin, long prismatic—crystals of tourmaline; blocky and small rectangular-appearing grains of quartz; rounded crystals of apatite; a small platelet of phlogopite; and minute, parallel-oriented needles and small platelets, possibly rutile. Tiny fractures were seen along partially healed fissures and also adjacent to various mineral inclusions. Chemical analyses of the three samples by energy-dispersive X-ray fluorescence (EDXRF) spectroscopy showed major amounts of Mg, Al and Si, minor amounts of Fe, and traces of Mn. Energy-dispersive spectroscopy on a slab of the cordierite by author GRR using a scanning electron microscope showed similar composition. The optical spectrum showed features of Fe^{2+} found in blue cordierite, plus water-related absorptions in the near-infrared, but also a strong absorption band near 500 nm that is the cause of the unusual orange-red to yellowish brown colour.

Further information on this new cordierite will be reported in a future publication.

Figure 7: These three Madagascar cordierites (2.55–3.63 ct) were analysed for this report. Photo by J. C. Zwaan.

Dr J. C. (Hanco) Zwaan (hanco.zwaan@naturalis.nl)
Netherlands Gemmological Laboratory
National Museum of Natural History 'Naturalis'
Leiden, The Netherlands

Dr Federico Pezzotta
Natural History Museum of Milan, Italy

Dr George R. Rossman
California Institute of Technology
Pasadena, California, USA

Reference

Deer W.A., Howie R.A. and Zussman J., 1986. *Rock-Forming Minerals—Disilicates and Ring Silicates*, Vol. 1B, 2nd edn. Longman, New York, 629 pp.

An Unusual Emerald and Pyrite Mixture from Colombia

Emeralds from Colombia are commonly associated with pyrite (for information on the geology of the deposits see, e.g., Pignatelli et al., 2015), and sometimes pyrite is found also as inclusions in the emeralds. In 2015, a new find of emerald from an undisclosed locality in Colombia produced intergrowths of pyrite, emerald and dolomite. Cabochons cut from this material are quite distinctive, and four of them were studied for this report (e.g. Figure 8).

The ratio of pyrite, emerald and dolomite in the samples was highly variable. In two of them, pyrite clearly crystallized first, forming euhedral cubic crystals up to 10 mm. In the other two cabochons, pyrite was present as irregular corroded masses surrounding small grains of emerald (e.g. Figure 9). The green areas of the stones were typically formed by a granular mixture of emerald and dolomite (again, see Figure 9)—except for the marquise-shaped cabochon, in which both minerals occurred separately. (The presence of emerald and dolomite in the cabochons was confirmed by Raman spectroscopy; pyrite does not produce a Raman spectrum with this author's unit.)

Figure 8: These cabochons from Colombia consist of intergrowths of pyrite, emerald and dolomite. The centre stone is 36 mm long. Photo by J. Hyršl.

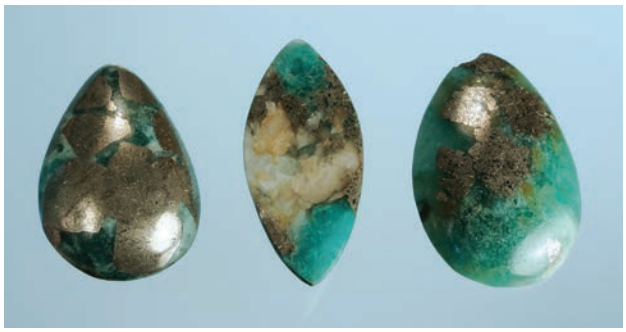

Overall, the polish lustre of the cabochons was mediocre due to the different hardness of the three minerals (Mohs 7½–8 for beryl, 6–6½ for pyrite, 3½ for dolomite). Within the mixed emerald-dolomite areas, the softer grains of dolomite could be easily distinguished with a loupe from the harder emerald by differences in their lustre.

Pyrite is a relatively unstable mineral, especially in humid conditions, and it is very fragile. For this reason, the studied cabochons are not suitable for jewellery use, but they represent interesting collector's objects.

Dr Jaroslav Hyršl (hyrsl@hotmail.com)
Prague, Czech Republic

Reference

Pignatelli I., Giuliani G., Ohnenstetter D., Agrosì G., Mathieu S., Morlot C. and Branquet Y., 2015. Colombian trapiche emeralds: Recent advances in understanding their formation. *Gems & Gemology*, **51**(3), 222–259, http://dx.doi.org/10.5741/gems.51.3.222.

Figure 9: The texture of the various minerals is visible on the base of this cabochon (35 mm long), which shows irregular corroded masses of pyrite and granular intergrowths of emerald and dolomite. Photo by J. Hyršl.

Garnet from Mahenge, Tanzania

The Mahenge area in the Morogoro region of south-central Tanzania is a well-known source of several gem varieties, particularly spinel and ruby. During the 2016 Tucson gem shows, Steve Ulatowski (New Era Gems, Grass Valley, California, USA) had some pink to orangey pink garnets from a new find in this area that he sold as 'Mahenge Malaya'. He obtained the rough material in mid-December 2015 in Arusha, Tanzania. Consisting of clean alluvial pebbles, the garnet ranged from pinkish orange to a saturated 'hot' pink. Most of the production was rather

Figure 10: Weighing 6.79 and 6.84 ct, these faceted garnets from Mahenge, Tanzania, are unusually large for this new find. Courtesy of Evan Caplan; photo by Jeff Scovil.

small sized, although Ulatowski encountered ~1 kg of material consisting of >0.5 g stones, with the largest pieces weighing >3 g. Faceting of two of the largest pieces yielded attractive pink and pinkish orange gemstones weighing 6.79 and 6.84 ct (Figure 10).

Ulatowski loaned a 3.22 ct triangular preform for examination, and the table facet was kindly polished during the show by Todd Wacks (Tucson Todd's Gems, Tucson, Arizona). Its colour was 'fleshy' pink with a faint brown tint (World of Color 2.5R5/6, Brownish Red) under daylight-equivalent lighting. Viewed with incandescent lighting, the brown tint was not evident and the stone appeared slightly more reddish pink (World of Color 2.5R5/10, Moderate Red). This colour behaviour is typical of many so-called Malaya or colour-shift garnets from East Africa. The stone had an RI of 1.751 and a hydrostatic SG of 3.82. Anomalous extinction was observed between crossed polarizers, and the garnet was inert to both long- and short-wave UV excitation. Magnetic susceptibility was not insignificant, with it being picked up by a 9-mm-diameter N-52 REE magnet, and easily dragged by smaller N-52 magnets. The stone appeared eye clean, but microscopic observation revealed several small, scattered, whitish, breadcrumb-like inclusions as well as what appeared to be fine strings of partially dissolved needles.

Figure 11: The visible-range spectrum of a 'fleshy' pink sample of Mahenge garnet showed absorptions related to both almandine and spessartine.

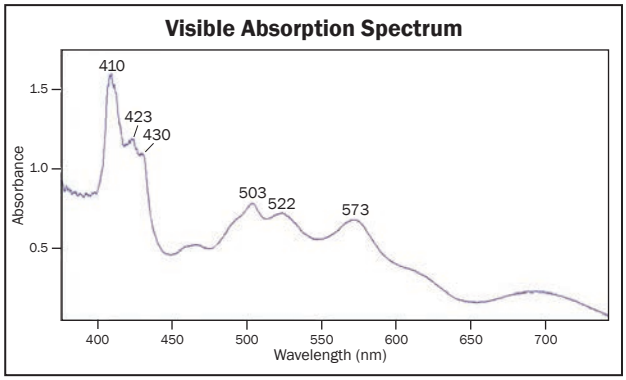

Pink is one of the rarer colours of garnet, and is typically seen in either the hydrogrossular or pyrope-dominant varieties. EDXRF chemical analyses with an Amptek X123-SDD spectrometer revealed major amounts of Mn and Fe, minor Ca, and traces of Cr. Although Mg was below accurate detection levels for this instrument, electron microprobe analysis of five samples of this garnet by John Attard (Attard's Minerals, San Diego, California, USA) revealed major amounts of Mg in all of them. They consisted mainly of pyrope with variable spessartine and almandine, and a very minor grossular component.

Visible-range spectroscopy using an Ocean Optics USB4000 spectrometer with a 7-inch integrating sphere showed weak almandine absorptions at 503, 522 and 573 nm, as well as spessartine absorptions at 410, 423 and 430 nm (Figure 11). Infrared spectroscopy with a PerkinElmer Spectrum100 Fourier-transform infrared (FTIR) instrument revealed a significant water content. The various water-related peaks between 3560 and 3675 cm^{-1} were consistent with OH absorption (Ogasawara et al., 2013).

This attractively coloured garnet is a welcome addition to the gem marketplace.

Cara Williams FGA and Bear Williams FGA
(info@stonegrouplabs.com)
Stone Group Laboratories
Jefferson City, Missouri, USA

Reference

Ogasawara Y., Sakamaki K. and Sato Y., 2013. Water contents of garnets from the Garnet Ridge, northern Arizona: H_2O behavior underneath the Colorado Plateau. American Geophysical Union, Fall Meeting, abstract #V23A-2754, http://adsabs.harvard.edu/abs/2013AGUFM.V23A2754O.

New Production of Grandidierite from Madagascar

Grandidierite, $(Mg, Fe^{2+})(AlFe^{3+})_3(SiO_4)(BO_3)O_2$, is an extremely rare collector's stone that is known in gem quality mainly from Madagascar, and less commonly from Sri Lanka. The material from Madagascar typically lacks transparency: Ostwald (1964) noted that "only massive [rough] material was available for study", and Mitchell (1977) stated that the small number of faceted stones and cabochons that he examined were "semitransparent, due to fissures and inclusions". Schmetzer et al. (2003) documented the first transparent faceted grandidierite (0.29 ct); it was also the first time this gem was reported from Sri Lanka.

During the 2016 Tucson gem shows, Frédéric Gautier (Little Big Stone, Antananarivo, Madagascar) had several pieces of transparent faceted grandidierite from new finds in the Androy region, Tuléar Province, southern Madagascar. The initial production occurred in late 2014, when some low-quality material was found. Better-quality stones were found during early- to mid-2015: approximately 300 kg were produced, with a very small percentage that was transparent. Most of the gem material consisted of small pieces, with some larger fractured pieces weighing 5–10 g. The colour ranged from pale to moderately saturated greenish blue to bluish green, in medium to dark tones. Gautier faceted 40 clean stones weighing 0.10–1.78 ct (e.g. Figure 12). Gemmological properties of a recently produced Malagasy grandidierite were described by Vertreist et al. (2015).

This new production from Madagascar marks the first time that a significant number of clean faceted grandidierites have become available, and also the largest pieces of transparent material ever to be cut. Hand mining of the deposit continues, and it is possible that more gem-quality rough will be produced. Nevertheless, grandidierite remains a very rare gem material.

Brendan M. Laurs FGA

References

Mitchell R.K., 1977. African grossular garnets; blue topaz; cobalt spinel; and grandidierite. *Journal of Gemmology*, **15**(7), 354–358, http://dx.doi.org/10.15506/jog.1977.15.7.354.

Ostwald J., 1964. Some rare blue gemstones. *Journal of Gemmology*, **9**(5), 182–184, http://dx.doi.org/10.15506/jog.1964.9.5.182.

Figure 12: Weighing 1.78 ct (left) and 1.08 ct (right), these grandidierites from Madagascar are exceedingly large and transparent for this rare gem material. Photos by Jeff Scovil.

Schmetzer K., Burford M., Kiefert L. and Bernhardt H.-J., 2003. The first transparent faceted grandidierite, from Sri Lanka. *Gems & Gemology*, **39**(1), 32–37, http://dx.doi.org/10.5741/gems.39.1.32.

Vertriest W., Detroyat S., Sangsawong S., Raynaud V. and Pardieu V., 2015. Gem News International: Grandidierite from Madagascar. *Gems & Gemology*, **51**(4), 449–450.

A Lalique Quartz Pendant, in Polarized Light

Singly polarized or cross-polarized light is often used by gemmologists when testing transparent and translucent rough or cut gem materials. The way the light is modified after passing through the material reveals important characteristics about the crystalline nature of the sample.

In October 2015, GGTL Laboratories in Geneva received for identification a colourless pendant (~37.1 × 34.3 × 5.1 mm; Figure 13) that displayed two human figures engraved in relief. The client indicated that René Lalique made the pendant. Lalique (1860–1945) was a famous designer and well-known for his glassmaking art, but he was also a jeweller who worked with a variety of gem materials (Passos Leite, 2008). At first sight the pendant appeared to be glass, but the cool sensation of the piece on the skin suggested it was quartz. (Glass has a lower thermal conductivity than quartz, and hence feels 'warmer' than quartz.)

Figure 13: This Lalique quartz pendant (~37.1 × 34.3 × 5.1 mm) displays two engraved human figures. Photo by C. Caplan.

Initial gemmological observations were done using a binocular microscope, first in transmitted light and then with crossed polarizers. Bright interference colours indicated the material was anisotropic. When we observed the pendant in the direction of the optic axis with a glass sphere (used as a convergent lens known as a conoscope), we immediately saw a 'bull's-eye' figure that is distinctive for quartz (Figure 14).

Quartz crystallizes in the trigonal system, and the tablet used for this pendant had been cut perpendicular to the optic axis (or three-fold symmetry axis). The common habit of quartz is an elongated prism with rhombohedral terminations, and the crystals are frequently

Figure 14: Viewed with crossed polarizers, the pendant shows a 'bull's-eye' interference figure with the conoscope, as expected for quartz. Distorted Dauphiné twinning interference patterns are visible in the minor rhombohedron at top and left. Photo by C. Caplan; image width ~28 mm.

Figure 15: The quartz pendant (~37.1 × 34.3 mm) shows various interference colours as the analyser is rotated over a stationary polarizer, from the front side (left) and the reverse side (right). Photos by C. Caplan.

twinned (O'Donoghue, 1987). Viewed with crossed polarizers, the quartz showed angular interference colour patterns on the top and left edges of the pendant due to twinning of the minor rhombohedron *z* faces (again, see Figure 14). Consistent with the fact that there was no colourless synthetic quartz available on the market during Lalique's time, the distribution and orientation of the twinning characteristics confirmed it was natural quartz (Notari et al., 2001; Payette, 2013).

This pendant provides a good example of how interference colours are influenced by the thickness of the observed material and by its crystallographic orientation versus the polarization direction of the light. The two groups of photos in Figure 15 show variations in the appearance of the pendant as the analyser was rotated over the stationary polarizer, from the front side (left) and the reverse side (right). The human figures remain colourless in the front view, while they show interference colours in the back view. The colours observed between crossed polarizers are complementary to those seen between parallel polarizers (Figure 15-right, third picture of each line). This appearance is due to a combination of diffusion and diffraction phenomena caused by the curved shape of the engraving. Further, when viewed only with fully crossed polarizers, completely different interference colours are produced as the pendant is rotated (Figure 16).

It is always interesting to examine gem materials with polarized light, and sometimes a simple colourless object can appear complexly beautiful. As shown by this pendant, such examination yields useful information, and may allow one to distinguish natural from synthetic quartz.

Candice Caplan (candice.caplan@ggtl-lab.org) and Franck Notari
GGTL Laboratories, Geneva, Switzerland

Figure 16: Different interference colours are also produced as the quartz pendant is rotated between crossed polarizers. Photos by C. Caplan; image width ~20 mm.

References

Notari F., Boillat P.Y. and Grobon C., 2001. Discrimination des améthystes et des citrines naturelles et synthétiques. *Revue de Gemmologie*, **141/142**, 75–80.

O'Donoghue M., 1987. *Quartz*. Butterworths, London, 110 pages.

Passos Leite M.F., 2008. *René Lalique at the Calouste Gulbenkian Museum*. Skira, Milan, Italy, 136 pages.

Payette F., 2013. A simple approach to separate natural from synthetic ametrine. *Australian Gemmologist*, **25**(4), 132–141.

Faceted Quartz with Petroleum Inclusions from Baluchistan, Pakistan

Euhedral quartz crystals with petroleum inclusions are well known from Baluchistan Province, western Pakistan (Koivula and Tannous, 2004; Koivula, 2008). These specimens typically have fluid inclusions containing yellow petroleum (with or without a colourless aqueous phase), a methane gas bubble and solid particles of black asphaltite. When exposed to UV radiation (particularly long-wave), the petroleum commonly luminesces a strong yellow or blue (see, e.g., Figure 28 [right] on p. 21).

Koivula and Tannous (2004) indicated that although gems can be cut from this quartz, the heat sensitivity of the inclusions requires caution to avoid fracturing them. It was therefore notable to see some of these faceted gemstones with Mark Kaufman (Kaufman Enterprises, San Diego, California, USA) during the 2016 Tucson gem shows (e.g. Figure 17). From 30 crystals that he purchased at the October 2015 Munich (Germany) show, Kaufman cut six stones weighing ~1–4 ct. He selected the crystals especially to show isolated petroleum inclusions after faceting, but unfortunately most of the inclusions were located too close to the surface of the crystals to avoid intersecting with the cutting wheel, causing the petroleum to leak out. Therefore, the greatest challenge that Kaufman faced while faceting this quartz was the difficulty of cutting around the inclusions without penetrating them.

Figure 17: Faceted Pakistani rock crystal quartz with petroleum inclusions (yellow) is seldom encountered in the marketplace. The stones shown here weigh 2.20–2.29 ct. Photo by Orasa Weldon.

For collectors who appreciate unusual inclusions, these quartz gems will provide interesting samples. *Brendan M. Laurs FGA*

References

Koivula J.I., 2008. Lab Notes: Unusual green fluid inclusions in quartz. *Gems & Gemology*, **44**(2), 161.

Koivula J.I. and Tannous M., 2004. Gem News International: Petroleum inclusions in quartz from Pakistan: A photo-essay. *Gems & Gemology*, **40**(1), 79–81.

Quartz Slabs from Inner Mongolia

Quartz crystals are prized by collectors for their transparency and prismatic crystal form, but some specimens are even more interesting when sliced into slabs to show their internal features. Such was the case for quartz tablets from Colombia that were recently described by Krzemnicki and Laurs (2014) as having a radiating fibrous structure.

During the 2016 Tucson gem shows, Luciana Barbosa (Gemological Center, Weaverville, North Carolina, USA) had some interesting quartz

Figure 18: These polished slices of quartz from Inner Mongolia (up to 2.8 cm tall) display various six-fold patterns. Courtesy of Mike and Pat Gray; photo by Jeff Scovil.

slabs from the Huanggang Fe-Sn deposit, Inner Mongolia, China. Polished perpendicular to the c-axis, some of them displayed snowflake-like patterns of dark inclusions, while others had transparent cores that showed complex patterns of interference colours between crossed polarizers (Figures 18 and 19).

Barbosa was told that the quartz was found in 2012. She obtained ~100 slices for the Tucson shows, with an additional ~50 pieces in the process of being slabbed. The slices typically ranged up to 3 cm across, with very few being any larger. Only some portions of the crystals gave attractive patterns when sliced. The dark inclusions have not yet been identified.

Brendan M. Laurs FGA

Reference

Krzemnicki M.S. and Laurs B.M., 2014. Gem Notes: Quartz with radiating fibres, sold as 'trapiche' quartz. *Journal of Gemmology*, **34**(4), 296–298.

Figure 19: Close-up images of the quartz slabs from Inner Mongolia reveal attractive radiating and concentric arrays of dark inclusions (left, 30 × 27 × 2 mm) and complex patterns of interference colours (right, 26 × 25 × 2 mm). Photos by Luciana Barbosa; crossed polarizers.

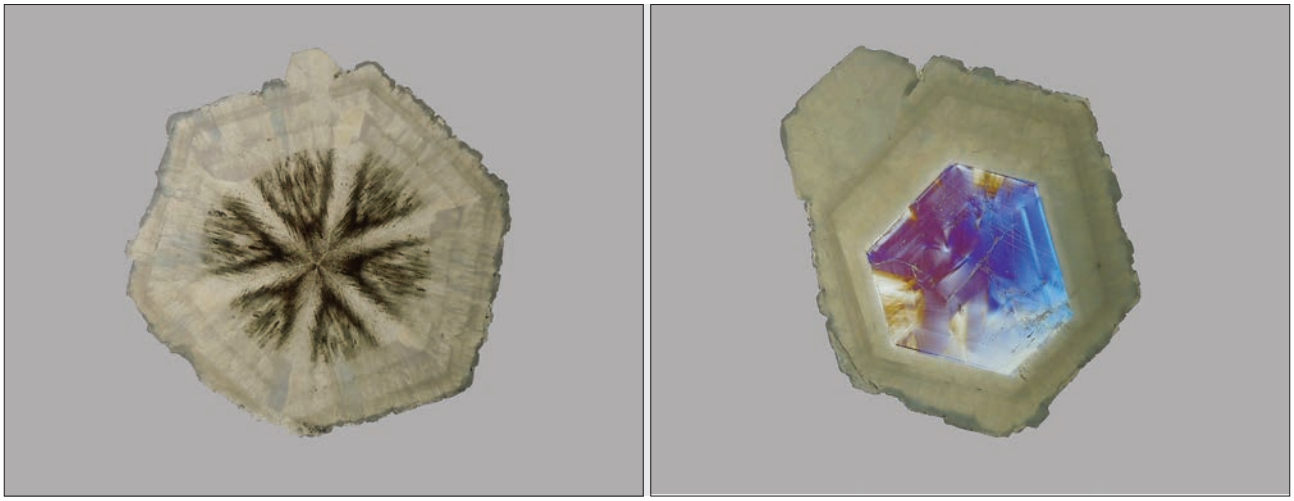

Sphalerite Inclusions in Quartz

During the 2016 Tucson gem shows, rare-stone dealer Luciana Barbosa had some faceted quartz with sphalerite inclusions from a new find in Goiás State, Brazil (e.g. Figure 20). Barbosa reported that about 80 stones were faceted from a single large quartz crystal that was mined in 2015, which contained numerous sphalerite crystals near the surface. The largest gem

Figure 20: This 34.20 ct quartz from a new find in Brazil contains two euhedral inclusions of sphalerite. Courtesy of Luciana Barbosa; photo by Jeff Scovil.

weighed over 100 ct, but most of the stones were <20 ct.

Although sphalerite inclusions have been reported previously in quartz (i.e. from tungsten deposits and various ore veins; Hyršl, 2006), this find is notable for the clarity of the host quartz and the perfection of the sphalerite crystals, some of which even display complex growth patterns on their faces (Figure 21).

Brendan M. Laurs FGA

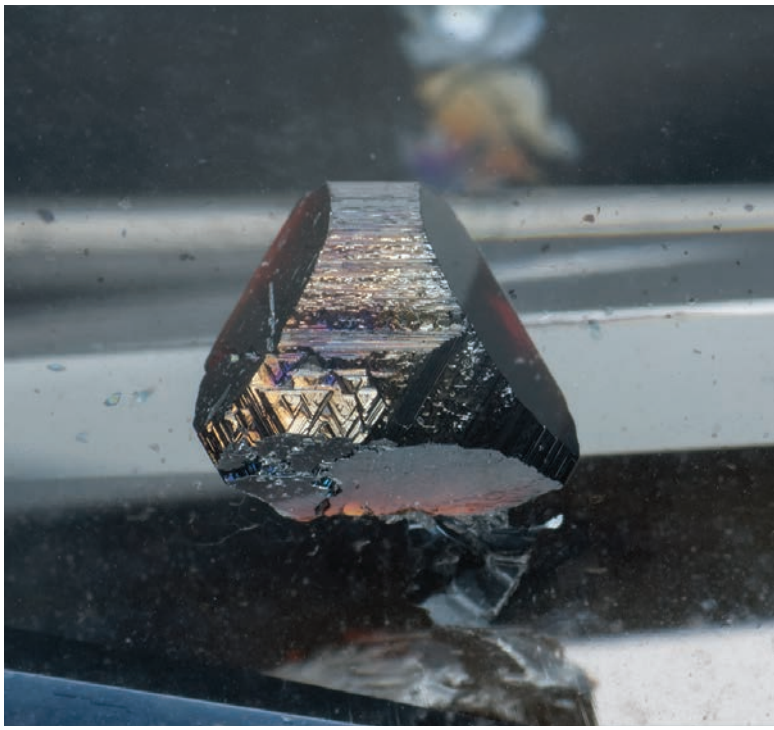

Figure 21: A closer view of the larger sphalerite inclusion (4 mm across) in Figure 20 shows interesting growth patterns on some of its faces. Photo by Jeff Scovil.

Reference

Hyršl J., 2006. Genetic classification of mineral inclusions in quartz. *Gems & Gemology*, **42**(3), 97–98.

Ruby from Liberia

Ruby from Liberia was reported relatively recently by Kiefert and Douman (2011) as small transparent pinkish red to red pebbles from the Mano River, and larger near-opaque purplish red crystals from Nimba Province near the Guinean border. During the 2015 and 2016 AGTA Tucson gem shows, Eric Braunwart (Columbia Gem House, Vancouver, Washington, USA) displayed ruby from Liberia that was different from either material mentioned above. While not of facet grade, it exhibited an attractive sparkliness in reflected light.

Braunwart loaned the sample in Figure 22 for examination. It consisted of a polished hexagonal plate weighing 3.32 ct and measuring 10.16 × 1.96 mm. It was a dull but saturated dark red (World of Color 2.5R3/6, Dark Red) with slight to moderate

Figure 22: This polished hexagonal plate (3.32 ct) of ruby from Liberia displays abundant sparkles in reflected light that are due to reflections from rutile inclusions and polycrystalline grain boundaries. Photo by B. Williams.

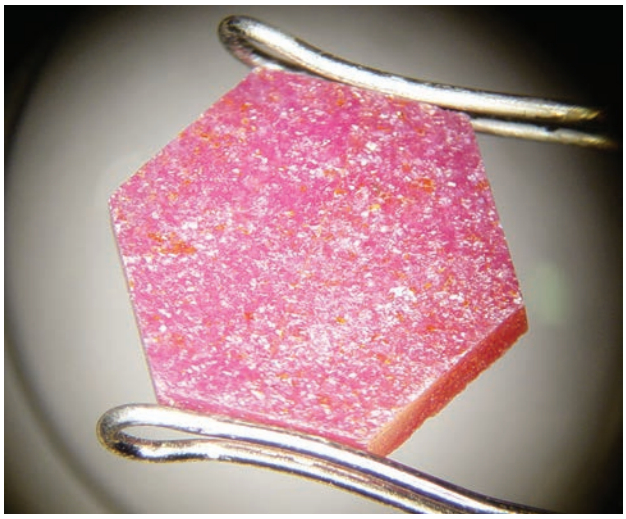

Figure 23: Seen here in oblique lighting, the 3.32 ct ruby shows a granular texture with orangey red domains corresponding to rutile inclusions. Photo by B. Williams.

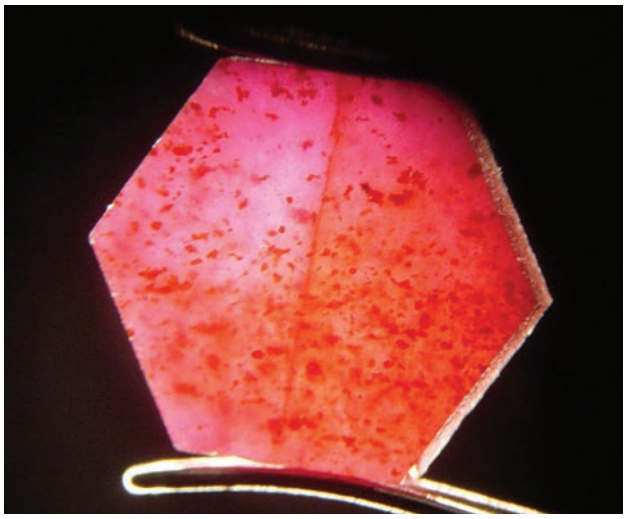

Figure 24: Viewing the 3.32 ct ruby with transmitted light highlights the presence of a partially healed fissure and abundant orangey red inclusions (rutile crystals). Photo by B. Williams.

translucency. Although the hexagonal slice had a shape reminiscent of a cross-section from a corundum crystal, the stone gave a polycrystalline reaction between crossed polarizers, remaining bright throughout a full rotation. Microscopic observation revealed a granular appearance with most individual grains appearing pinkish red, while a few were orangey red (Figure 23). While this might be suggestive of ruby dichroism, the orangey red domains proved to consist of inclusions. Transmitted light revealed numerous translucent, deep orangey red, blocky, crystalline inclusions that were randomly oriented, as well as one partially healed fissure running through the centre of the stone (Figure 24). No other inclusions were observed. RI measurements of the sample yielded a single, weak shadow edge near 1.763. Specific gravity was measured as 3.81; this relatively low value is possibly due to the corundum's polycrystalline structure. The stone was inert to both long- and short-wave UV excitation. Raman analysis with a GemmoRaman-SG instrument confirmed it to be corundum.

It is the sparkly appearance that makes this ruby intriguing. Under magnification, numerous micro-reflections were seen emanating from the polycrystalline grain boundaries, as well as from the inclusions mentioned above. Several of the surface-reaching inclusions were identified as rutile by an Enwave 785 micro-Raman spectrometer. The presence of abundant rutile inclusions is consistent with the elevated Ti content obtained for the sample with an Amptek X123-SDD EDXRF spectrometer. The chemical analysis also revealed the Cr and Fe that are presumed responsible for the red colour of the ruby and lack of fluorescence, respectively.

While ruby with rutile needles is commonly encountered, this material in unusual for having rutile present as reflective grains mixed with polycrystalline ruby.

Cara Williams FGA and Bear Williams FGA

Reference

Kiefert L. and Douman M., 2011. Gem News International: Ruby from Liberia. *Gems & Gemology*, **47**(2), 128.

Yellow Sapphire with Unstable Colour—in Reverse

Irradiated yellow sapphires are rarely encountered in today's market. Although it is possible to irradiate a colourless sapphire to turn it yellow, this treatment is highly unstable and readily fades to colourless upon exposure to light (Nassau and Valente, 1987). We were therefore surprised to learn about a yellow sapphire with unstable colour—in reverse. Harold Dupuy FGA of Stuller

Figure 25: This 1.07 ct sapphire shows an unusual 'reverse' colour change. The more stable yellow state fades to colourless after low-temperature heating, and the yellow colour can be restored by exposure to long-wave UV radiation or daylight. Photos by B. Williams.

Inc., Lafayette, Louisiana, USA, reported that they sold a 1.07 ct white sapphire to a retailer who returned the stone after it turned yellow. The client mounted the white sapphire into a ring, and sold it to a consumer who wore the ring for a few months before returning it to the retailer. Stuller immediately exchanged the stone for another comparable white sapphire, but the question remained of how and why the change in coloration occurred.

The sapphire was sent to Stone Group Laboratories for testing. Upon receipt, the stone was yellow (Figure 25, left). The refractometer showed the expected RI values of 1.76–1.77 and Raman spectroscopy confirmed it was corundum. Detailed microscopic examination and FTIR spectroscopy revealed the absence of thermal enhancement in this metamorphic sapphire. With Dupuy's permission, various experiments were performed to test the colour stability of the stone.

First the sapphire was subjected to low-temperature heating of 260°C for one hour, which rendered it colourless (e.g. Figure 25, right). Then it was exposed to a 4 W long-wave UV lamp for 30 minutes, after which it again appeared light yellow. Reheating as before returned it to colourless. Such reversible coloration is commonly related to energy-induced trapped hole centres, which can vary in their stability (Nassau and Valente, 1987). A reversible colour change also has been observed by the present authors in some blue zircons that exhibit brown-to-green tints upon exposure to strong UV radiation, then revert to their previous (heated) blue colour over a period of days when exposed to a broad-spectrum visible light (cf. Renfro, 2013), or more quickly revert to blue with slight heating.

Jay Boyle (Jay Boyle Co., Fairfield, Iowa, USA), who has been dealing in untreated yellow and white sapphires for 35 years, says he has encountered a small number of yellow stones that exhibited this colour behaviour. He believes it to be observed only in approximately 1 in 3,000 yellow sapphires. In such cases, the yellow colour is more stable, and fades to colourless when exposed to heat (such as during the jewellery-making process), but reverts to the original yellow upon exposure to sunlight for a few days.

In the present sapphire, ultraviolet-visible-near infrared (UV-Vis-NIR) spectroscopy showed a small absorption at 450 nm in both colour states that is indicative of iron (not responsible for the colour phenomenon). The spectra also revealed a very subtle difference between colour states in the form of a broad absorption band in the 460–480 nm range for the yellow state, which was most likely related to the observed change in coloration.

All of the conditions that were found capable of altering the colour of this sapphire are commonly experienced by gem materials in general. Long-wave UV radiation is encountered in the laboratory environment as well as in tanning beds. Of course, sunlight is an even more common source of long-wave UV wavelengths. Heating to a temperature of 260°C is comparatively mild, such that it may be produced by typical kitchen ovens, and jewellery processes can often expose gems to much higher temperatures. Heating of this sapphire to 260°C did not induce a 3309 cm^{-1} band in the FTIR spectra, such as seen in heated corundum. More research is required to understand the coloration of this sapphire, which is best described as containing a rare but unstable energy-activated colour centre.

Cara Williams FGA and Bear Williams FGA

References

Nassau K. and Valente G.K., 1987. The seven types of yellow sapphire and their stability to light. *Gems & Gemology*, **23**(4), 222–231, http://dx.doi.org/10.5741/gems.23.4.222.

Renfro N.D., 2013. Reversible color modification of blue zircon by long wave ultraviolet radiation. *Geological Society of America Abstracts with Programs*, **45**(7), 835.

Petroleum Inclusion in Pink Spinel

Recently, American Gemological Laboratories had the opportunity to examine an unusual 1.69 ct pink spinel that reportedly came from Sri Lanka (Figure 26). Microscopic examination revealed some inclusions commonly seen in spinel, consisting of variously sized octahedral crystals, planar internal growth structures and open fissures. However, most conspicuous was a sizeable two-phase inclusion positioned under the table and in the heart of the stone. The euhedral negative crystal contained a viscous yellow fluid and a spherical bubble (Figure 27, left). As the stone was turned, the bubble slowly moved through the thick yellow fluid. When viewed in a darkened room with long-wave UV radiation (365 nm), the fluid in this inclusion displayed a chalky blue-white reaction underlying the distinct reddish glow of the host spinel (Figure 28, left). Raman analysis could not be used to analyse the fluid due to strong chromium luminescence that swamped the detector. However, focused infrared spectroscopy using a paper mask around the inclusion (Figure 29) identified the fluid as petroleum. The spherical bubble was presumably a gas, although it could have been an immiscible fluid, such as water.

Figure 26: This 1.69 ct pink spinel, reportedly of Sri Lankan origin, contains a unique petroleum-bearing inclusion under the table facet. Photo by Bilal Mahmood.

Similar negative crystals are well-known in rock crystal quartz from Baluchistan, Pakistan (see e.g. Koivula, 2008), which contain petroleum and a bubble of methane gas. The petroleum fluid in this spinel has a similar viscous yellow character (see Figure 27, right) and displays the same chalky blue-white long-wave UV reaction (see Figure 28, right) as the petroleum in quartz from Pakistan.

To the authors' knowledge, this is the first time that a petroleum-bearing inclusion has been documented in spinel.

Monruedee Chaipaksa (mchaipaksa@aglgemlab.com) and Christopher P. Smith
American Gemological Laboratories
New York, New York, USA

Reference

Koivula J.I., 2008. Lab Notes: Unusual green fluid inclusions in quartz. *Gems & Gemology*, **44**(2), 161.

Figure 27: Left: The large, two-phase negative crystal in the spinel contains a viscous yellow fluid (petroleum) and a spherical bubble consisting of a gas or immiscible fluid. The bubble could be seen to slowly migrate through the petroleum as the stone was turned. Photomicrograph by M. Chaipaksa; magnified 70×. Right: A similar appearance is displayed by petroleum-filled negative crystals in colourless quartz crystals from Baluchistan, Pakistan. Photomicrograph by C. P. Smith; magnified 24×.

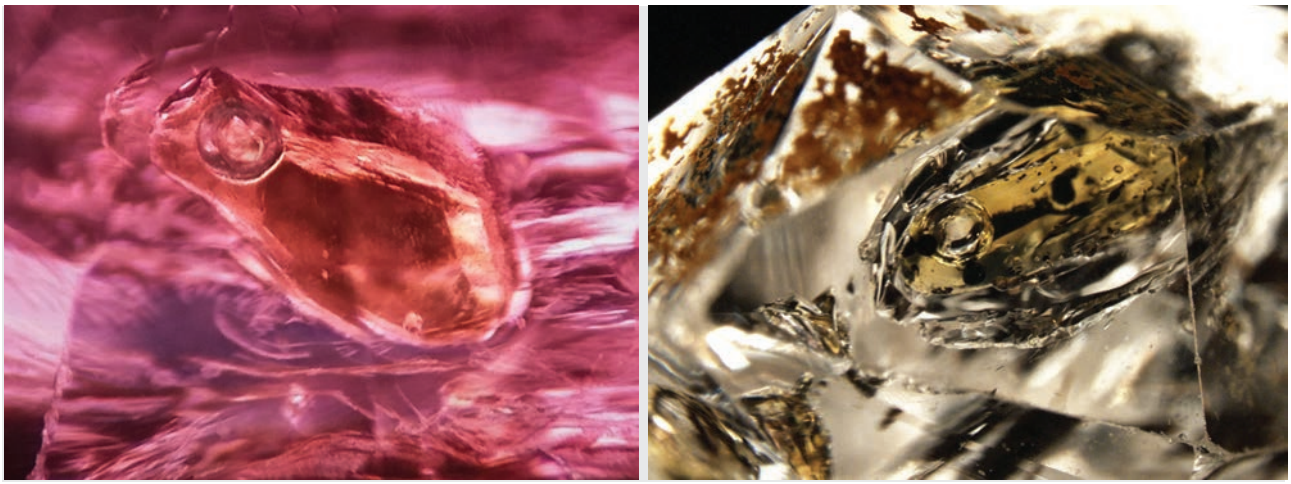

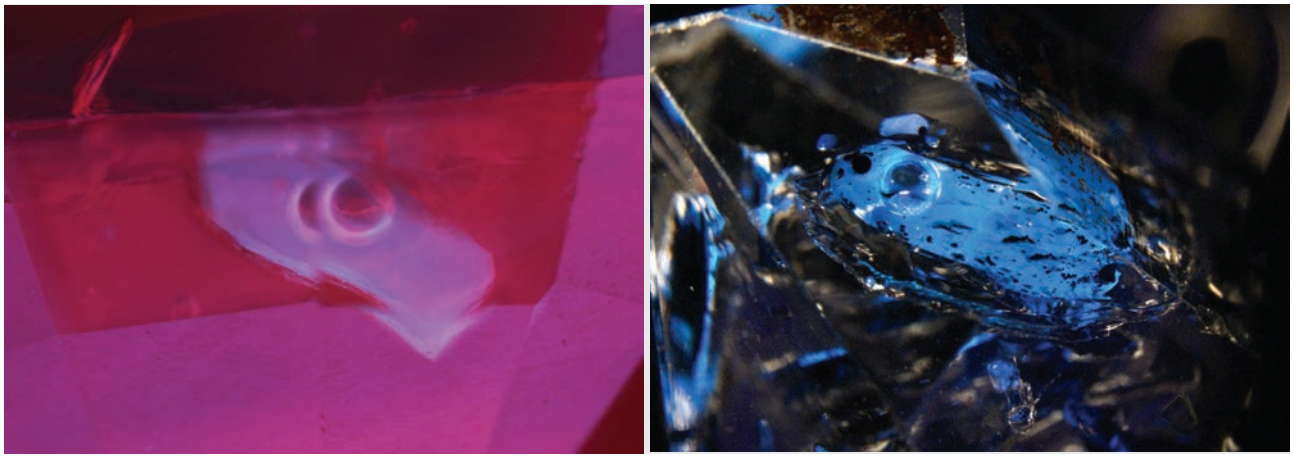

Figure 28: Left: Under long-wave UV radiation (365 nm), the petroleum exhibits a chalky blue-white reaction that was somewhat muted by the dominant red luminescence of the host spinel. Right: Such fluorescence also is displayed by petroleum inclusions in a Pakistani quartz. Photomicrographs by C. P. Smith; magnified 40×.

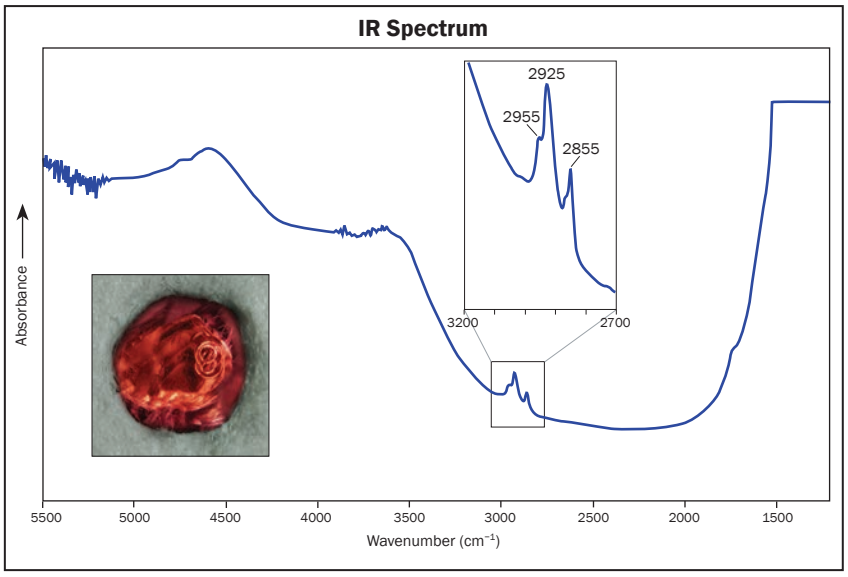

Figure 29: Focused infrared spectroscopy of the negative crystal in the spinel identified the viscous yellow fluid as petroleum, with lines at 2955, 2925 and 2855 cm^{-1}. The inclusion was isolated for the analysis by using a 1.5-mm-wide paper mask (inset photomicrograph by C. P. Smith).

Spurrite from New Mexico, USA

Spurrite is a calc-silicate mineral with the formula $Ca_5(SiO_4)_2(CO_3)$ and a Mohs hardness of 5. It typically forms in contact metamorphic rocks (in particular, skarn deposits) as granular masses ranging from colourless to greyish violet (Bernard and Hyršl, 2004). The mineral has only rarely been used for lapidary purposes (e.g. purple beads and polished slabs or freeform pieces from Mexico and south-western USA; Koivula and Misiorowski, 1986; Wentzell, 2004).

During the 2015 Tucson gem shows, Mauro Pantò (The Beauty in the Rocks, Laigueglia, Italy) had faceted spurrite from Tres Hermanas Mountains, Luna County, New Mexico, USA (cf. Homme and Rosenzweig, 1970). He had 15 pieces that averaged 3 ct each (e.g. Figure 30). Pantò kindly donated one of the spurrites to Gem-A, and the gem was characterized by authors CW and BW.

The following properties were recorded from the 1.86 ct stone: colour—greyish lilac purple; diaphaneity—translucent; RI—approximately 1.67 (indistinct, using the bright line technique); hydrostatic SG—3.00; fluorescence—inert to long- and short-wave UV radiation; polariscope—

aggregate reaction; Chelsea filter—light pinkish red; and no absorption features were visible with a desk-model spectroscope. These properties are consistent with those reported for spurrite in the literature, except that Wentzell (2004) documented faint 'cobalt'-blue long-wave UV luminescence in samples from Mexico. Microscopic examination revealed little other than minor surface-reaching fissures, grain boundaries typical of a polycrystalline material and a few tiny dark masses.

Raman analysis using an Enwave L-Series spectrometer with a 785 nm laser gave a very good match to spurrite in the RRUFF database and in our own reference spectra. EDXRF chemical analyses using an Amptek X123-SDD instrument with a DP5 preamplifier showed that Fe was the main impurity, along with minor-to-trace amounts of Mn, Cr, Zn and Pb. The presence of small amounts of mineral impurities (such as carbonates) was documented by Wentzell (2004) in spurrite from Mexico. Minute amounts of mineral impurities also were present in our sample from New Mexico, as indicated by the anomalous trace elements and the tiny black masses.

Figure 30: These translucent purple gemstones (3.14–5.73 ct) are spurrite from New Mexico, USA. Photo by Mauro Pantò.

Spurrite is dimorphous with paraspurrite, which has mostly overlapping gemmological properties but is known only from Inyo County, California, USA (Bernard and Hyršl, 2004).

Cara Williams FGA, Bear Williams FGA and Brendan M. Laurs FGA

References

Bernard J.H. and Hyršl J., 2004. *Minerals and Their Localities*. Granit, Prague, Czech Republic.

Homme F.C. and Rosenzweig A., 1970. Contact metamorphism in the Tres Hermanas Mountains, Luna County, New Mexico. In L.A. Woodward, Ed., *New Mexico Geological Society Fall Field Conference Guidebook – 21: Tyrone–Big Hatchet Mountains–Florida Mountains Region*, 141–145.

Koivula J.I. and Misiorowski E., 1986. Gem News: Tucson 1986. *Gems & Gemology*, **22**(2), 114–115.

Wentzell C.Y., 2004. Lab Notes: Spurrite. *Gems & Gemology*, **40**(1), 63–65.

Update on Tsavorite Mining at the Scorpion Mine, Kenya

The history and mining of tsavorite at Kenya's Scorpion mine and surrounding claims was described by Bridges and Walker (2014), and since then many important developments have occurred. After a six-year hiatus, the operations were reopened in January 2015. This was accomplished after major investments in infrastructure and staffing, improved mining processes and newly implemented safety measures—all in an effort to ramp-up tsavorite production.

Among the infrastructural improvements, access roads to the Scorpion mine and outlying claim areas were upgraded for better access, and a new road to the Green Garnet 3 (GG3) operation was constructed after the old road was destroyed by past rainy seasons. The GG2 site has been renovated to repair most of the damage done by many years of illegal mining. The former 'CW' open pit (where very fine-colour tsavorite and some tourmaline were previously mined) has been reclaimed. Both the main camp and supervisor camp were restored after elephant attacks caused severe damage. The staff quarters also were upgraded to accommodate a labour force that expands to approximately 100 people during the height of the mining season. The main camp has been

Figure 31: Miners sort through waste rock at the working face of Scorpion mine tunnel No. 4. The ceiling in this area has been reinforced with split-sets. Photo by Louis Brunet.

entirely equipped with solar power, and a new workshop has been constructed.

To improve mining efficiency, an 85 kVA generator was installed at the Scorpion mine to power larger fans and two mono-winches that can be used to remove approximately 4–5 tonnes of waste rock per hour. To enable the use of two rock drills simultaneously, a high-pressure compressed air pipe has been installed into both the No. 2 and No. 4 inclines. The existing ventilation system was also upgraded to improve air circulation. Two new airlift pumps were purchased that run on compressed air instead of petrol/diesel, for a safer and cleaner work environment. Six new rock-drilling machines were obtained that are specially designed for operating with water and compressed air. These make drilling much easier and also minimize the drillers' exposure to silica dust. A 40,000 litre water tank has been installed at the Scorpion mine to ensure a continuous water supply, and a water bowser (tanker rig) was built for transporting water to other locations such as GG3. To improve underground safety, split-sets (roof bolts) have replaced the timber and steel girder supports previously utilized in the No. 2 and No. 4 tunnels (e.g. Figure 31). Problematic areas of the tunnels have been reinforced with welded mesh to help retain friable hanging-wall material.

Production of tsavorite from the Scorpion mine (and later from GG2) resumed in mid-July 2015, and several small-to-medium-sized nodules have been encountered so far. Most of the gem rough (e.g. Figure 32) consisted of pieces weighing 0.1–0.5 g, with a small percentage in the 1–20 g range. The colour ranged from a vivid light yellowish green to a vibrant deep bluish green, with some attractive medium green stones produced (e.g. Figure 33). Tsavorite in larger calibrated sizes such as 7 × 5 mm, 8 × 6 mm, 9 × 7 mm, etc. has always been extremely hard to come by. However, the recent production has enabled the creation of complete tsavorite suites (e.g. Figure 34). For the first time in many years, multiple suites of graduated and calibrated tsavorite rounds have been cut, ranging from 2.0 to 8.5 mm. The largest faceted stone from recent production weighed 17.20 ct.

To help ensure future production of tsavorite, several knowledgeable geologists were brought on to assess the mining areas and assist with mapping the local geology and reef zones at Scorpion and GG2. In addition, around Snake Hill and at other tsavorite-bearing locations, approximately 350 cubic metres of earth were removed for bulk sampling.

Unfortunately, activities by illegal miners and bandits remain a problem in the lease areas, and some encroachers have been arrested by the

Figure 32: Recently produced tsavorite rough from the Scorpion mine is in the process of being sorted. Photo by B. Bridges.

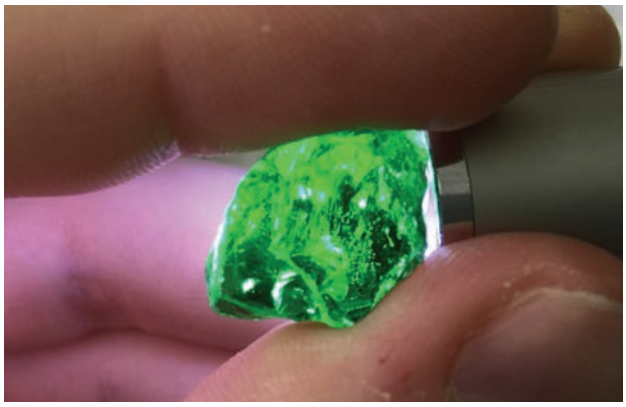

Figure 33: This large (~7 g) piece of tsavorite displays an excellent medium green colour and a good shape for cutting. Photo by B. Bridges.

Kenya Police. There is a strong push by a large Kenyan organized crime syndicate to take over the tsavorite mining region in southern Kenya. Our activities continue to be impacted by threats of violence similar to that which led to the murder of the mine's original owner, Campbell Bridges, in 2009.

With the mine finally in production once more, this represents a new chapter for tsavorite in Kenya, which has contributed to the excitement and optimism the gem industry shares for the future of the Bridges' mining operation. The family is hopeful that they will be able to continue with minimal outside interference and be allowed to further develop their tsavorite reserves.

Bruce Bridges (brucebridges@tsavorite.com)
Bridges Tsavorite, Tucson, Arizona, USA

Reference

Bridges B. and Walker J., 2014. The discoverer of tsavorite—Campbell Bridges—and his Scorpion mine. *Journal of Gemmology*, **34**(3), 230–241, http://dx.doi.org/10.15506/jog.2014.34.3.230.

Figure 34: The graduated and calibrated round brilliants in this tsavorite suite range from 3.5 to 8.5 mm for the necklace stones, and the matched pair has a total weight of 10.76 ct. Photo by Jeff Scovil for Bridges Tsavorite.

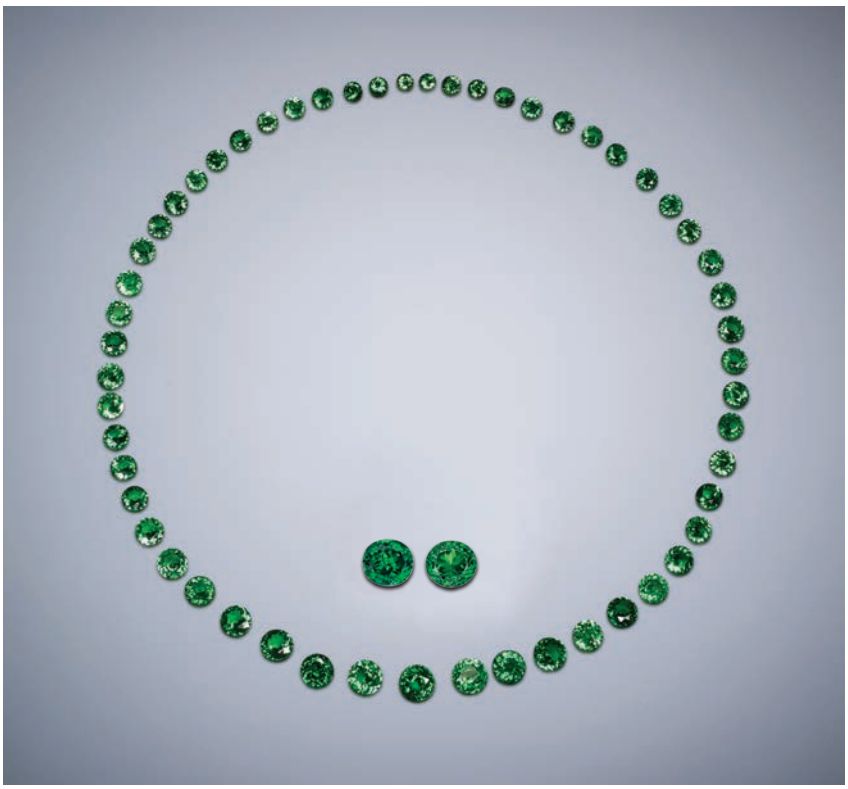

PEARLS

Natural Mussel Pearls from the Philippines

In the Philippines, the brown mussel (*Modiolus philippinarum*) is harvested for food on a subsistence basis, and also has been used as an inexpensive source of aquaculture feed (e.g. Napata and Andalecio, 2011). Natural mussel pearls from *Modiolus philippinarum* are virtually unknown in the gem trade, and it was therefore surprising to see hundreds of them during the 2016 Tucson gem shows with one pearl dealer, K.C. Bell (KCB Natural Pearls, San Francisco, California, USA). Bell reported collecting the pearls from his Philippine supplier for at least 10 years. All of them were drilled and strung, and he divided them into three general varieties (e.g. Figure 35) consisting of the following pieces:

1. Black round
   - Three lines: each ~17.5″ (44.5 cm) long, 1.0–5.3 mm diameter, 65.86 ct total weight
   - Two tassels: each 2″ (5.1 cm) long, 3.0–6.5 mm diameter, 54.75 ct total weight
2. Black baroque
   - Two lines: each ~16″ (40.6 cm) long, 2.0–9.4 mm diameter, 150.76 ct total weight
   - Two tassels: each 2.5″ (6.4 cm) long, 2.0–9.5 mm diameter, 74.00 ct total weight
3. Mauve (mostly baroque)
   - Two lines: each ~18″ (45.7 cm) long, 1.5–6.0 mm diameter, 90.67 ct total weight
   - One graduated line: 4.61″ (11.7 cm) long, 2.0–5.3 mm diameter, 10.62 ct total weight
   - Two tassels: each 2.5″ (6.4 cm) long, 1.5–3.0 mm diameter, 73.72 ct total weight

The 'black' pearls were mostly medium-to-dark purple with some light-coloured pieces (particularly among the rounds) in various purple, blue and golden shades. Overtones of pink and lavender were visible in some of the rounds. The mauve pearls consisted of light-to-medium shades of cream, brown and grey, with silver overtones. Various surface features included dimples and wrinkles; only a few circled pearls were present.

Although *Modiolus philippinarum* pearls are rarely encountered, this collection shows how large numbers can be amassed over a long time.

Brendan M. Laurs FGA

Reference

Napata R.P. and Andalecio M.N., 2011. Exploitation and management of brown mussel (*Modiolus philippinarum*) resources in Iloilo, Philippines. *Philippine Journal of Social Sciences and Humanities*, **16**(2), 22–34.

Figure 35: These are some of the natural pearls (up to 9 mm) collected in the Philippines from the brown mussel Modiolus philippinarum. *From left to right, pearl varieties have been classified into mauve, black round and black baroque. Photo by Jeff Scovil.*

An innovator in gemstone reporting

• Identification of colored gemstones • Country of origin determination • Full quality and color grading analysis

AMERICAN GEMOLOGICAL LABORATORIES AGL

580 5th Ave • Suite 706 • New York, NY 10036, USA
www.aglgemlab.com • +1 (212) 704 - 0727

First Circular & Call for Paper

Save your dates

GIT 2016

14 -15 November

"The Fullmoon of GemUnity"

The 5th GIT International Gem and Jewelry Conference

with Pre - and Post - Conference Excursions

PATTAYA, THAILAND

The Fullmoon of GEMUnity

November 14–15, 2016, Pattaya, Thailand

Conference Dates:

November 14-15, 2016: Technical session, oral & poster presentations
November 9-13, 2016: Pre-conference excursion to the legendary Mogok gem deposits, Myanmar
November 16-18, 2016: Post-conference excursion to Chanthaburi, the world's capital of colored stones & Trat, home of the renowned Siamese Ruby

Venue:

Pattaya, the world's premiere beach resort, Thailand
Special rates offered for accommodations
Further information announced on the GIT website

Important Dates

- Topics submission by May, 2016
- Extended abstract submission by August, 2016

Themes:

- Gem & precious metal deposits, exploration and responsible mining
- Bangkok rendezvous of the World's Ruby
- Innovation identification & characterization
- Treatment & synthetics update and disclosure
- Gem quality standards & gem optics and color science
- Jewelry trend & design
- Manufacturing & cutting edge technology
- Ethical, policy & good governance issues
- World gem & jewelry trading and ASEAN market

Registration Fees:

- Early bird USD 200, after Sep 30 USD 300
- Student USD 100, after Sep 30 USD 150
- On-Site USD 350
- *Pre-conference excursion to Mogok USD 1,800 or less (Air ticket to Mandalay and Visa for Myanmar excluded)
- *Post-conference excursion to Chanthaburi & Trat, Thailand USD 300
  (*Limited seats available for excursion only on the first come first serve basis)

Highlights:

- Keynote addresses by top-notched speakers
- Creative forums by top designers, gemologists and business leaders
- CSR from the mine to the market
- Global gem and jewelry networking
- Adventurous excursions to gem fields and historical sites
- Intimate gem community rendezvous

Secretariat Office:

Tel: +66 2634 4999 ext. 453
Email: git2016@git.or.th
Website: www.git.or.th

สถาบันวิจัยและพัฒนาอัญมณีและเครื่องประดับแห่งชาติ (องค์การมหาชน)
The Gem and Jewelry Institute of Thailand (Public Organization)

Characterization of Oriented Inclusions in Cat's-eye, Star and Other Chrysoberyls

Karl Schmetzer, Heinz-Jürgen Bernhardt and H. Albert Gilg

Milky-appearing alexandrite samples from Tanzania (Lake Manyara) and India (Kerala) were examined, as were chatoyant and asteriated chrysoberyl/alexandrite from India (Orissa), Brazil, Madagascar and Sri Lanka, and also phenomenal synthetic alexandrite from Kyocera in Japan. Sixteen oriented thin sections were studied by a combination of optical microscopy, micro-Raman spectroscopy, and electron microprobe techniques employing backscattered electron (BSE) imaging, qualitative point analysis and Ti compositional mapping. Rutile was identified as needle-like inclusions and V-shaped platelets in planes perpendicular to the a-axis, elongated parallel to the c-axis, and parallel to symmetry-equivalent <011> directions. Additional structures consisting of rutile needles and/or channels in various samples were oriented parallel to the a-axis. Also observed were single or multiple-intergrown rutile platelets elongated parallel to the a-axis, and rutile platelets showing rectangular, L-shaped or zigzag cross-sections parallel to <012> directions. In a four-rayed star chrysoberyl, elongated ilmenite particles were oriented along the c-axis. Various optical effects such as a whitish appearance, asterism or chatoyancy are caused by, and depend upon, the presence, size and concentration of the combined different types of needle-like or platy inclusions.

The Journal of Gemmology, **35**(1), 2016, pp. 28–54, http://dx.doi.org/10.15506/JoG.2016.35.1.28

Background

The examination of needle-like mineral inclusions and elongated cavities or channels in gem materials has always been of interest to gemmologists because these features are responsible for chatoyancy and asterism in cabochon-cut samples. Identifying such inclusions, however, has often proved problematic since their dimensions are frequently below the resolution of gemmological microscopes (magnification up to 100×).

By analogy, numerous studies have dealt with the examination and identification of the needle-like precipitates in corundum (specifically Ti-doped synthetic and Fe- and Ti-bearing natural material). The different phases present as acicular inclusions have been characterized via transmission electron microscopy using electron diffraction and/or other micro-analytical techniques. The inclusions often have been described as twinned rutile needles, although the presence of rhombic or monoclinic

Figure 1: This pendant features a cat's-eye alexandrite, presumably from Sri Lanka, and is shown in daylight (left) and incandescent light (right). The stone measures 13.62 × 13.72 × 9.05 mm and weighs 14.52 ct. Courtesy of David Humphrey, Pacific Palisades, California, USA; photo by Erica and Harold Van Pelt.

TiO_2 phases and even the formation of Al_2TiO_5 have been reported as well (Phillips et al., 1980; Langensiepen et al., 1983; Moon and Phillips, 1991; Xiao et al., 1997; Viti and Ferrari, 2006; He et al., 2011).

Oriented structures in chrysoberyl, in contrast, have received less attention. It is evident from the observed optical phenomena that oriented inclusions are present in both cat's-eye (e.g. Figure 1) and star chrysoberyl. The chatoyancy has been ascribed to hollow channels or needle-like mineral inclusions such as rutile (Eppler, 1958), a view broadly repeated in standard gemmological texts. Through examinations involving a large number of samples from sources worldwide, a consistent orientation for these inclusions has been established. The needle-like or channel structures were found to be parallel to the crystallographic a-axis [100], with the single light band of the cat's-eye being observed perpendicular to the needle axis (Schmetzer and Hainschwang, 2012).

With respect to asteriated material, six-rayed natural chrysoberyl is almost unknown and only has been mentioned occasionally (Kumaratilake, 1997; McClure and Koivula, 2001), while four-rayed chrysoberyl is extremely rare, originating mostly from Sri Lanka (Schmetzer, 2010). In the latter material, the two intersecting light bands normally show different intensities, and the needle-like inclusions or channels that cause these bands have not been identified unequivocally.

In a study of cat's-eye and non-phenomenal chrysoberyls from Brazil, precipitates (exsolu-

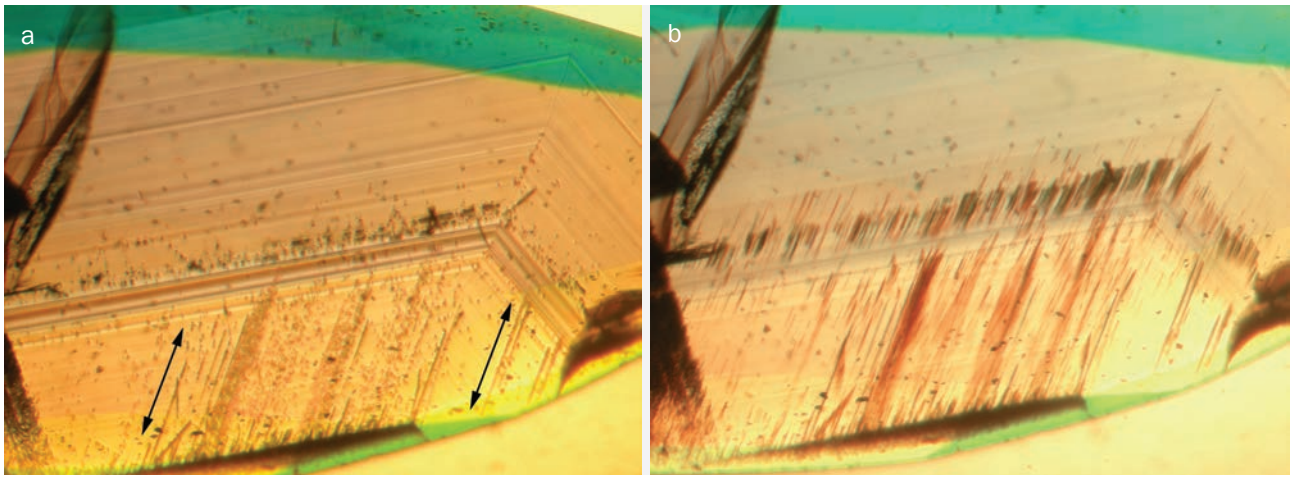

*Figure 2: This alexandrite from Lake Manyara, Tanzania, shows relatively large needle-like inclusions (rutile needles and/or channels) parallel to the a-axis. (a) In a view exactly parallel to the a-axis, the inclusions appear as small rounded dots forming sequences of parallel lines (indicated by arrows), and growth planes parallel to the **i** prism faces appear sharp. (b) In a view inclined to the a-axis, the elongate nature of the inclusions is visible. Immersion, field of view 2.7 × 2.0 mm; photomicrographs by K. Schmetzer.*

tions) of rutile were identified by electron diffraction and micro-analytical techniques in one chatoyant sample (Marder and Mitchell, 1982). The rutile inclusions were described as "elongated plates about 0.1 µm thick", but their orientation was not mentioned. Nonetheless, an analogy between chrysoberyl and corundum was proposed, with the three directions in chrysoberyl parallel to the c-axis [001] and parallel to <011> directions being equivalent to the three directions observed for rutile needles in corundum. (For an explanation of the nomenclature referring to crystallographic directions and their respective axes in chrysoberyl as employed in this article, see Box A.) More recently, two series of oriented inclusions described as rutile precipitates along **k** and **–k** {021} faces were studied by electron diffraction in a chrysoberyl from Brazil (Drev et al., 2015). The equivalent directions of those elongated structures would be <012>, and the maximum length of the precipitates was 0.05 µm. The relationship between the crystal structures of the chrysoberyl host and those of the rutile exsolutions was discussed in detail by Drev et al. (2015), but the dimensions of the precipitates in the direction parallel to the a-axis [100] has not yet been determined (Prof. A. Rečnik [Jožef Stefan Institute, Ljubljana, Slovenia], pers. comm., 2016).

Synthetic alexandrite grown by Kyocera of Japan shows three series of needle-like inclusions (most likely rutile exsolutions) lying in planes perpendicular to the a-axis; within these planes, the inclusions are oriented parallel to the c-axis [001] and to the **i** and **–i** {011} prism faces (Schmetzer et al., 2013), equivalent to orientations parallel to the [001] and <011> directions (see again Box A; for simplicity, this latter nomenclature convention will generally be used herein). Accordingly, the three different series of needles form angles of ~60° with each other.

Authors' Previous Work and the Aim of This Study

In alexandrite from the Lake Manyara deposit in Tanzania, various types of oriented inclusions are observed, mainly in milky-appearing crystals exhibiting pervasive cloudy whiteness throughout the entire piece, or in samples with alternating milky areas and transparent green growth zones. An initial study revealed that the inclusions are developed as needles or channels elongated parallel to the a-axis [100] and as small particles concentrated in planes perpendicular to the a-axis (Schmetzer and Malsy, 2011; see Figures 2 and 3). A polished thin section oriented almost perpendicular to the a-axis showed at high magnification three series of flattened needles or platelets oriented with their flat faces parallel to that plane.

In a subsequent study of a completely milky, translucent alexandrite crystal from Lake

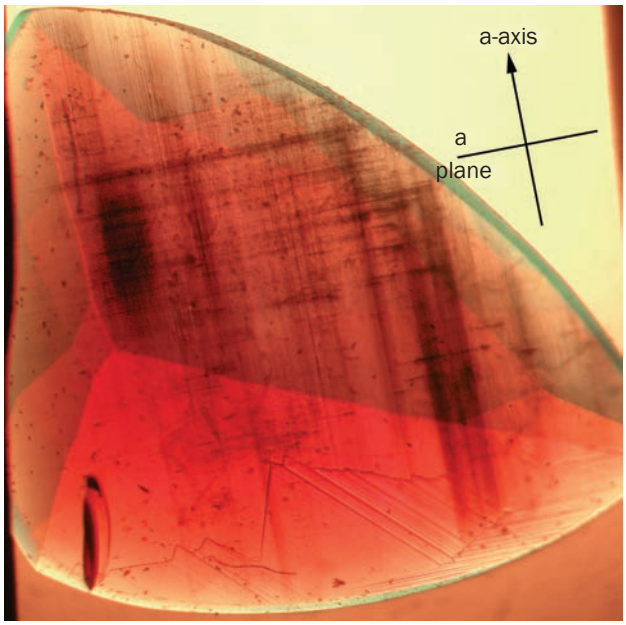

*Figure 3: Alexandrite (shown here) and chrysoberyl from Lake Manyara frequently contain areas with needles or channels oriented parallel to the a-axis, as well as minute inclusions in layers parallel to the **a** plane. View perpendicular to the a-axis, immersion, polarized light, field of view 4.5 × 4.5 mm; photomicrograph by K. Schmetzer.*

Manyara, polished thin sections were prepared in orientations perpendicular to the a-axis and almost perpendicular to the c-axis (Schmetzer and Bernhardt, 2012; Figures 4 and 5). The inclusion pattern observed in the section cut perpendicular to the a-axis (Figure 4) was similar to that described by Schmetzer and Malsy (2011), but like the earlier work, this study did not report the compositional nature of the inclusions.

The current examination was undertaken to further investigate the presence and nature of oriented inclusions in milky-appearing alexandrite from Lake Manyara. Moreover, this study offered an opportunity for wider applicability in understanding similar natural and synthetic materials. For instance, the inclusion pattern described above and pictured in Figure 3 is seen not only in material from Lake Manyara, but also in alexandrite from other localities (e.g. India). Therefore, this study was expanded in an effort to elucidate whether alexandrite/chrysoberyl from other locations might likewise show a pattern of oriented inclusions analogous to that observed in the Lake Manyara material. An example is presented here for semi-transparent samples from the state of Kerala in India.

Yet another opportunity to augment this inclusion study was afforded by chatoyant and asteriated material. As noted above, the elongated inclusions responsible for the chatoyancy in chrysoberyl from various sources were found to be parallel to the a-axis [100] (Schmetzer and Hainschwang, 2012). Additionally, from the orientation of the two intersecting light bands in natural four-rayed star chrysoberyl, presumably from Sri Lanka, it had been concluded that

Figure 4: In a thin section cut perpendicular to the a-axis, this alexandrite from Lake Manyara displays needle-like inclusions oriented in three directions. Intergrowths between two needles commonly form V-shaped angular structures or even triangular platelets. Transmitted light, field of view 120 x 90 µm; photomicrograph by H.-J. Bernhardt.

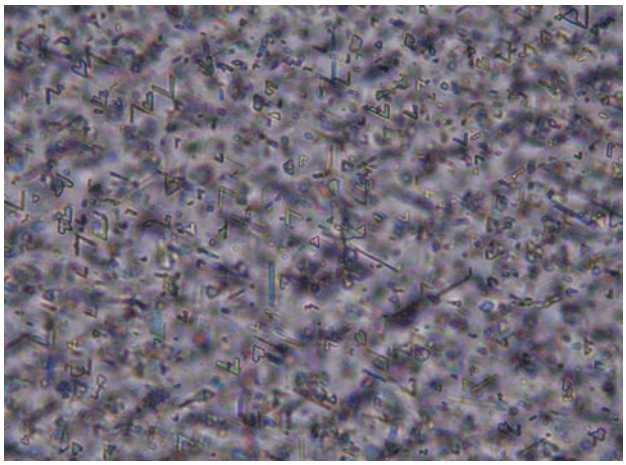

*Figure 5: In this view of a thin section cut approximately perpendicular to the c-axis, a Lake Manyara alexandrite has needle-like inclusions parallel to the a-axis. In some areas, other inclusions are concentrated on **a** (100) planes (perpendicular to the a-axis), and cross-sections of these inclusions are seen in this orientation of the thin section. Transmitted light, field of view 140 × 105 µm; photomicrograph by H.-J. Bernhardt.*

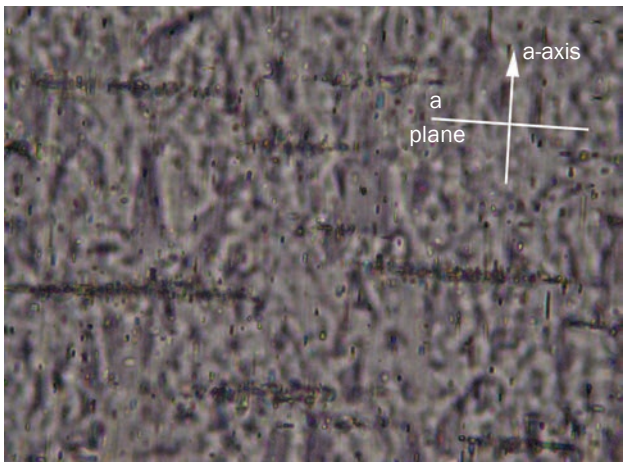

Box A: Nomenclature for Crystal Faces and Crystallographic Directions in Chrysoberyl

To facilitate understanding of the orientation of elongated inclusions (needle-like, channel or platelet structures) in chrysoberyl varieties, and especially to avoid excessive repetition in the text, this box gives a few general points about designating faces and directions in the orthorhombic crystal system.

The three crystallographic axes of chrysoberyl are normally indicated using the simple letters a, b and c. The three crystal faces perpendicular to these axes are correspondingly designated as **a**, **b** and **c**. A more detailed system of notation employing what are referred to as Miller indices in parentheses (hkl) specifies the faces perpendicular to the three axes as (100) for **a**, (010) for **b** and (001) for **c**. A similar notation involving three numbers in brackets [uvw] can be applied to the axes: [100] for the a-axis, [010] for the b-axis and [001] for the c-axis (Table A-1). For purposes of the present paper, cell dimensions of a = 4.42 Å, b = 9.39 Å and c = 5.47 Å were used for the three crystallographic axes.

All symmetry-equivalent faces of a crystal are referred to as a crystal form, and the faces of such a crystal form are symbolized using braces. For example, chrysoberyl has four symmetry-equivalent **i** (011) prism faces, i.e. (011), (01$\bar{1}$), (0$\bar{1}$1) and (0$\bar{1}\bar{1}$), which are identified by the symbol {011} for the crystal form equivalent to all four such crystal faces (Figure A-1).

Crystallographic directions other than the three crystal axes are also designated with the symbol [uvw]. They commonly represent edges between two crystal faces. There are, for instance, four symmetry-equivalent edges between the four **i** {011} prism faces and the **a** (100) pinacoid. These four edges [011], [01$\bar{1}$], [0$\bar{1}$1] and [0$\bar{1}\bar{1}$] are indicated jointly by the symbol <011>.

Table A-1: Oriented inclusions in chrysoberyl varieties; nomenclature of crystal faces and crystallographic directions.

Crystal Axes and Faces

Crystal axis	Symbol [uvw]	Cell dimensions (Å)	Face perpendicular to the crystal axis	Miller index (hkl)
a-axis	[100]	4.42	Pinacoid **a**	(100)
b-axis	[010]	9.39	Pinacoid **b**	(010)
c-axis	[001]	5.47	Pinacoid **c**	(001)

Needle-like Inclusions or Channels Parallel to Crystal Axes

Orientation	Symbol	Observed in chrysoberyl
‖ a-axis	[100]	Yes
‖ b-axis	[010]	No
‖ c-axis	[001]	Yes

Needle-like Inclusions or Rectangular Cross-Sections Parallel to the Edges Formed by Two Intersecting Crystal Faces

First face	Miller index (hkl)	Second face	Miller index {hkl}	Direction of crystal edges <uvw>	Angles between symmetry-equivalent crystal edges
Pinacoid **a**	(100)	Prism **i**	{011}	<011>	60.44° and 119.56°
Pinacoid **a**	(100)	Prism **k**	{021}	<012>	81.28° and 98.72°

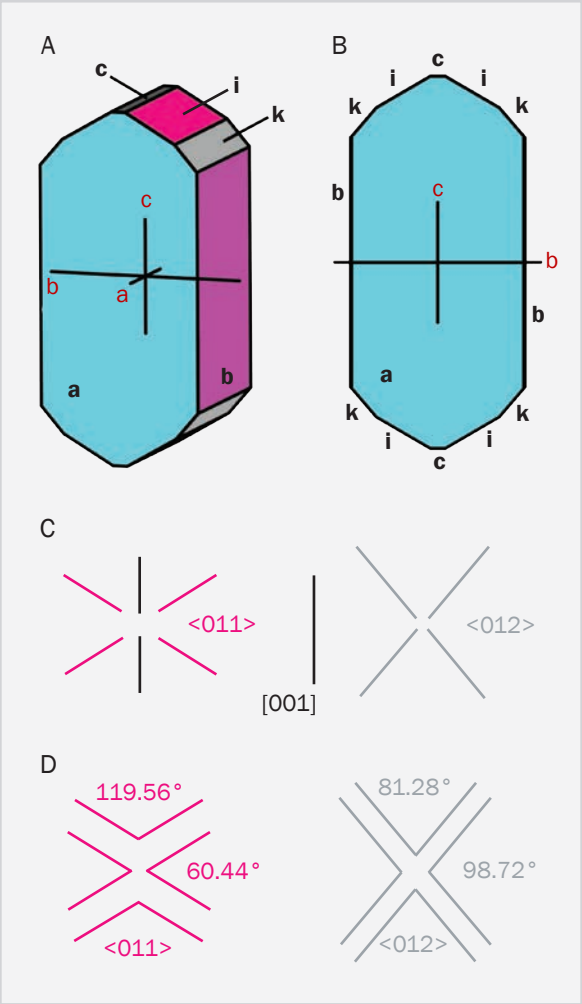

Figure A-1: This diagram shows the morphology of chrysoberyl and alexandrite crystals and the orientations of their acicular inclusions or platelets. Drawing A is an idealized clinographic projection of a crystal formed by the pinacoids **a** *{100},* **b** *{010} and* **c** *{001} in combination with the prisms* **i** *{011} and* **k** *{021}. Drawing B is a view of the same crystal parallel to the a-axis, representing the orientation of thin sections cut perpendicular to the a-axis. Part C displays the orientation of different series of needle-like inclusions in such thin sections, showing needles oriented parallel to the c-axis [001] and to the <011> directions (left), and cross-sections of flattened needles or elongated platelets parallel to the <012> directions (right). Part D depicts the possible orientations of intergrown structures or twins parallel to the <011> and <012> directions, giving the angles formed by the needles parallel to <011> and by the inclusion cross-sections parallel to <012>. All drawings by K. Schmetzer.*

Crystal edges between two faces with Miller indices $(h_1k_1l_1)$ and $(h_2k_2l_2)$ are easily calculated with the formula:

$$u = k_1 \bullet l_2 - l_1 \bullet k_2$$
$$v = l_1 \bullet h_2 - h_1 \bullet l_2$$
$$w = h_1 \bullet k_2 - k_1 \bullet h_2$$

In chrysoberyl, several series of needle-like inclusions, platelets of various shapes, channels and/or cross-sections of such structures are observed. Specifically, needles or channels lie parallel to the a-axis [100], parallel to the c-axis [001], and parallel to the edges between the **a** (100) pinacoid and the **i** {011} prism faces, symbolized by <011>. The cross-sections of flattened needles or narrow platelets elongated in the a-axis [100] direction are parallel to the four edges between the **a** (100) pinacoid and the **k** {021} prism faces, symbolized by <012>. All needles or channels parallel to the directions [001] or <011>, and the inclusion cross-sections parallel to <012>, are located within the **a** (100) plane or are observed in sections parallel to the **a** (100) plane. The various forms of needles, platelets or channels with cross-sections seen parallel to the a-axis [100] extend perpendicular to that plane.

Also in chrysoberyl, symmetry-equivalent needle-like inclusions parallel to <011> may be intergrown or twinned, forming angles of 60.44° and 119.56°. Flattened needles or platelets elongated parallel to the a-axis [100] with cross-sections parallel to <012> may also be intergrown, forming angles of 81.28° and 98.72°.

*Table I: Samples of chrysoberyl varieties containing oriented inclusions.**

Locality	Type	Sample no.	No. polished thin sections	Orientation of thin sections	Notes
Lake Manyara, Tanzania; alexandrite	Crystal	A	1	⊥ a-axis [100]	One Ti map; see also Schmetzer and Malsy (2011)
	Crystal	B	2	⊥ a-axis [100] ≈⊥ c-axis [001]	Two Ti maps; see also Schmetzer and Bernhardt (2012)
Kerala, India; alexandrite	Crystal	C	2	⊥ a-axis [100] ≈⊥ c-axis [001]	Two Ti maps
Kyocera, Japan; synthetic alexandrite (six-rayed star or cat's-eye according to cut orientation)	Cabochon	F	1	⊥ a-axis [100]	See also Schmetzer et al. (2013)
	Cabochon	G	1	⊥ b-axis [010]	
	Cabochon	H	1	⊥ b-axis [010]	
Orissa, India; cat's-eye chrysoberyl	Cabochon	E	2	⊥ a-axis [100] Perpendicular to the other section	
Brazil; cat's-eye chrysoberyl	Cabochon	I	1	⊥ a-axis [100]	
Ilakaka, Madagascar; cat's-eye chrysoberyl	Crystal	J	3	⊥ a-axis [100] ⊥ b-axis [010] ⊥ c-axis [001]	
Sri Lanka; star chrysoberyl (four-rayed)	Cabochon	D	2	≈⊥ b-axis [010] Perpendicular to the other section	Two Ti maps

* Groups of similar samples are highlighted in the same colour. All thin sections were 60 µm thick except for sample A, which was 20 µm thick.

the series of needles or channels causing the somewhat stronger light band was oriented parallel to the a-axis [100], while the second set of needles was found at a right angle to that direction, in the bc-plane (Schmetzer, 2010). Synthetic asteriated alexandrite, on the other hand, shows six rays when cabochons are cut with the base perpendicular to the a-axis (Schmetzer and Hodgkinson, 2011), and the formation of rutile precipitates in such crystals has been described in numerous patent applications (see the overview given by Schmetzer et al., 2013). In commercially available synthetic material grown Kyocera, the light bands of these six-rayed stars are formed by three series of needles in the **a** (100) plane.

Consequently, the present study delves into the apparent differences between cat's-eyes, four-rayed stars, and six-rayed stars, comparing chatoyant and asteriated natural and synthetic alexandrite/chrysoberyl samples.

Materials and Methods

Samples

Table I presents a summary of the samples and the orientation of the corresponding polished thin sections studied for this report. The thin-section orientations were chosen by taking into account the size and morphology of the samples, in combination with information available from the literature (especially from author KS's own studies cited above) on the inclusion directions.

The crystallographic orientation of the crystals, in turn, was determined by considering sample morphology and optical features such as growth structures, position of the optic axes and pleochroism (for alexandrite). The position of the crystallographic axes of the cabochon-cut samples was also established by optical examination, primarily by searching for both optic axes with the immersion microscope. To prepare thin sections of good transparency that

Figure 6: Alexandrite crystals and fragments from Lake Manyara frequently show a somewhat cloudy or milky appearance throughout the complete body of the samples or as alternating milky and transparent green growth zones. The tabular crystal at top-centre measures 9.6 × 6.8 mm. Daylight, photo by K. Schmetzer.

would contain sufficient oriented inclusions, a thickness of 60 µm was selected, which is larger than the sections typically used for petrographic studies (~25 µm).

With the goal of collecting more information about oriented needle-like inclusions in chrysoberyl and alexandrite, the present study started with crystals from Lake Manyara having milky-appearing areas (Figure 6) that were already known to contain such oriented inclusions. Three polished thin sections from two Lake Manyara alexandrites, which were previously prepared and examined by Schmetzer and Malsy (2011) and Schmetzer and Bernhardt (2012), were used. An alexandrite crystal presumably from the Trivandrum District in Kerala, southern India, was then selected for the preparation of two polished thin sections, based on observations of a somewhat similar whitish appearance (Figure 7) and a specific network of inclusions seen with the gemmological microscope. The exact source of this sample within the Trivandrum District is unknown, although alexandrites from various locations in the southern Indian states of Kerala and Tamil Nadu have been briefly mentioned in the literature (Menon et al., 1994; Manimaran et al., 2007; Fernandes and Choudhary, 2010).

Next, again drawing upon prior work that had indicated the existence of relevant oriented inclusions in material grown by the Japan-based company Kyocera, three polished thin sections with two different orientations were added to the present study; these had been prepared earlier for a study of cat's-eye and star synthetic alexandrites (see, e.g., Figure 8; Schmetzer et al., 2013).

Figure 7: These alexandrite crystals and fragments, presumably from the Trivandrum District, Kerala State, southern India, show a somewhat cloudy or milky appearance. The crystal in the upper right measures 8.4 × 4.2 mm. Daylight, photo by K. Schmetzer.

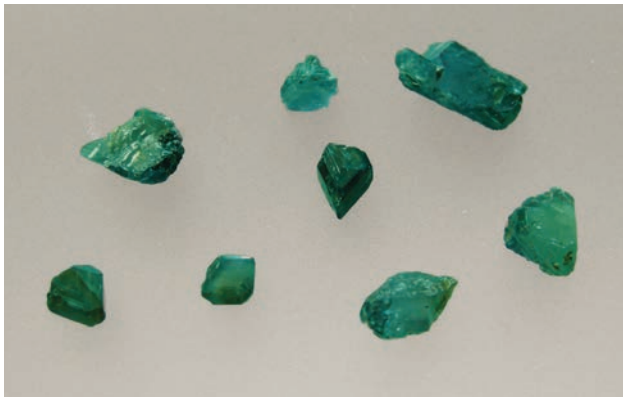

Figure 8: This six-rayed asteriated synthetic alexandrite produced by Kyocera weighs 1.63 ct and measures 8.3 mm in diameter. Daylight, photo by K. Schmetzer.

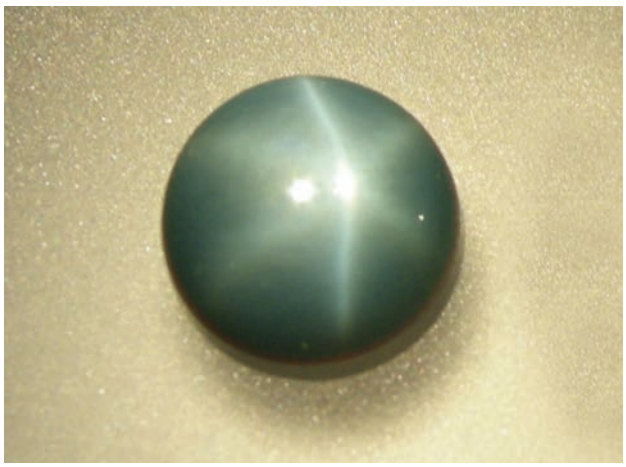

Figure 9: These cat's-eye chrysoberyl cabochons, presumably from Orissa State, India, range from 0.54 to 1.07 ct, and the smallest sample measures 5.0 × 3.7 mm. Incandescent light, photo by K. Schmetzer.

Figure 10: This cat's-eye chrysoberyl from Brazil weighs 1.38 ct and measures 5.9 × 5.8 mm. Incandescent light, photo by K. Schmetzer.

Then, operating on the premise that natural cat's-eye and star chrysoberyl should also contain at least one or two series of needle-like inclusions, a cat's-eye cabochon from a group of chrysoberyls (Figure 9) presumably from the state of Orissa, India (see Fernandes and Choudhary, 2010), was selected for the preparation of two oriented polished thin sections.

To characterize the inclusion pattern of a natural cat's-eye chrysoberyl from a second source, we used a transparent, high-quality cabochon (Figure 10) from one of the numerous Brazilian occurrences (see, e.g., Cassedanne and Roditi, 1993). This sample was sliced parallel to the sharp light band.

Because cat's-eye chrysoberyl is also known from the famous gem mining area of Ilakaka, Madagascar (Milisenda et al., 2001), this study was further supplemented by a milky-appearing, only slightly translucent chrysoberyl crystal from that locality. Oriented thin sections were prepared in all three directions perpendicular to the crystal axes of this sample. Additionally, after the three slices had been removed, the edges of the remaining portion were ground and the surface was polished. The resulting irregularly shaped but rounded sample resembled a tumble-polished pebble, and a strong light band completely encircled its surface.

Finally, the authors were allowed to cut a 1.9-mm-thick slice from a four-rayed star chrysoberyl cabochon from Sri Lanka (top-right sample in Figure 11), despite the fact that such samples are extremely rare and normally not available for destructive examination. The removal of this slice from the base did not influence the visual appearance of the stone after cutting, and the slice was used to prepare two oriented polished thin sections.

Figure 11: In these four-rayed star chrysoberyls, presumably from Sri Lanka, the b-axis of the crystals is almost perpendicular to the base of the cabochons. The weight of the samples ranges from 4.49 to 10.37 ct, and the cabochon at the lower right weighs 6.25 ct and measures 9.6 × 9.3 mm. A slice of the cabochon in the upper right was used for the preparation of two thin sections (sample D). Incandescent light, photo by K. Schmetzer.

Methods

To resolve acicular inclusions and small platelets, all thin sections were examined at higher magnification (up to 1,000×) than normally applied in gemmology, in both reflected and transmitted light, using a Leitz Ortholux II Pol-BK polarizing microscope or a Leica DM LM polarizing microscope.

Because previous work (especially on corundum but also on some natural or synthetic chrysoberyls; see references cited above) suggested that Ti-bearing phases might play an important role in forming acicular inclusions, multiple techniques were employed using a Cameca SX 50 electron microprobe to evaluate the chemical nature of the inclusions. Preliminary qualitative point analyses of individual inclusions, guided by BSE images (which depict differences in mean atomic mass as variations in brightness levels), were performed for several inclusions that were clearly exposed at the surface of the polished thin sections. In addition, X-ray compositional maps for Ti were obtained by scanning seven of the thin sections, to which a carbon coating had been applied. BSE images of certain scanned areas were taken as well. The Ti-mapped areas consisted of 512 × 512 analytical points (pixels) with a step-width (point distance) of 0.119 µm, which resulted in a scanned area of ~61 × 61 µm consisting of 262,144 points for each compositional map. To achieve the greatest possible resolution, the maximum available focus of the electron beam (~1 µm in diameter) was used. The measurement time per pixel was 140 ms, the beam current was 20 nA and the acceleration voltage was 15 kV.

Quantitative microprobe analyses of the host chrysoberyl also were obtained from samples from both localities in India (Kerala and Orissa) to further characterize material obtained from the trade.

The mineral phases forming the Ti-bearing inclusions in all of the samples were analysed by micro-Raman spectroscopy using a Horiba Jobin Yvon XploRA PLUS confocal Raman microscope. The spectrometer was equipped with a frequency-doubled Nd:YAG laser (532 nm, with a maximum power of 22.5 mW) and an Olympus 100× long-working-distance objective with a numerical aperture of 0.9. The measurements were performed with a 1,200 mm^{-1} grating, a 300 µm pinhole and a 100 µm slit. Two accumulations of 5 sec counting time were used for each spectrum.

Results

The numerous Ti-bearing needles, narrow rectangular platelets, V-shaped and triangular platelets, and L-shaped and zigzag clusters examined by micro-Raman spectroscopy in combination with microprobe analysis were identified as rutile, on the basis of four characteristic bands at ~142 cm^{-1} (weak), ~239 cm^{-1} (medium), ~445 cm^{-1} (very strong) and ~611 cm^{-1} (very strong) [Figure 12a; see, e.g., Porto et

Figure 12: Raman spectra are shown for a rutile inclusion in chrysoberyl from Ilakaka, Madagascar (a), and for an ilmenite inclusion in asteriated chrysoberyl from Sri Lanka (b). Spectra from the host chrysoberyl are shown for both samples for comparison.

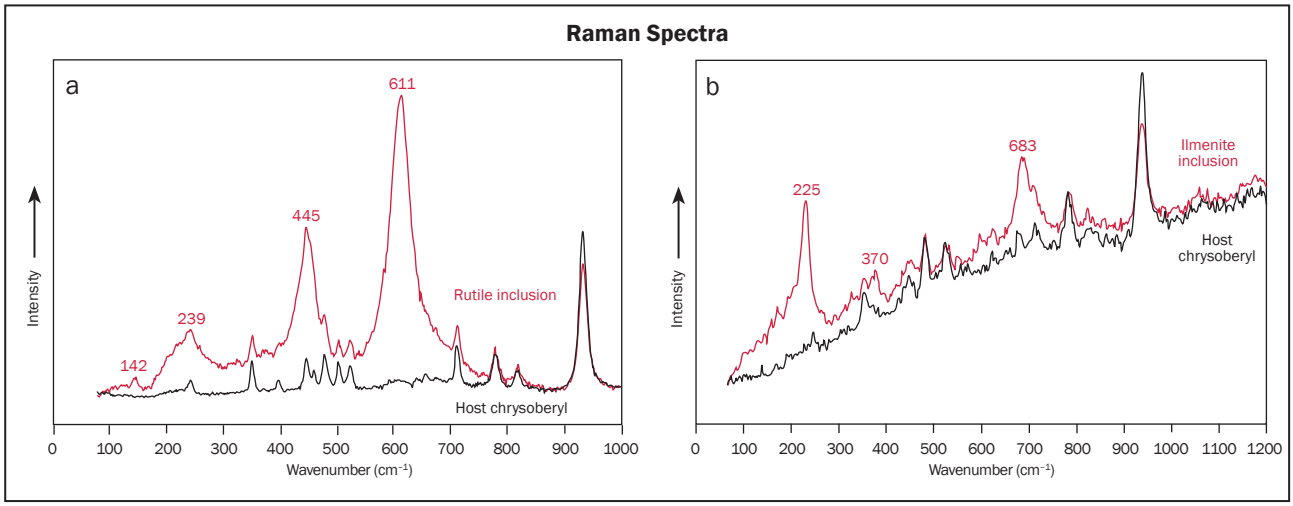

Table II: Oriented needle-like inclusions or platelets in chrysoberyl varieties.[a]

Locality and variety	Sample no.	Orientation of inclusions, optical microscopy						
		Single needles in **a** (100) plane		Single needles, channels or platelets elongated parallel to [100]		Intergrown structures		
		Elongation parallel to [001][b]	Elongation parallel to <011>	Cross-sections parallel to <012>, forming narrow rectangles (single 'stripe')	Cross-sections rounded or rectangular	Elongation parallel to <011>, forming V-shaped or triangular platelets	Elongation parallel to <011> and [001]	Elongation parallel to [100], with cross-sections parallel to <012>, forming L-shaped and zigzag platy clusters (multiple 'stripes')
Lake Manyara, Tanzania; alexandrite	A	Common	Common		Common	Common		
	B	Common	Common		Common	Common		
Kerala, India; alexandrite	C	Rare	Common	Rare	Larger channels	Common		Rare
Kyocera, Japan; synthetic alexandrite (six-rayed star or cat's-eye according to cut orientation)	F, G, H	Common	Common			Common	Rare	
Orissa, India; cat's-eye chrysoberyl	E	Very rare	Rare	Rare		Rare	Very rare	Common
Brazil; cat's-eye chrysoberyl	I	Rare	Rare		Common	Rare		
Ilakaka, Madagascar; cat's-eye chrysoberyl	J	Common	Common	Common		Common		Rare
Sri Lanka; star chrysoberyl (four-rayed)	D	Common			Common			

[a] Dominant inclusions of a similar type are highlighted in the same colour.

[b] Larger growth tubes parallel to the c-axis [001] are occasionally observed in chrysoberyl and alexandrite from various locations, but such channels were not seen in the present samples (see, e.g., Schmetzer and Krzemnicki, 2015).

al., 1967]. Only the inclusions in the four-rayed star chrysoberyl from Sri Lanka were identified as ilmenite needles based on Raman bands at ~225 cm^{-1} (very strong), ~370 cm^{-1} (weak) and ~683 cm^{-1} (very strong) [Figure 12b; cf. Wang et al., 2004].

Other than for the ilmenite, the Raman spectra were all more-or-less identical and indistinguishable from the spectra for rutile available in the literature. No other crystalline TiO_2 phases were detected. Therefore, the Ti-bearing particles, which were also characterized extensively by microscopy in combination with microprobe analysis, are in general designated herein simply as rutile.

Moreover, as a preface to describing observations for different samples in detail, it should be mentioned that additional orientations of needles or platelets or of cross-sections of flattened inclusions were encountered beyond those described below, especially in the sample from Kerala, India. However, we would need to study thin sections cut in different orientations to fully characterize these additional inclusion types.

A summary of the results discussed below is presented in Table II.

Alexandrite from Lake Manyara, Tanzania

Alexandrite from Lake Manyara was described in detail by Schmetzer and Malsy (2011), and the oriented inclusions were examined by Schmetzer and Bernhardt (2012). As reported in those publications, both of the polished thin sections cut perpendicular to the a-axis showed needle-like to plate-like structures (Figure 4). In samples A and B, three series of single elongated needles were observed in directions parallel to the c-axis [001] and parallel to <011>, forming angles of ~60° with each other (Figure 13). Frequently, two needles parallel to the <011> directions were intergrown or twinned, forming acute-angled, V-shaped platelets with re-entrant angles measuring ~60°. Due to the differing dimensions and thicknesses of the needles within the **a** (100) plane, the open space between the two sides of these V-shaped structures varied widely. Some exhibited large spaces between the arms; others were essentially triangular platelets with almost no interstitial space. Obtuse-angled

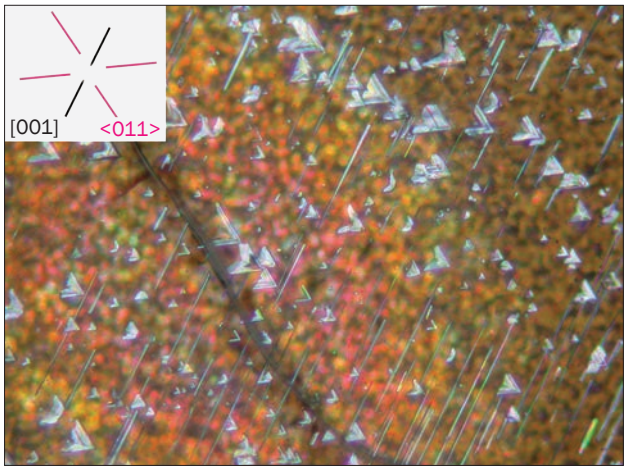

Figure 13: In a thin section cut perpendicular to the a-axis of alexandrite from Lake Manyara (sample B), elongated inclusions are observed in three different orientations parallel to [001] and <011>. Some of the needles or elongated inclusions parallel to <011> meet at one end, forming V-shaped angular structures or triangular platelets. View parallel to the a-axis, reflected light, field of view 140 × 105 µm; photomicrograph by H.-J. Bernhardt.

structures consisting of two intergrown needles forming angles of ~120° were rare. Intergrown needles comprising crystals elongated parallel to one <011> direction and parallel to the c-axis [001] were not seen in the Lake Manyara material during the investigations to date.

No systematic distribution for these different structures was apparent in the crystals examined. Some areas within the same crystal showed mainly single needle-like features, while other zones contained primarily angular structures of two intergrown or twinned needles/platelets. In still other areas of the crystal, both types of structures were observed together.

Qualitative point analyses of surface-reaching inclusions indicated only Ti as the main element. For the compositional mapping of Ti by the electron microprobe, areas were selected within the thin sections that in transmitted and reflected light showed numerous inclusions, including both single needles and intergrown structures (Figure 14a). The distribution of Ti correlated well with bright spots in BSE images of the same areas; several needles and acute-angled structures were observed within the surrounding chrysoberyl matrix (Figure 14c,e), representing the section perpendicular to the a-axis, sample B). Weaker Ti signals corresponding to several

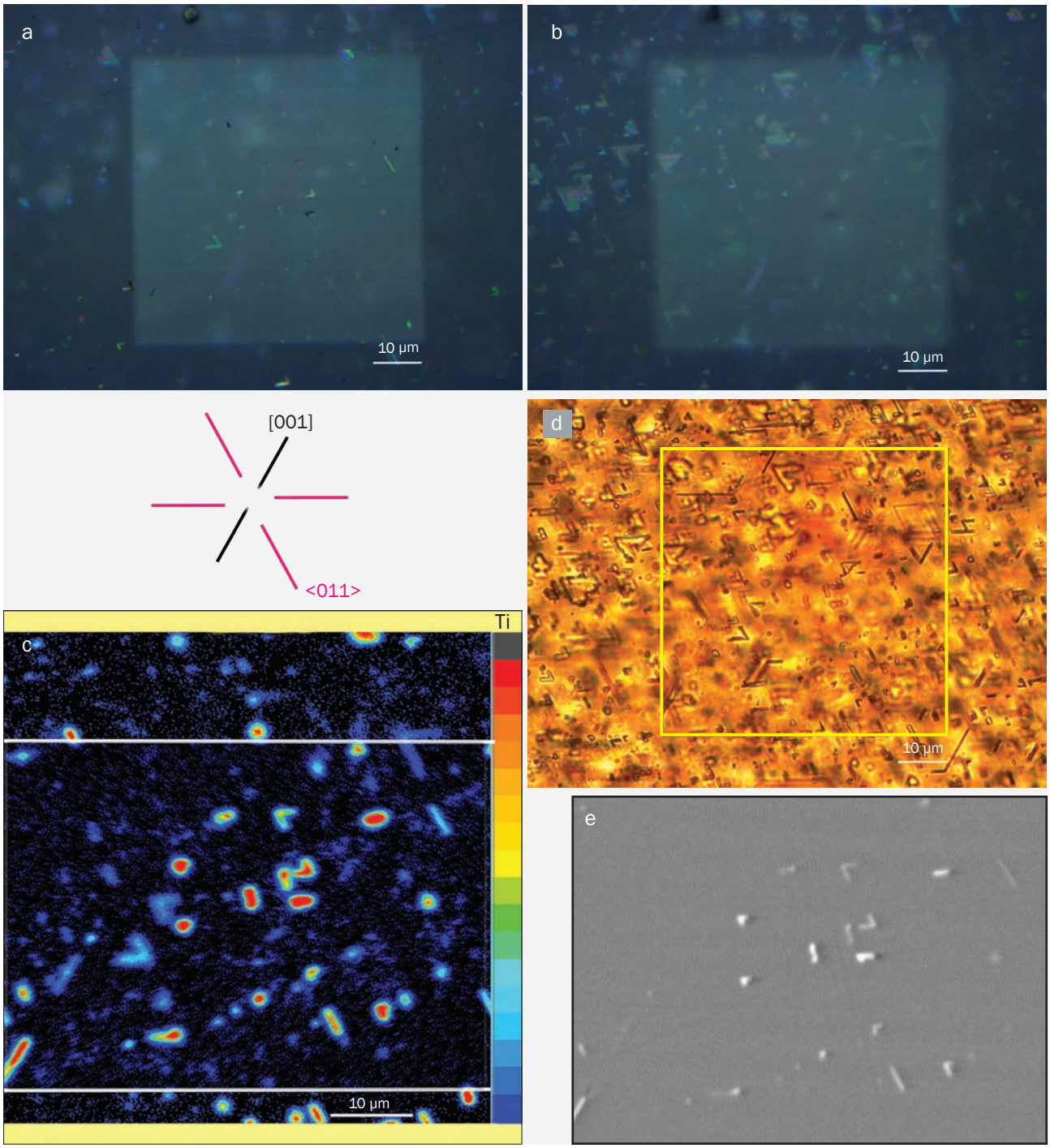

Figure 14: In a thin section cut perpendicular to the a-axis of alexandrite from Lake Manyara (sample B), elongated inclusions are observed in photomicrographs in reflected light (a,b) and in transmitted light (d) compared to a Ti compositional map (c) and a BSE image (e). The scanned area measuring ~61 × 61 µm is clearly seen in reflected light due to the alteration of the carbon coating from the electron beam of the microprobe. In reflected light, the surface of the sample (a) shows rutile needles and V-shaped platelets that are also represented in the Ti compositional map (c). Focusing the optical microscope below the surface of the thin section (b) shows inclusions that generally are not seen in the Ti map. In transmitted light (d), inclusions both at the surface and below are seen. The BSE image (e) shows only rutile needles and V-shaped rutile platelets exposed at the surface of the thin section. The compositional map (c) shows Ti signals corresponding to these inclusions, as well as somewhat weaker Ti signals for inclusions located within the chrysoberyl host, but close to the surface. The scanned area (c) is outlined in (a), (b) and (d); the area of the BSE image (e) is outlined in (c); the intensity of the Ti signal in (c) ranges from weak (blue) to strong (red). Field of view ~112 × 84 µm (a,b,d); photomicrographs and Ti map by H.-J. Bernhardt.

needles and acute-angled structures also were seen within the X-ray map, indicating inclusions not exposed at, but close to, the surface of the chrysoberyl host.

After the Ti compositional mapping was complete, the scanned area remained clearly outlined in the carbon coating in reflected light (Figure 14a,b). It was therefore possible to directly compare the microscopic view in transmitted/reflected light with the BSE image (Figure 14e) and the Ti compositional map (Figure 14c). When the optical microscope was focused on the surface of the sample (Figure 14a), the pattern of inclusions observed in reflected light closely resembled that seen in the BSE image, and these inclusions provided relatively strong Ti signals in the compositional map (Figure 14c). However, if the optical microscope was focused some microns further below the surface, a completely different inclusion picture was revealed in reflected light, consisting of needles and platelets located entirely within the chrysoberyl host (Figure 14b). Most of these inclusions were not indicated in the Ti map. In transmitted light, a denser pattern of inclusions was visible (Figure 14d) that could thus be characterized as an overlap or summation of the inclusions seen in reflected light at various depths within the polished thin section. All these needles or platelets proved to be rutile by Raman analysis, with the individual needles or platelets having—in the direction of the a-axis—a thickness in the range of 1–2 µm or even smaller.

The microscopic features of the thin section of sample B that was cut almost perpendicular to the c-axis revealed two principal types of inclusions: (1) those concentrated in planes perpendicular to the a-axis, and (2) tiny needle-like structures, sometimes slightly flattened, running parallel to the a-axis [100] (Figure 5). For the former type of inclusions, the BSE image depicted numerous single bright spots, and occasionally somewhat elongated points or short lines. The compositional map also showed a high concentration of Ti in these areas. Raman spectroscopy of several highly reflective particles with almost square or rectangular (sometimes slightly rounded) cross-sections yielded clear rutile spectra.

Conversely, the needle-like structures running parallel to the a-axis [100]—the second type of inclusions—were not clearly resolved in the Ti map. However, micro-Raman spectroscopy of numerous tiny needles with this orientation showed rutile spectra for some of them. Others revealed only spectra of the chrysoberyl host, which might indicate that these needles were simply too small for the Raman technique applied or that the structures were channels.

The orientation of the thin section cut almost perpendicular to the c-axis (Figure 5) is a rectangular slice through the section shown in Figures 13 and 14. If rutile needles with a thickness in the micrometre range (see above) are cut in such a way, their representation on the Ti map would be single points. If triangular rutile platelets are cut in this way, the Ti map would show small lines. Both types of reflective structures were identified as rutile by Raman spectroscopy.

The lack of any Ti-related features in the compositional map corresponding to the tiny needle-like structures running parallel to the a-axis [100] indicates either (1) that any Ti signals from these inclusions were below the resolution of the microprobe, if in fact these needles were rutile and exposed to the surface, or (2) that only channels were present. Nonetheless, the Raman examination showed, at least for some of these small needles, that they were indeed rutile. Consequently, the presence of tiny rutile needles parallel to the a-axis [100] was established, but the additional presence of channels in the same direction could not be ruled out.

The observations from optical microscopy, BSE imaging and Ti compositional mapping for sample A from Lake Manyara, obtained from a thin section cut perpendicular to the a-axis, generally showed results similar to those of sample B with the same orientation and therefore are not repeated here. Additionally, in one area of the thin section, cross-sections of needles or channels elongated parallel to the a-axis [100] were observed (Figure 15), appearing in this orientation as parallel lines comprising individual somewhat rounded structures. In reflected light, some of these structures were highly reflective and could be identified as rutile by Raman spectroscopy. However, as with the results just described for sample B, it is possible that channels having the same orientation might also be present.

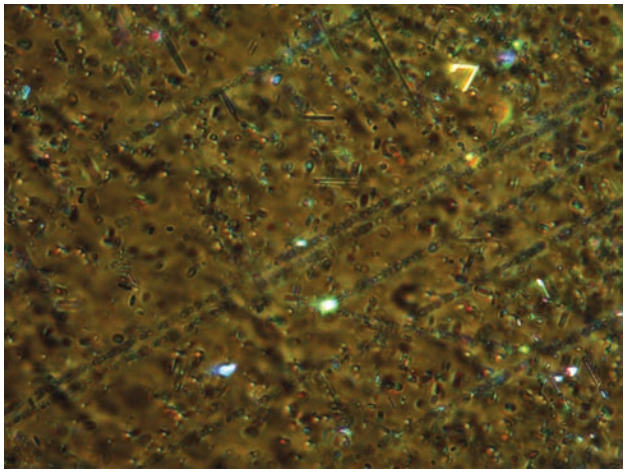

Figure 15: Cross-sections of several sequences of needle-like inclusions are seen in a thin section cut perpendicular to the a-axis, in alexandrite from Lake Manyara (sample A). The individual somewhat rounded cross-sections form numerous parallel lines. Some of these inclusions are highly reflective and were identified as cross-sections of rutile needles. Reflected light, crossed polarizers, field of view 167 × 125 µm; photomicrograph by H.-J. Bernhardt.

Alexandrite from Kerala, India

Alexandrite from Trivandrum in the Kerala State of southern India has been mentioned in the literature, but a detailed description is unknown to the present authors. The material available for this study comprised primarily broken crystal fragments, along with a few complete crystals and some tabular contact twins. Microprobe analyses of six samples of this alexandrite yielded 0.25–0.85 wt.% Cr_2O_3, 0.03–0.05 wt.% V_2O_3 and 0.81–1.35 wt.% Fe_2O_3.

In the gemmological microscope, most samples showed a distinct network of fine needle-like inclusions oriented parallel to the <011> directions (Figure 16). Furthermore, a dense series of needles or channels parallel to the a-axis [100] was present in most samples. A similar inclusion pattern has been described for some alexandrite from Sri Lanka and Madagascar (Schmetzer, 2010).

Examination of the two polished thin sections at higher magnification, in combination with Ti compositional mapping by electron microprobe, showed a number of similarities with the Lake Manyara material. In the thin section oriented perpendicular to the a-axis, Ti-bearing needles or platelets were present, and the inclusion pattern differed substantially depending on whether the focus was at the surface of the thin section (Figure 17a) or slightly below the surface (Figure 17b). The Ti map (Figure 17c), which represented only the surface of the thin section, registered three relatively large rutile needles within the chrysoberyl host. Transmitted light provided a composite view of inclusions at multiple depths within the sample (Figure 17d). Several of these inclusions were identified as rutile by micro-Raman spectroscopy.

Most of the rutile needles were elongated parallel to the <011> directions of the host (Figures 17 and 18). Needles parallel to the c-axis [001] were occasionally present, but less commonly than in the Lake Manyara material. Moreover, the needles and platelets in the sample from Kerala were larger than in material from Lake Manyara, although they, too, were up to 1–2 µm thick in the direction parallel to the a-axis [100]. The pleochroism, as observed in different parts of the rutile platelets or V-shaped rutile crystals (Figures 18 and 19), established that the inclusions consisted of two different parts with different crystallographic orientations.

Figure 16: Observed parallel to the a-axis (as shown by inset), an alexandrite from Kerala State, India, reveals a dense network of needle-like structures parallel to the <011> directions. Immersion, field of view 2.7 × 3.6 mm; photomicrograph by K. Schmetzer.

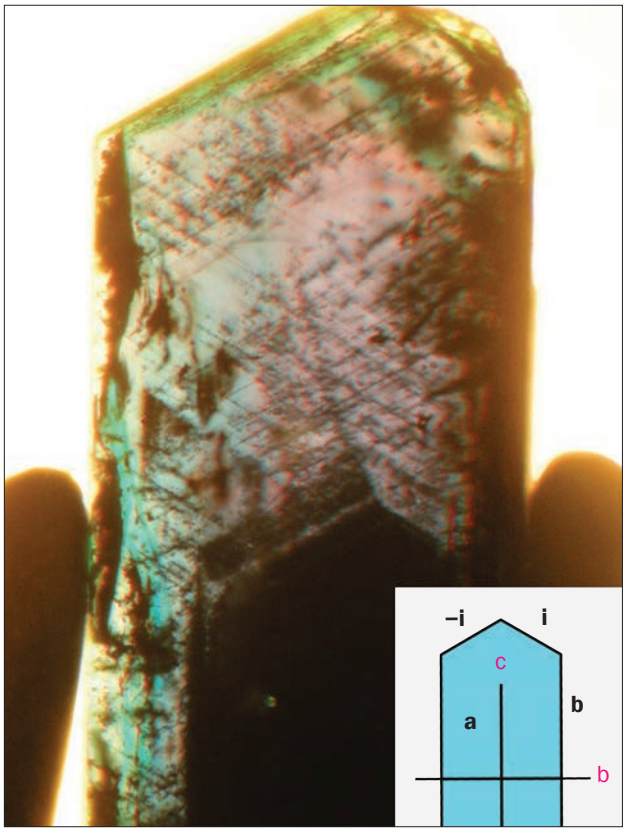

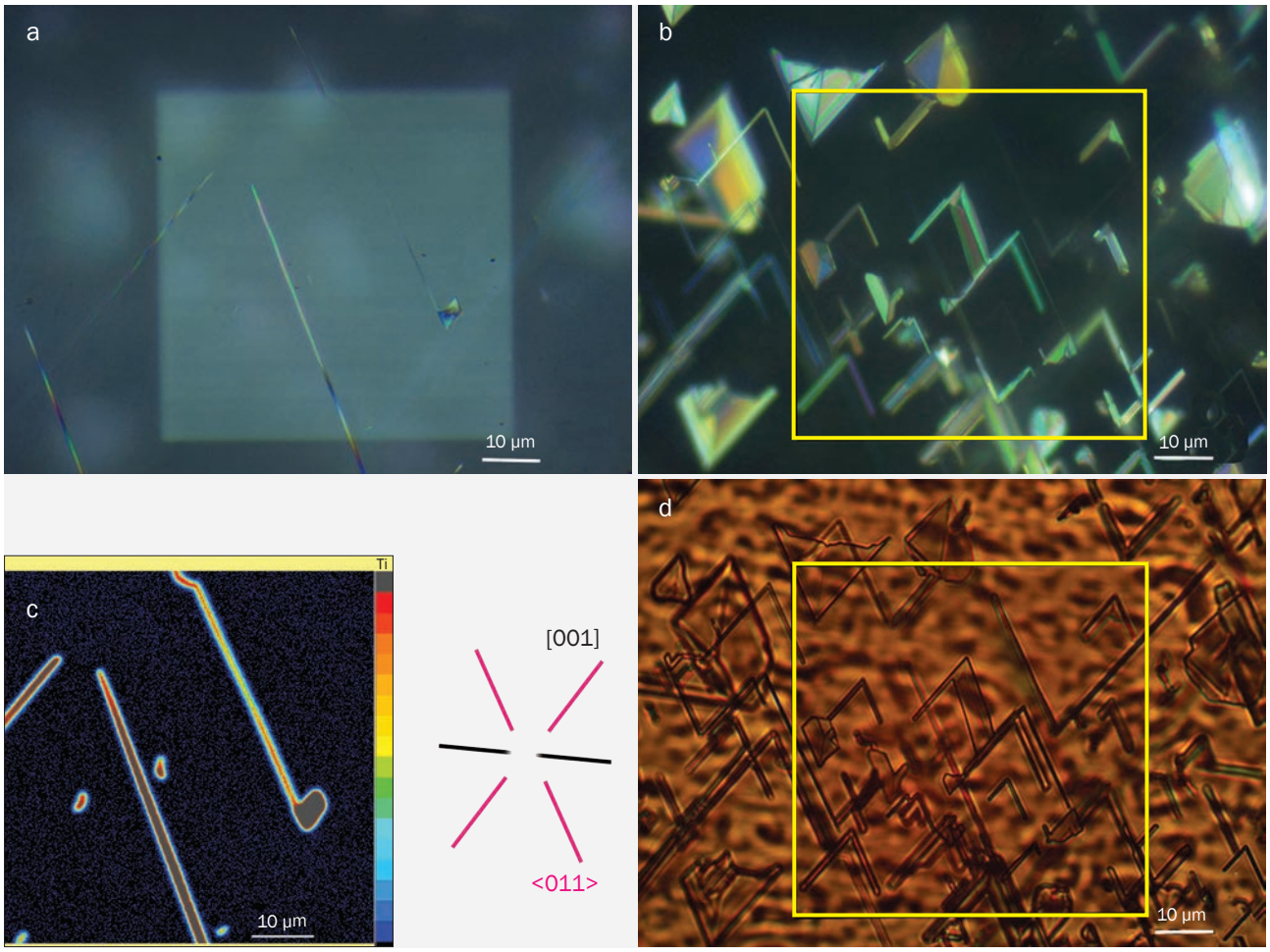

Figure 17: An alexandrite from Kerala (sample C), cut perpendicular to the a-axis, is shown in reflected (a,b) and transmitted light (d) compared to the Ti compositional map (c). In reflected light, the view of the surface of the sample (a) shows the scanned area (measuring ~61 × 61 µm), with rutile needles that are also represented in the Ti distribution map (c). Focusing the optical microscope slightly below the surface of the thin section with crossed polarizers shows inclusions (b) that generally are not observed in the Ti distribution map. In transmitted light (d), inclusions both at the surface and at various depths below the surface are seen. The scanned area (c) is outlined in (a), (b) and (d); the intensity of the Ti signal in (c) ranges from weak (blue) to strong (red). Field of view ~112 × 84 µm; photomicrographs and map by H.-J. Bernhardt.

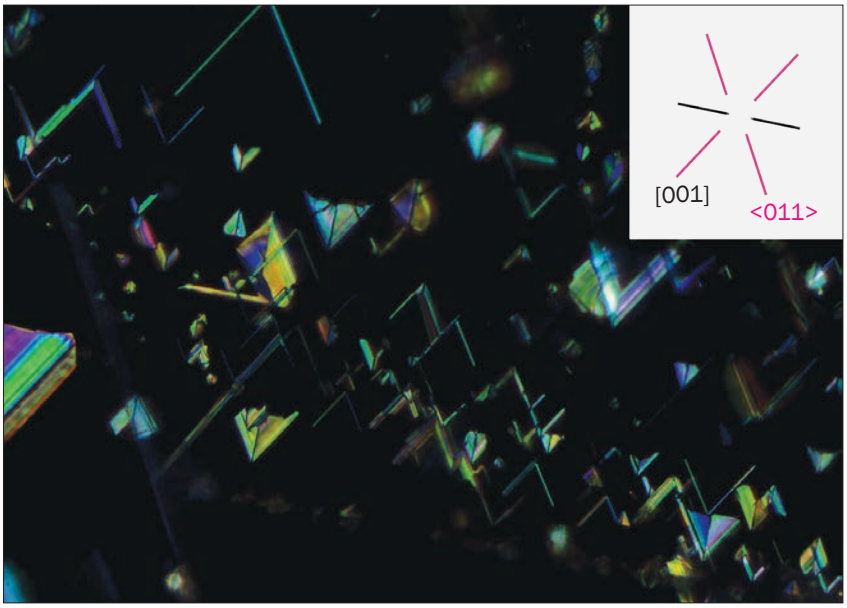

Figure 18: An alexandrite crystal from Kerala, cut perpendicular to the a-axis (sample C), shows elongated rutile inclusions in different orientations parallel to <011>. Some of them meet at one end, forming V-shaped angular structures or platelets; single needles parallel to the c-axis are only rarely seen. View parallel to the a-axis, reflected light, crossed polarizers, field of view 224 × 160 µm; photomicrograph by H.-J. Bernhardt.

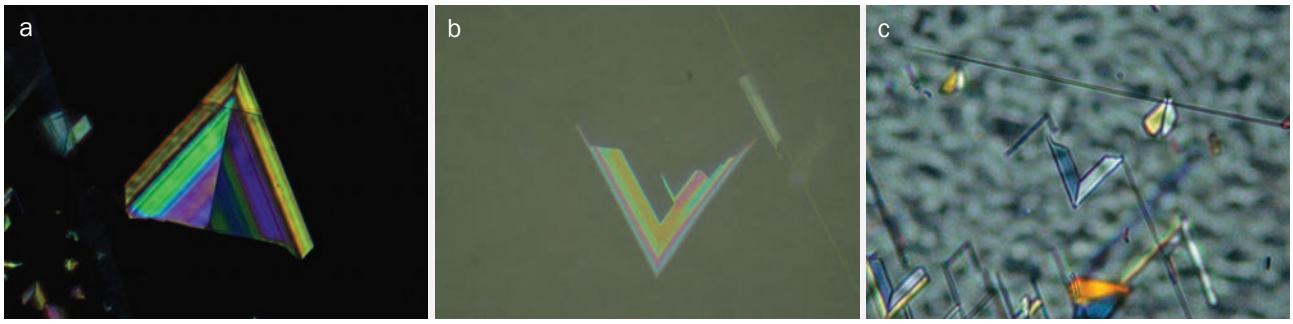

Figure 19: Somewhat larger V-shaped or triangular rutile platelets in the alexandrite from Kerala, cut perpendicular to the a-axis (sample C), are shown in these images (a, b and c). View parallel to the a-axis, reflected light, crossed polarizers, field of view 112 × 84 µm; photomicrographs by H.-J. Bernhardt.

More atypically, in one area of the Kerala thin section cut perpendicular to the a-axis, structures appearing as short lines were observed parallel to the <012> directions of the chrysoberyl host, and were often connected to form L-shaped or zigzag patterns (Figure 20). Such an orientation was recently described in a chrysoberyl from Brazil (Drev et al., 2015). In the Kerala sample, these inclusions also were identified as rutile by Raman spectroscopy. As further explained below in connection with the Orissa material, these structures represented cross-sections of platelets elongated parallel to the a-axis [100].

The other thin section of the alexandrite from Kerala, cut with an orientation almost perpendicular to the c-axis, showed needle-like structures of different lengths, and the compositional map recorded simply Ti-bearing spots or somewhat elongated Ti-rich areas. Again, these are the typical patterns expected if needles or V-shaped platelets such as those depicted in Figures 17–19 are cut at a right angle to the **a** (100) face.

Kyocera Synthetic Alexandrite

Asteriated and chatoyant synthetic alexandrites from Kyocera in Japan were described in detail by Schmetzer and Hodgkinson (2011) and by Schmetzer et al. (2013). The thin section of this Ti-bearing material oriented perpendicular to the a-axis (sample F) showed small elongated particles in three directions, with the three series of needles forming angles of ~60° with each other (Figure 21a). Several intergrown particles were seen, mostly with re-entrant angles of 60° and rarely with angles of 120° (Figure 21b). However, due to the small size of these particles and the dense pattern, it was sometimes difficult to determine if two needles were intergrown or if they were merely exsolved at different depths close to each other and thereby overlapped in the microscopic view of the thin section. The needles were too small for either

Figure 20: In this area of the Kerala alexandrite thin section shown in Figures 18 and 19, cross-sections of elongated inclusions are observed in different orientations parallel to <012>. Some of these structures meet, forming L-shaped or zigzag patterns. View parallel to the a-axis, reflected light (top), reflected light and crossed polarizers (bottom), field of view 112 × 84 µm; photomicrographs by H.-J. Bernhardt.

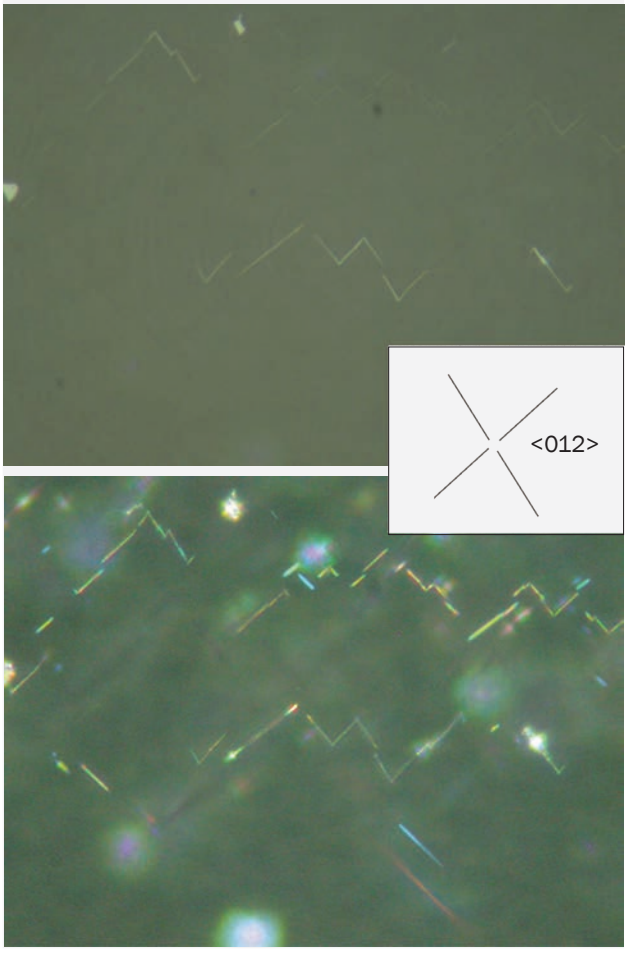

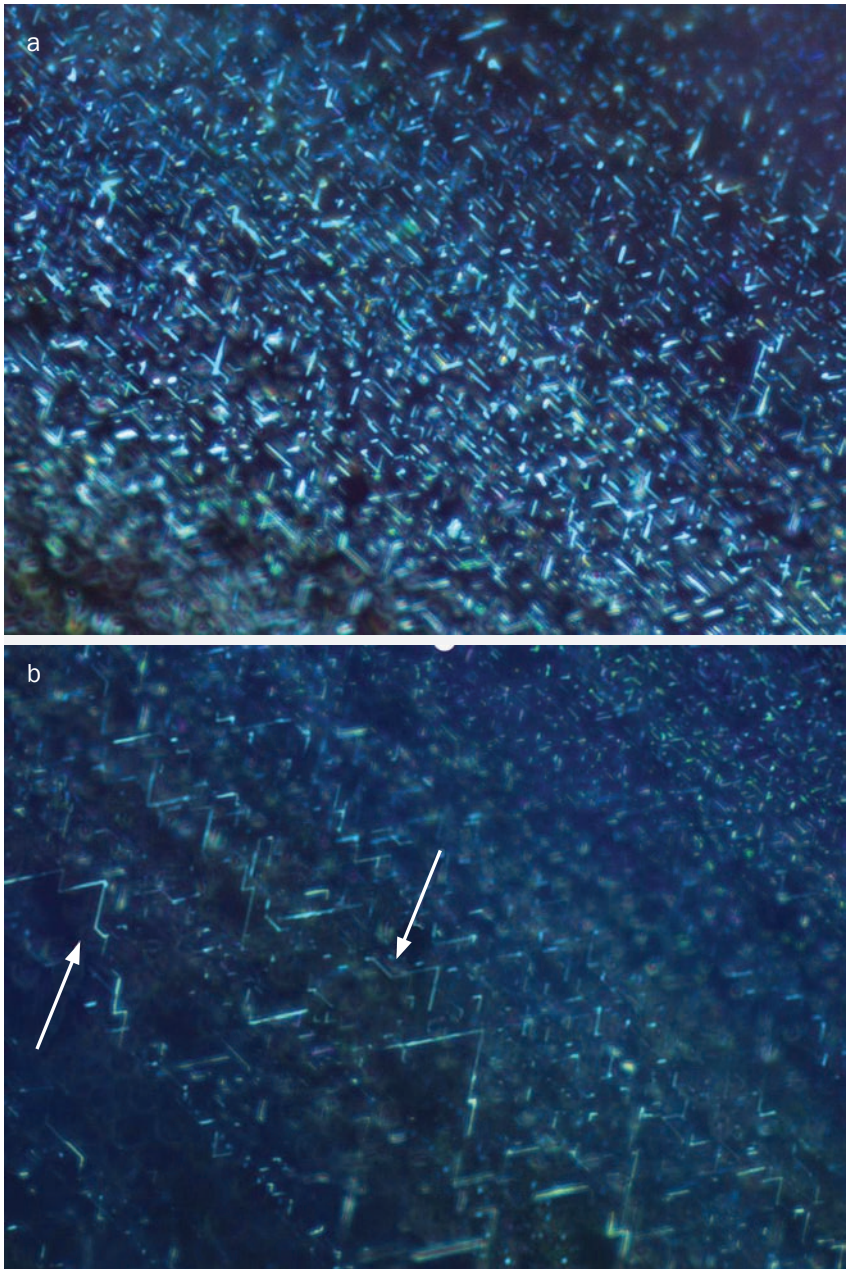

Figure 21: A thin section cut perpendicular to the a-axis of a synthetic asteriated alexandrite grown by Kyocera (sample F) shows a dense network of needles oriented in the <011> and [001] directions. In general, isolated needles or needles that are intergrown forming an angle of ~60° are observed (a), whereas two needles forming an angle of 120° (b, indicated by arrows) are less common. Reflected light, field of view 112 x 84 µm; photomicrographs by H.-J. Bernhardt.

microprobe analyses or micro-Raman spectroscopy. The examination of samples G and H, both cut perpendicular to the b-axis, did not reveal additional information, only corroborating what was learned from sample F. For further details, the reader is referred to the publications cited above.

Chatoyant Chrysoberyl from Orissa, India

Cat's-eye chrysoberyl from Orissa has been known in the trade for several years. The faceted chrysoberyl and alexandrite, as well as their chatoyant varieties, frequently have a low-saturation greenish or a light greyish colour in daylight, with a colour change to grey or light purple, respectively, in incandescent light. In a previous study, some samples described as colour-change chrysoberyl showed low concentrations of both V and Cr in comparable amounts (Schmetzer, 2010).

The chatoyant chrysoberyl selected for the present study (sample E) was chosen from a group of cabochons (e.g. Figure 9) that were slightly greenish grey in daylight and grey in incandescent light. Four samples from the group were analysed by electron microprobe, which recorded 0.05–0.07 wt.% V_2O_3, 0.03–0.05 wt.% Cr_2O_3, and 0.45–0.61 wt.% Fe_2O_3. These measurements are comparable with published data for faceted material from Orissa (Schmetzer, 2010).

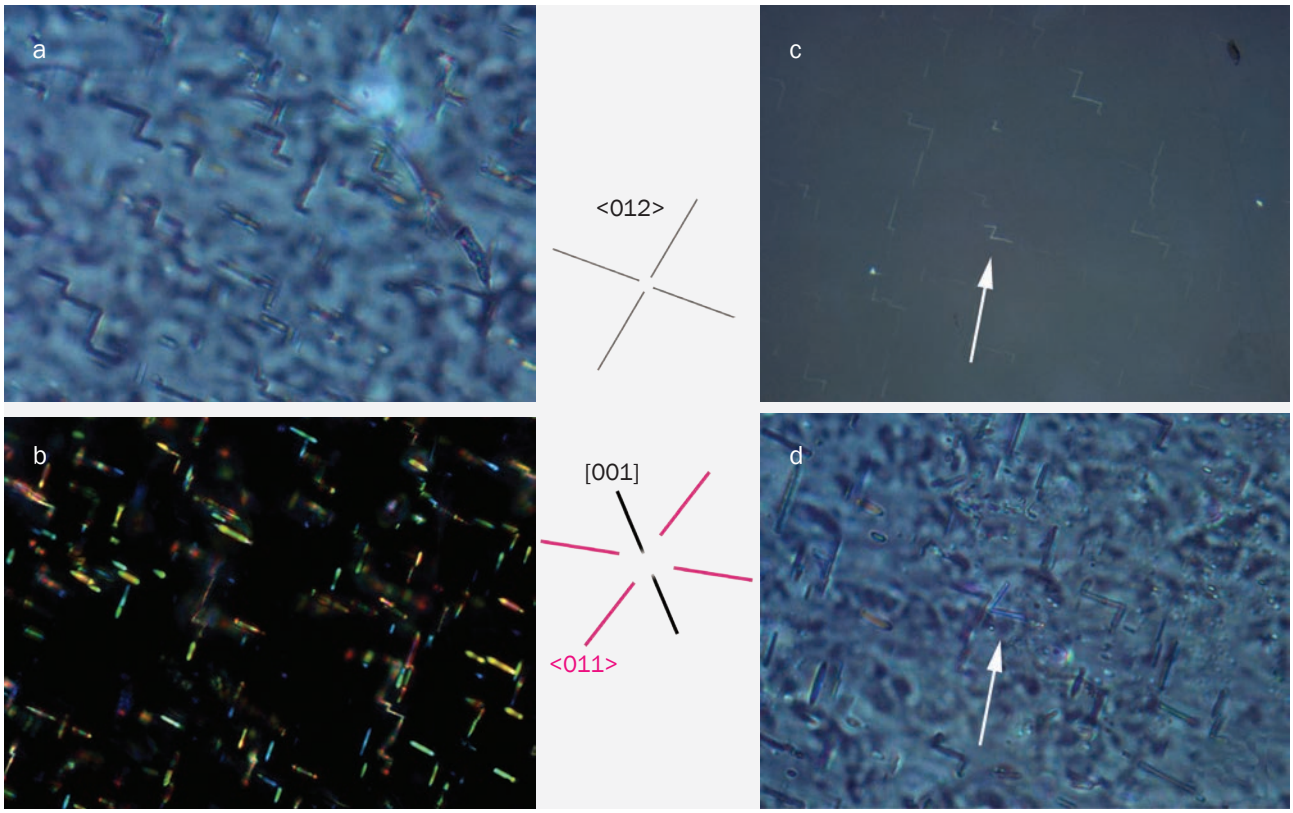

Figure 22: Photomicrographs in reflected light (a,c,d) and in reflected light with crossed polarizers (b) of a thin section cut perpendicular to the a-axis of a cat's-eye chrysoberyl from Orissa (sample E) show a network of L-shaped or zigzag cross-sections of rutile platelets parallel to <012> (a,b). Only a few cross-sections oriented parallel to <011> are observed in one small area of the thin section (c,d; indicated by arrows). Field of view 112 × 84 µm; photomicrographs by H.-J. Bernhardt.

The thin section from sample E (cut perpendicular to the a-axis and parallel to the light band of the cabochon) showed a network of reflective rectangular structures parallel to the <012> directions of the host chrysoberyl (Figure 22a,b). Typically, two, three or even more of these inclusions were linked together, forming an L-shaped or zigzag pattern. In one area of this thin section, similar structures parallel to the <011> directions were also observed (Figure 22c,d). Numerous examples of both types of inclusions revealed Raman spectra for rutile.

The thin section cut perpendicular to that just described showed a dense network of what appeared to be linear structures elongated parallel to the a-axis [100]. This pattern was best seen in transmitted light (Figure 23). Upon detailed inspection, it was observed that typically two or three, but occasionally more, of these linear structures existed within a somewhat larger platy inclusion. The linear structures traversed the larger platelet and gave it the appearance of being comprised of multiple narrow parts, connected by the linear structures. It was further seen that the different narrow parts of these complex platelets came into focus at different depths,

Figure 23: Chrysoberyl cat's-eye from Orissa (sample E) shows a dense network of complex rutile platelets elongated parallel to the a-axis. The platelets are composed of multiple narrow parts or 'stripes' that are inclined to each other and intergrown. Linear junctions connecting these parts or 'stripes' are also oriented parallel to the a-axis. Transmitted light, field of view 225 × 168 µm; photomicrograph by H.-J. Bernhardt.

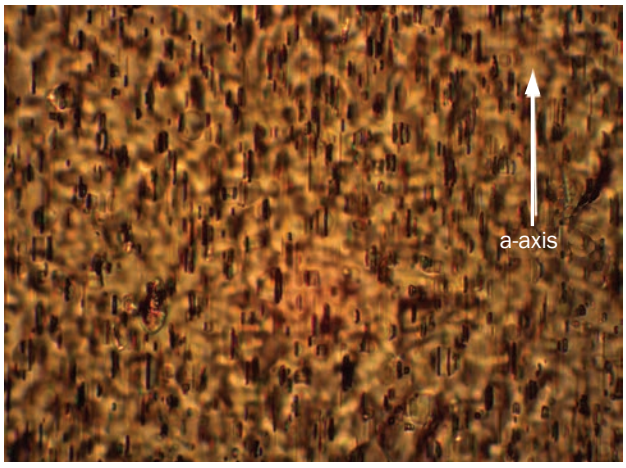

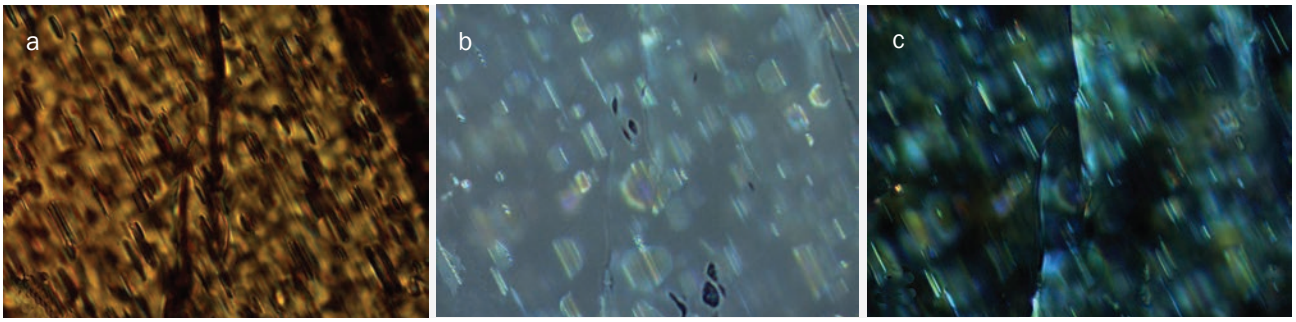

Figure 24: A dense network of complex platelets with internal linear junctions oriented parallel to the a-axis is shown in a cat's-eye chrysoberyl from Orissa (sample E). The small rutile platelets consisting of several parts or 'stripes' each reflect and scatter light. Transmitted light (a), reflected light (b) and reflected light with crossed polarizers (c), field of view 112 × 84 µm; photomicrographs by H.-J. Bernhardt.

indicating that they were inclined to the plane of the polished thin section. Many such platelets were examined by micro-Raman spectroscopy and showed rutile spectra.

Taking into consideration the observations of both the slice cut perpendicular to the a-axis (Figure 22) and the slice cut parallel to the a-axis [100] (Figure 23), it was concluded that the L-shaped and zigzag patterns of rectangular rutile particles along <012> depicted in Figure 22 represented cross-sections of the platy inclusions with internal linear structures elongated parallel to the a-axis [100] depicted in Figure 23. As such, the linear structures along the a-axis [100] and at right angles to the L-shaped and zigzig patterns represented the junctions between the different parts of the larger platy rutile inclusions. Moreover, taking into account the description by Drev et al. (2015) of rectangular structures along <012> as intergrown rutile clusters, it could further be concluded that: (1) the larger platy inclusions or complex platelets described above were rutile clusters, and (2) the linear structures elongated parallel to the a-axis [100] represented the edges or interconnections between the different inclined parts of the platy clusters. In other words, the platy rutile clusters were composed of narrow inclined sections elongated parallel to the a-axis [100] that caused the platelets to appear 'striped' when viewed perpendicular to the a-axis. When viewed in cross-section, two such narrow intergrown 'stripes' formed the L-shaped pattern parallel to the <012> directions of the host, while more than two such 'stripes' formed the zigzag pattern, likewise parallel to the <012> directions.

When lit from above, the different parts or 'stripes' of the platy rutile clusters reflected and scattered the incident illumination (Figure 24). When the chrysoberyl was cut as a cabochon, it was this scattered and reflected light that formed the bright band of the cat's-eye.

Chatoyant Chrysoberyl from Brazil

In the immersion microscope, the transparent cat's-eye chrysoberyl from Brazil revealed a dense pattern of needles with an orientation parallel to the a-axis [100]. These oriented needles visually resembled the inclusion scenario seen in the alexandrite from Lake Manyara in Figure 2. In the polished thin section cut perpendicular to the needle axis, numerous highly reflective cross-sections of such needles could be observed (Figure 25). These were determined to be rutile

Figure 25: Cat's-eye chrysoberyl from Brazil (sample I) is shown here in transmitted light in a thin section cut perpendicular to the a-axis. The photo shows cross-sections of rutile needles elongated parallel to [100], together with a few needles and V-shaped platelets elongated parallel to <011>; some needles along [001] are also observed. Field of view 150 × 112 µm; photomicrograph by H. A. Gilg.

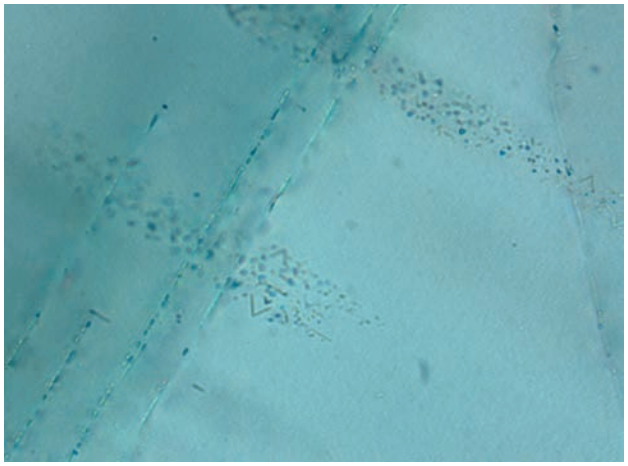

by micro-Raman spectroscopy. Likewise seen were a few needles and V-shaped platelets with an orientation parallel to the a-plane (100), and again Raman examination identified them as rutile.

Chatoyant Chrysoberyl from Ilakaka, Madagascar

Cat's-eye chrysoberyl from Ilakaka is mostly seen in the trade as cabochons prepared from high-quality transparent material; in addition, samples with a milky appearance are known. One such slightly waterworn crystal (sample J), which showed a clear morphology consisting of the pinacoids **a** (100) and **b** (010) in combination with **i** {011} prism faces and **o** {111} dipyramids, was selected for the preparation of three polished thin sections perpendicular to the three crystallographic axes a, b and c. As noted previously, the part of the Ilakaka crystal remaining after removal of these slices was ground and polished into a rounded, irregularly shaped specimen, which displayed a bright, reflective light band encircling the sample.

The thin section cut perpendicular to the a-axis showed an inclusion scene consisting of needles and V-shaped platelets parallel to the a-plane (100) and cross-sections of platelets elongated parallel to the a-axis [100] (Figures 26 and 27). As explained above for the Orissa sample, the narrow platelets elongated parallel to the a-axis [100] had rectangular cross-sections parallel to <012>. In the Madagascar sample, however, only a few of these inclusions were intergrown, and L-shaped cross-sections were rare. Applying the descriptions used for the Orissa sample, the platelets elongated parallel to the a-axis [100] in the Ilakaka stone might be characterized as representing only one narrow part or 'stripe'.

Figure 26: This view of a chrysoberyl from Ilakaka, Madagascar (sample J), in a thin section cut perpendicular to the a-axis, shows the inclusion pattern and a cross-cutting healed fracture. The chrysoberyl host shows a high concentration of rutile needles and platelets, whereas the area within the healed fracture is free of rutile particles and shows only some larger fluid inclusions trapped during the healing process. Transmitted light, field of view 300 × 222 µm; photomicrograph by H. A. Gilg.

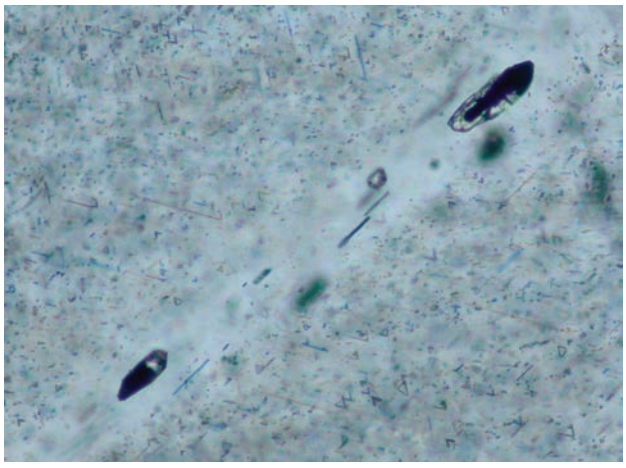

The thin sections cut perpendicular to the b- and c-axes both showed a similar inclusion pattern of narrow platelets elongated parallel to the a-axis [100], consisting of a single part or 'stripe' each, and cross-sections of the needles and platelets oriented parallel to the a-plane (100) (Figure 28). Micro-Raman spectroscopy of numerous inclusions of all the types just mentioned showed spectra for rutile.

Asteriated Chrysoberyl from Sri Lanka

Star chrysoberyl from Sri Lanka has been mentioned in the gemmological literature as an extremely rare phenomenal gemstone. Subsequent to a previous study dealing with four-rayed chrysoberyl (Schmetzer, 2010), the first author was able to examine six additional four-rayed star samples of varying quality (e.g. Figure 11). Such asteriated chrysoberyls are frequently heavily included and only translucent. However, it was possible by optical examination (correlation of the crystal orientation with the positions of both optic axes) to determine the location of the b-axis [010] in four of these six samples as being more-or-less at the centre of the stars. Together with samples examined previously, this optical orientation in four-rayed star chrysoberyls has now been established for a total of six samples. These results indicate an orientation of two series of needles or channels perpendicular to this axis in the ac-plane.

The slice examined for the present study (sample D) had been cut from, and parallel to, the flat base of such a four-rayed star chrysoberyl (top-right in Figure 11). As stated earlier, two thin sections were prepared from the slice, perpendicular to each other. The slight inclination of the arms of the star was a consequence of

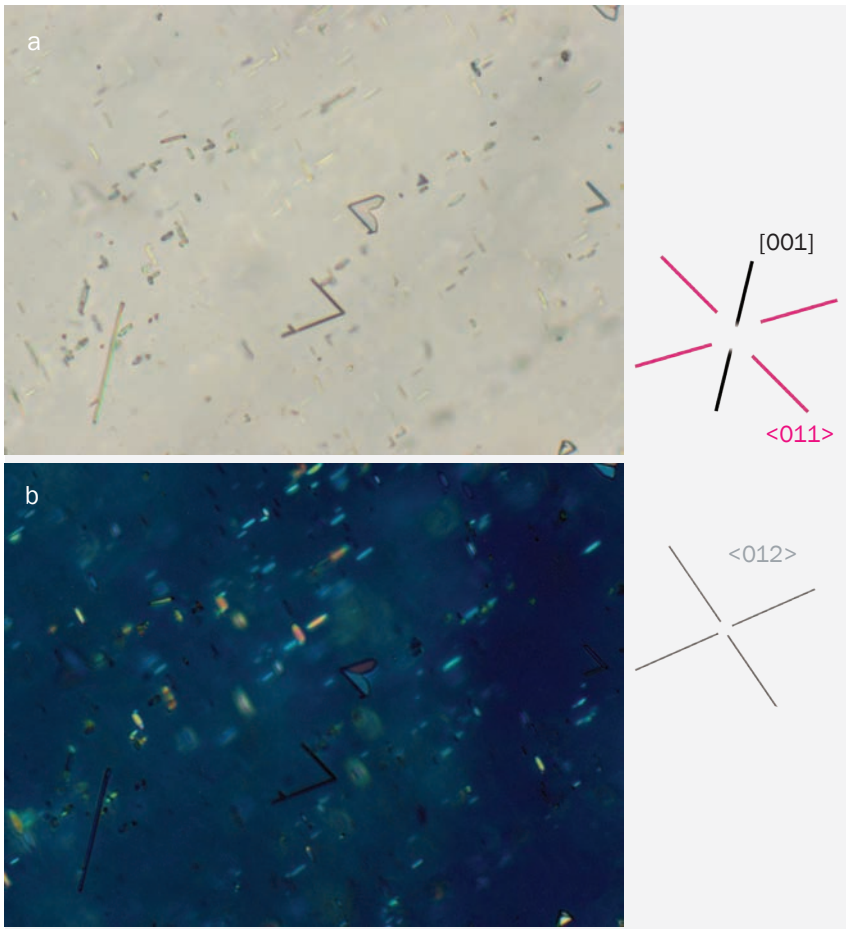

Figure 27: The Ilakaka sample in Figure 26 is shown here in transmitted light (a) and in transmitted light with crossed polarizers (b). Evident is a high concentration of rutile platelet cross-sections elongated parallel to <012>, together with needles and V-shaped platelets elongated parallel to <011>; some needles along [001] are also observed. Field of view 83 × 62 µm; photomicrographs by H. A. Gilg.

the b-axis [010] being inclined by about 30° in relation to the base of the cabochon. Upon tilting the cabochon by approximately that angle, the four-rayed star became orthogonal.

Microscopic examination of the thin section cut parallel to the base of the cabochon showed two series of inclusions oriented parallel to the a-axis [100] and parallel to the c-axis [001] (Figure 29a,b,d). The series parallel to the c-axis [001] was highly reflective and showed Ti signals in the compositional map (Figure 29c). Unexpectedly, micro-Raman spectroscopy of several of these elongated inclusions did not show the pattern for rutile, but instead a spectrum assigned to ilmenite, $FeTiO_3$.

The series of needles or channels parallel to the a-axis [100] was not reflective when viewed in the polarization microscope. If the thin section was rotated so the chrysoberyl appeared dark between crossed polarizers, these elongated particles also invariably appeared dark. Hence, they seemed to show no birefringence. Furthermore, the compositional map (Figure 29c) did not reflect any Ti concentrations for these particles, and the electron microprobe did not record high concentrations of other elements that

Figure 28: In a thin section cut perpendicular to the c-axis, the Ilakaka chrysoberyl (sample J) shows a high concentration of rutile platelets and needles elongated parallel to the a-axis. Most of the platelets consist of only a single part or 'stripe'. Transmitted light, field of view 150 × 112 µm; photomicrograph by H. A. Gilg.

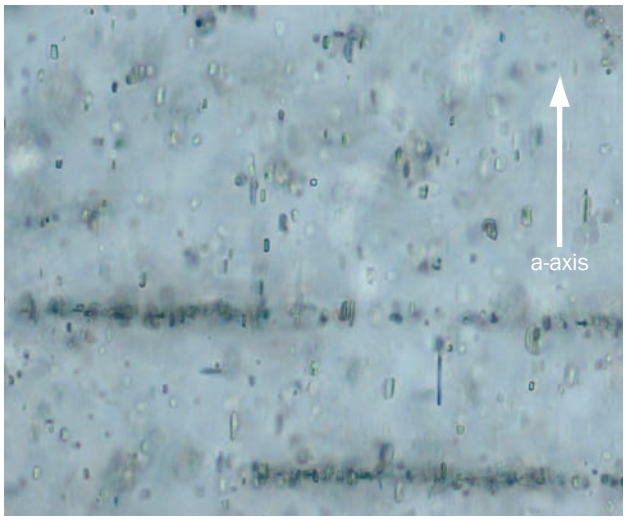

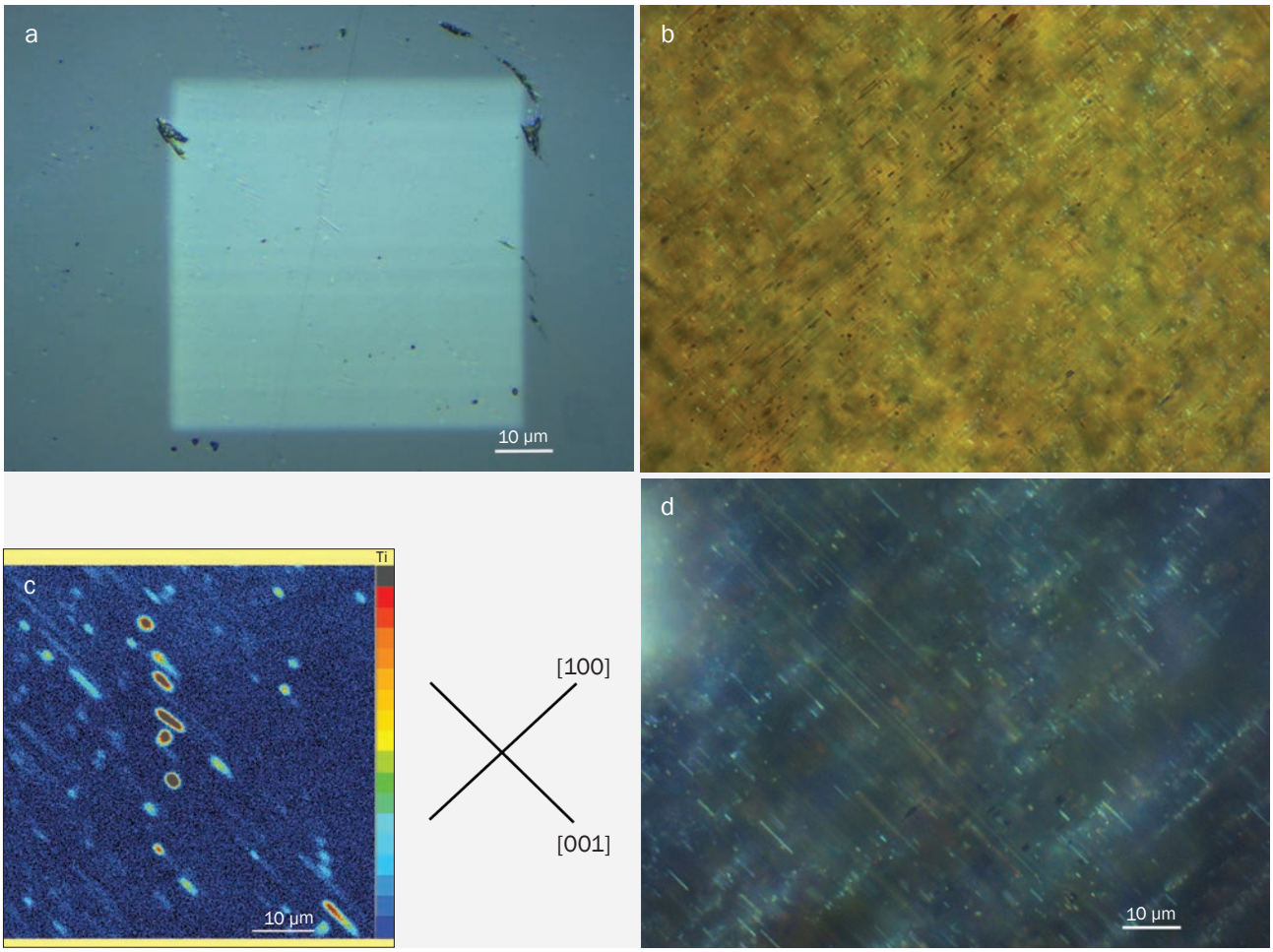

Figure 29: A thin section of an asteriated chrysoberyl from Sri Lanka (sample D), representing a section approximately perpendicular to the b-axis, is shown in reflected light (a) and in reflected light with crossed polarizers (b,d) compared to a Ti compositional map (c). In reflected light, focusing on the surface of the sample (a) shows the scanned area (measuring ~61 × 61 µm), with one series of parallel ilmenite needles that are also represented on the Ti distribution map (c); a second series of needles or channels perpendicular to the first series shows no Ti. The intensity of the Ti signal in (c) ranges from weak (blue) to strong (red). Field of view 112 × 84 µm (a,d) and 224 × 168 µm (b); photomicrographs and map by H.-J. Bernhardt.

could suggest the presence of an alternative type of elongated inclusion. In addition, micro-Raman spectroscopy showed only the Raman lines of the chrysoberyl host. Consequently, these elongated inclusions along the a-axis [100] might represent channels. Nonetheless, given the small size of rutile precipitates in a Brazilian chrysoberyl found by Drev et al. (2015) through use of a transmission electron microscope, there remains the possibility that similarly minute rutile needles might be present in the star chrysoberyl from Sri Lanka that did not generate conclusive signals with our instruments.

The thin section cut perpendicular to the base of the asteriated cabochon revealed only a few highly reflective and somewhat rounded inclusions, which may be understood as the rectangular cross-sections of the ilmenite needles. The compositional map depicted numerous corresponding spots with high Ti concentration. These data confirm the results described above that were obtained from the thin section oriented parallel to the base of the cabochon.

Discussion and Conclusions

The combination of immersion microscopy of gem materials at low magnification, optical microscopy of polished thin sections cut in preferred orientations at high magnification, micro-Raman spectroscopy and electron microprobe techniques (qualitative point analysis, BSE imaging and Ti compositional mapping) showed that two primary groups of rutile inclusions existed in the chrysoberyl and

alexandrite samples examined for this study. Their concentrations varied among the different sources. One group was characterized by needles and platelets on planes perpendicular to the a-axis, whilst the other group consisted of needles and platelets elongated parallel to the a-axis [100]. More specifically:

1. In one group, three different series of needle-like to flat tabular rutile inclusions oriented in planes parallel to the **a** (100) pinacoid were found in natural as well as synthetic samples. These rutile needles were elongated parallel to the c-axis [001] and along symmetry-equivalent <011> directions. Frequently, V-shaped rutile platelets with re-entrant angles of ~60°, rarely ~120°, and/or triangular rutile platelets were formed by such flattened rutile needles and platelets.
2. In the other group, rutile needles and platelets consisting of one or more narrow rectangular parts or 'stripes' elongated in directions parallel to the a-axis [100] were observed. In the optical microscope, the rutile needles showed rectangular, somewhat rounded cross-sections. Rutile platelets consisting of only a single part or 'stripe' showed rectangular cross-sections parallel to the <012> directions of the host. More complex platelets were formed by clusters of intergrown and inclined rutile parts or 'stripes', with internal linear junctions elongated parallel to the a-axis [100] direction. Cross-sections of such complex platelets were oriented along several symmetry-equivalent <012> directions, with re-entrant angles of ~81° or ~99° formed by the different parts of these clusters. These cross-sections displayed an L-shaped or zigzag pattern.

The inclusion pattern seen in any given alexandrite or chrysoberyl, as demonstrated by various samples in this study (see, e.g., Figure 3), may represent both of these groups, that is needles or V-shaped platelets on planes perpendicular to the a-axis, and needles or platelets elongated parallel to the a-axis [100]. These primary groups may also be augmented by further types of inclusions. For instance, in the four-rayed star chrysoberyl, elongated ilmenite particles were seen parallel to the c-axis [001]. Also present were needle-like inclusions parallel to the a-axis [100] that could not be identified as mineral inclusions by the methods applied. This latter type may consist of channels or minute rutile needles.

In samples A and B from Lake Manyara, Tanzania, and in sample C from Kerala, India, the rutile platelets or needles located in the **a** (100) plane were highly reflective and birefringent, and caused the samples to appear whitish in a view parallel to the a-axis [100], i.e. perpendicular to the triangular rutile platelets, flattened rutile needles or V-shaped rutile structures. These small needles or platelets with a thickness in the a-axis [100] direction in the micrometre range (or even smaller) were distributed throughout the completely milky-appearing crystals or within the cloudy areas of zoned samples.

If such inclusions are not exposed at the surface of a crystal or a polished thin section, they still reflect light and are clearly visible in the microscope. They generally do not, however, contribute to the intensity of the Ti signal recorded by the detector of the electron microprobe. As a result, previous studies (Schmetzer and Malsy, 2011; Schmetzer and Bernhardt, 2012) are not inconsistent with the present, more complete work employing multiple techniques.

Although the Ti-bearing needles or platelets in samples from Lake Manyara and Kerala showed a somewhat cloudy, milky appearance in reflected light, no sharp six-rayed asteriated chrysoberyls have been reported to date from these two areas. The presence of both needles and platelets, combined with the relatively large dimensions of these inclusions, prevents such a phenomenon. Conversely, synthetic asteriated alexandrite from Kyocera showed a dense network consisting of three series of distinctly smaller needles in the same orientations as in the Lake Manyara and Kerala examples, but no larger platelets were seen in the synthetic alexandrite. Thus, the Kyocera synthetics, when cut as cabochons with the base parallel to the **a** (100) pinacoid (e.g. sample F in the present study) showed six-rayed asterism. If the base of a synthetic alexandrite cabochon was different from this particular orientation (samples

G and H), only one light band was commonly observed, and such samples are described in the trade as synthetic cat's-eye alexandrite.

Perpendicular to the **a** (100) plane (i.e. parallel to the a-axis [100]), larger channels or needles of sufficient size to be resolved with the magnification of the gemmological microscope were seen in a previous study of samples from Lake Manyara (Figure 2), and now also in the cat's-eye chrysoberyl from Brazil (sample I) and in the alexandrite crystals from Kerala. Smaller elongated particles with the same orientation were found in samples A and B from Lake Manyara and in sample D, the asteriated chrysoberyl from Sri Lanka.

The particles along the a-axis [100] in the four-rayed star chrysoberyl from Sri Lanka could not definitively be identified as rutile by optical examination in combination with electron microprobe analysis and micro-Raman spectroscopy. These inclusions are therefore possibly elongated channels, although it must be considered that very small rutile needles of the size described by Drev et al. (2015) would probably not be seen with the methods applied in the present study.

In contrast, rutile spectra were recorded for numerous tiny needles parallel to the a-axis [100] in samples A and B from Lake Manyara, for both elongated needles (sample B) and cross-sections of needles (sample A). Similar cross-sections of rutile needles also were positively identified in the cat's-eye chrysoberyl from Brazil. Consequently, at least a subset of particles elongated parallel to the a-axis [100] can be characterized as rutile needles.

If a dense concentration of such minute particles (channels and/or rutile needles) elongated along the a-axis [100] is present, these structures cause a light band with an orientation perpendicular to the needle axis. Such a light band formed the chatoyancy in the cat's-eye chrysoberyl from Brazil and was one of the bands observed in four-rayed asteriated chrysoberyl from Sri Lanka (sample D). The second light band in the Sri Lankan star studied here was generated by ilmenite needles along the c-axis [001].

In crystals from Lake Manyara or Kerala, the scattering of light by these elongated inclusions (channels and/or rutile needles) was responsible for the milky appearance of such samples in all directions perpendicular to the a-axis. Given that larger **c** (001) faces are extremely rare in natural chrysoberyl or alexandrite, a whitish appearance is normally visible in a view toward the **b** (010) pinacoid or the **i** {011} prism faces, which are frequently well developed in chrysoberyl.

Complex rutile platelets formed by various narrow intergrown parts or 'stripes' elongated parallel to the a-axis [100], with L-shaped or zigzag cross-sections along the <012> directions, were observed in the cat's-eye chrysoberyl from Orissa, India (sample E). The internal edges or junctions between the inclined parts or 'stripes' likewise ran along the a-axis [100]. These complex platy structures represent a previously undocumented type of inclusion as well as a new mechanism for forming the light band in cat's-eye chrysoberyl. The same type of inclusion also was observed in a small area within the thin section of alexandrite from Kerala, India (sample C). Furthermore, elongated rutile platelets consisting of only one narrow part or 'stripe' each, with simple rectangular cross-sections, were found in high concentration in sample J from Madagascar. The sizes of the rutile inclusions with a similar orientation as described by Drev et al. (2015), for a section perpendicular to the a-axis in one chrysoberyl from Brazil, were much smaller.

In both chrysoberyls with a high concentration of rutile platelets (samples E and J), chatoyancy was observed in the direction perpendicular to the elongation of the platelets. These platelet-derived light bands correspond to those formed by needles in certain other chatoyant chrysoberyls such as sample I from Brazil.

If both types of inclusions are present—that is, rutile platelets or flattened needles in the **a** (100) plane and a dense network of channels and/or rutile needles/platelets elongated in the a-axis [100] direction—then the crystal appears somewhat whitish in most directions, as observed for sample B from Lake Manyara and especially for sample J from Ilakaka, Madagascar. This indicates that a whitish appearance in alexandrite or chrysoberyl is caused by more than one mechanism, and the direction of view parallel or perpendicular to the a-axis allows these mechanisms to be distinguished.

References

Cassedanne J. and Roditi M., 1993. The location, geology, mineralogy and gem deposits of alexandrite, cat's-eye and chrysoberyl in Brazil. *Journal of Gemmology*, **23**(6), 333–354, http://dx.doi.org/10.15506/jog.1993.23.6.333.

Drev S., Komelj M., Mazaj M., Daneu N. and Rečnik A., 2015. Structural investigation of (130) twins and rutile precipitates in chrysoberyl crystals from Rio das Pratinhas in Bahia (Brazil). *American Mineralogist*, **100**(4), 861–871, http://dx.doi.org/10.2138/am-2015-5120.

Eppler W.F., 1958. Notes on asterism in spinel and chatoyancy in chrysoberyl, quartz, tourmaline, zircon and scapolite. *Journal of Gemmology*, **6**(6), 251–263, http://dx.doi.org/10.15506/jog.1958.6.6.251.

Fernandes S. and Choudhary G., 2010. *Understanding Rough Gemstones*. Indian Institute of Jewellery, Mumbai, 211 pp.

He J., Lagerlof K.P.D. and Heuer A.H., 2011. Structural evolution of TiO_2 precipitates in Ti-doped sapphire (α-Al_2O_3). *Journal of the American Ceramic Society*, **94**(4), 1272–1280, http://dx.doi.org/10.1111/j.1551-2916.2010.04217.x.

Kumaratilake W.L.D.R.A., 1997. Gems of Sri Lanka: A list of cat's-eyes and stars. *Journal of Gemmology*, **25**(7), 474–482, http://dx.doi.org/10.15506/jog.1997.25.7.474.

Langensiepen R.A., Tressler R.E. and Howell P.R., 1983. A preliminary study of precipitation in Ti^{4+}-doped polycrystalline alumina. *Journal of Materials Science*, **18**(9), 2771–2776, http://dx.doi.org/10.1007/bf00547594.

Manimaran G., Bagai D. and Chacko P.T.R., 2007. Chrysoberyl from southern Tamil Nadu of South India, with implications for Gondwana studies. In S. Rajendran, S. Aravindan and K. Srinivasamoorthy, Eds., *Mineral Exploration*, New India Publishing Agency, New Delhi, 63–76.

Marder J.M. and Mitchell T.E., 1982. The nature of precipitates in cat's-eye chrysoberyl. *40th Annual Meeting of Electron Microscopy Society of America*, **1982**, Washington DC, USA, 556–557.

McClure S.F. and Koivula J.I., 2001. A new method for imitating asterism. *Gems and Gemology*, **37**(2), 124–128, http://dx.doi.org/10.5741/gems.37.2.124.

Menon R.D., Santosh M. and Yoshida M., 1994. Gemstone mineralization in southern Kerala, India. *Journal of the Geological Society of India*, **44**(3), 241–252.

Milisenda C.C., Henn U. and Henn J., 2001. New gemstone occurrences in the south-west of Madagascar. *Journal of Gemmology*, **27**(7), 385–394, http://dx.doi.org/10.15506/jog.2001.27.7.385.

Moon A.R. and Phillips M.R., 1991. Titania precipitation in sapphire containing iron and Ti. *Physics and Chemistry of Minerals*, **18**(4), 251–258, http://dx.doi.org/10.1007/bf00202577.

Phillips D.S., Heuer A.H. and Mitchell T.E., 1980. Precipitation in star sapphire. I. Identification of the precipitate. *Philosophical Magazine A*, **42**(3), 385–340, http://dx.doi.org/10.1080/01418618008239365.

Porto S.P.S., Fleury P.A. and Damen T.C., 1967. Raman spectra of TiO_2, MgF_2, ZnF_2, FeF_2, and MnF_2. *Physical Review*, **154**(2), 522–526.

Schmetzer K., 2010. *Russian Alexandrites*. Schweizerbart Science Publishers, Stuttgart, Germany, 141 pp.

Schmetzer K. and Bernhardt H.-J., 2012. Oriented inclusions in alexandrite from the Lake Manyara deposit, Tanzania. *Australian Gemmologist*, **24**(11), 267–271.

Schmetzer K. and Hainschwang T., 2012. Origin determination of alexandrite – A practical example. *InColor*, **21**, 36–39.

Schmetzer K. and Hodgkinson A., 2011. Synthetic star alexandrite. *Gems&Jewellery*, **20(3), 9–11.**

Schmetzer K. and Krzemnicki M.S., 2015. Nail-head spicules as inclusions in chrysoberyl from Myanmar. *Journal of Gemmology*, **34**(5), 434–438, http://dx.doi.org/10.15506/jog.2015.34.5.434.

Schmetzer K. and Malsy A.-K., 2011. Alexandrite and colour-change chrysoberyl from the Lake Manyara alexandrite-emerald deposit in northern Tanzania. *Journal of Gemmology*, **32**(5–8), 179–209, http://dx.doi.org/10.15506/jog.2011.32.5.179.

Schmetzer K., Bernhardt H.-J. and Hainschwang, T., 2013. Ti-bearing synthetic alexandrite and chrysoberyl. *Journal of Gemmology*, **33**(5–6), 137–148, http://dx.doi.org/10.15506/jog.2013.33.5.137.

Viti C. and Ferrari M., 2006. The nature of Ti-rich inclusions responsible for asterism in Verneuil-grown corundums. *European Journal of Mineralogy*, **18**(6), 823–834, http://dx.doi.org/10.1127/0935-1221/2006/0018-0823.

Wang A., Kuebler K.E., Jolliff B.L. and Haskin L.A., 2004. Raman spectroscopy of Fe-Ti-Cr-oxides, case study: Martian meteorite EETA79001. *American Mineralogist*, **89**(5–6), 665–680, http://dx.doi.org/10.2138/am-2004-5-601.

Xiao S.Q., Dahmen U. and Heuer A.H., 1997. Phase transformation of TiO_2 precipitates in sapphire (α-Al_2O_3) induced by the loss of coherency. *Philosophical Magazine A*, **75**(1), 221–223, http://dx.doi.org/10.1080/01418619708210292.

The Authors

Dr Karl Schmetzer FGA
D-85238 Petershausen, Germany
Email: SchmetzerKarl@hotmail.com

Dr Heinz-Jürgen Bernhardt
ZEM, Institut für Geologie, Mineralogie und Geophysik, Ruhr-University Bochum
D-44780 Bochum, Germany

Prof. Dr H. Albert Gilg
Lehrstuhl für Ingenieurgeologie
Technische Universität München
D-80333 Munich, Germany

Acknowledgements

Samples for this study, other than those taken from the personal collection of one of the authors (KS), were kindly provided by the late George Bosshart (Horgen, Switzerland), Dr Thomas Hainschwang (Balzers, Liechtenstein), Alan Hodgkinson (Portencross, Scotland), Dr Jaroslav Hyršl (Prague, Czech Republic), Dr Michael S. Krzemnicki (from the Henry A. Hänni collection housed at the Swiss Gemmological Institute SSEF, Basel, Switzerland) and Martin P. Steinbach (Idar-Oberstein, Germany). The technical laboratories at Bochum and München Universities are also thanked for the careful preparation of the polished thin sections.

SSEF

SCHWEIZERISCHES GEMMOLOGISCHES INSTITUT
SWISS GEMMOLOGICAL INSTITUTE
INSTITUT SUISSE DE GEMMOLOGIE

ORIGIN DETERMINATION · TREATMENT DETECTION

DIAMOND GRADING · PEARL TESTING

EDUCATION · RESEARCH

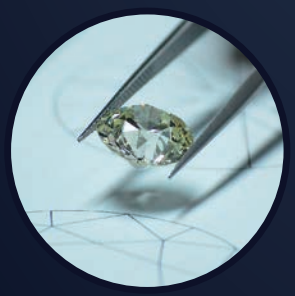

THE SCIENCE OF GEMSTONE TESTING©

Aeschengraben 26, CH-4051 Basel, Switzerland Tel. +41 61 262 06 40 Fax + 41 61 262 06 41 admin@ssef.ch www.ssef.ch

The Great Mughal and the Orlov: One and the Same Diamond?

Anna Malecka

One of the most famous stones mentioned in the gemmological literature is the so-called Great Mughal diamond, described and depicted in a 17th-century work of Jean-Baptiste Tavernier. According to Tavernier, this specimen weighed ~286 metric carats (upon recalculation from Eastern units); it was not mentioned in later sources referring to the Mughal court. In the 18th century, however, a diamond reminiscent of the Great Mughal appeared on the market—it is known today as the Orlov (189.62 ct). Some researchers have suggested that these specimens could be identical, if not for the fact that the Orlov weighs about 90 ct less than the stone reported by Tavernier. This discrepancy may be explained by the inference that Tavernier never actually examined the stone, but he only described it from accounts given by others. This deduction, together with new evidence showing that the stone actually weighed ~193.5 ct, indicates a high likelihood that the Great Mughal is the same as the Orlov diamond.

The Journal of Gemmology, **35**(1), 2016, pp. 56–63, http://dx.doi.org/10.15506/JoG.2016.35.1.56

Introduction

In the work of Jean-Baptiste Tavernier (1605–1689), French diamantaire and traveller to India and other exotic locales (Figure 1), there is a description of one of the largest diamonds in the collection of the Mughal emperor Aurangzeb (reigned 1658–1707)—a specimen weighing ~286 ct known as the Great Mughal (or Great Mogul). Most who have written on the history of this diamond do not question the credibility of Tavernier's account (King, 1867; Jagnaux, 1885; Shipley, 1955; Bruton, 1970; Moneta Cavenago-Bignami, 1980; Harlow, 1998; Balfour, 2009). The Frenchman's information regarding this stone is examined further in this article, and its possible relation to the Orlov diamond is explored.

Background

One of the most frequently cited historical European travel writers is Jean-Baptiste Tavernier. This privately active gem merchant made six journeys to the East during the period 1630–1668, visiting among other countries Turkey, Persia and India (e.g. Figure 2). In this last region—the first known source of diamonds—Tavernier was most interested in just these stones, which was reflected in the work he published in 1676, wherein he described the methods used to mine them and problems connected with their trade.

Even though the Frenchman's reports pertaining to these issues are not the only ones from this period, his writings also contain an account of unique value regarding the gems

Figure 1: Jean-Baptiste Tavernier is shown wearing an Oriental costume in this portrait by Nicolas de Largillière. The painting currently resides at Herzog Anton Ulrich Museum, Braunschweig, Germany.

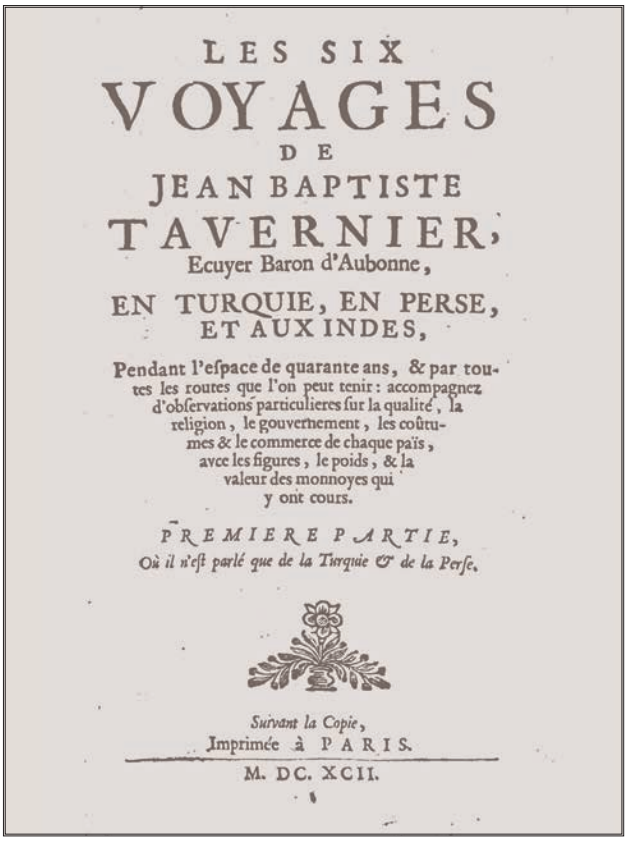

LES SIX
VOYAGES
DE
JEAN BAPTISTE
TAVERNIER,
Ecuyer Baron d'Aubonne,
EN TURQUIE, EN PERSE,
ET AUX INDES,
Pendant l'eſpace de quarante ans, & par toutes les routes que l'on peut tenir : accompagnez d'obſervations particulieres ſur la qualité, la religion, le gouvernement, les coûtumes & le commerce de chaque païs, avec les figures, le poids, & la valeur des monnoyes qui y ont cours.
PREMIERE PARTIE,
Où il n'eſt parlé que de la Turquie & de la Perſe.
Suivant la Copie,
Imprimée à PARIS.
M. DC. XCII.

Figure 2: Tavernier's travels to the East were recorded in various manuscripts, such as this one from 1692.

of Aurangzeb, the ruler of the Mughal Empire (Howard, 1677; Master, 1911; Moreland, 1931; de Coutre, 1991). Aurangzeb's valuables were shown to Tavernier by the imperial gem keeper, Akel Khan. Most of these were not especially notable by Mughal standards, as they 'only' weighed from several carats to about 60 ct. However, according to Tavernier (1692), there was one exceptional stone (as quoted in and translated by Streeter, 1882, pp. 69–70; see also Balfour, 2009):

> The first piece that Akel Khan placed in my hands was the great diamond, which is rose cut, round and very high on one side. On the lower edge there is a slight crack, and a little flaw in it. Its water is fine, and weighs 319½ ratis [*sic*], which makes 280 of our carats, the rati being ⅞ of a carat.

Tavernier, who included a drawing of this gem in his account (Figure 3), claimed that the keeper allowed him to personally examine and weigh the diamond. He also reported that the original rough stone weighed about 790 carats, and in 1656 it was given as a gift to Aurangzeb's father Emperor Shah Jahan (reigned 1628–1658; Figure 4) by Mir Jumla, previously a dignitary in the court at Golconda, in recognition of his support of the Mughals. The stone was most probably pilfered from one of the temples in Karnataka, India, by soldiers of Mir Jumla during military operations conducted there in 1642–1652 (Gemelli Careri, 1700). The diamond was reportedly cut by a Venetian, Hortensio Borgio, who worked in India

Figure 3: Tavernier's drawing of the Great Mughal diamond appeared in his 1692 monograph.

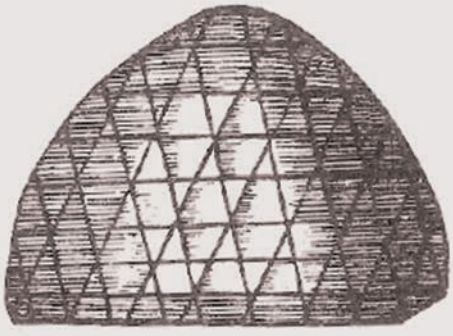

Figure 4: Emperor Shah Jahan is shown on a throne, flanked on the left by his three eldest sons—Dara Shikoh, Shah Shuja and Aurangzeb—while their maternal grandfather, Asaf Khan, stands to the right. The painting dates from the Mughal Period, circa AD 1628. Source: Aga Khan Museum, www.agakhanmuseum.org/collection/artifact/shah-jahan-his-three-sons-and-asaf-khan-akm124.

during the second part of the 17th century. The reported weight of the resulting stone, 319½ rattis—indicated by Tavernier (1692) as being equivalent to 280 'of our carats'—probably is equal to ~286 metric carats (see below).

The diamond described by Tavernier has not been mentioned in later sources referring to the Mughal period.

Figure 5: The 189.62 ct Orlov diamond is shown here in the Imperial Sceptre, part of the Diamond Fund collection of the Moscow Kremlin. Photo © Elkan Wijnberg.

Correlations with the Orlov Diamond

The stone from Tavernier's drawing and description has been noted as being similar to the Mughal-cut Orlov diamond (Figures 5 and 6), which weighs 189.62 ct and is presently kept at the Moscow Kremlin in Russia (Rybakov, 1975; Polynina, 2012; Malecka, 2014b; Shcherbina, 2014). Several legends circulate about the origins of the Orlov diamond. The most popular of them, which can be dated to Europe in the late 18th century, states this gem was taken by a French soldier from an Indian temple in Srirangam in present-day Tamil Nadu State (Dutens, 1783). Another rumour indicated that this stone was to have been an ornament for the throne of Nadir Shah, ruler of Persia, who in 1739 plundered the Mughal treasury (Pallas, 1805; Fersman 1924–25). However, according to documents from Russian archives, during the rule of Nadir Shah (1736–1747), the Orlov was in fact the property of the Persians (although it was not necessarily kept in Persia). We do know for certain that it was taken from the Persian city of Isfahan to Amsterdam by an Armenian merchant. In Amsterdam, it was sold to Catherine II, the empress of Russia (Malecka, 2014b; Malecka, in prep.-b).

Both the Great Mughal and Orlov diamonds have the same type of cut. According to Balfour (2009), "the pattern of facets is not dissimilar" and, even more importantly, there is a small indentation in the Orlov that corresponds to the small crack on the stone described by Tavernier. Even though the similarity of these gems was already noticed in the 19th century by European writers, they were restrained from equating the stones by the information on the weight of the Great Mughal diamond as given by Tavernier. Some writers justified the differences in weight by pointing out Tavernier's probable mistake when weighing Aurangzeb's stone, or that this specimen decreased in size (i.e. through recutting) at a later time (Anonymous, 1853; Schrauf, 1869; Ball, 1889; Fersman, 1922; Fersman 1924–25).

However, Aziz (1942) reported that some Mughal authors pointed to a different weight for this stone than that given by Tavernier (see page 60). He did not correlate the identity of this gem with the Orlov diamond, perhaps because the weight of the Orlov was usually given by older authorities as 185 Amsterdam or Russian carats, whereas Aziz described it as weighing 194.75 ct, similar to that given by some 19th century Russian sources (Anonymous, 1866; Aziz, 1942; Kuznetsova, 2009; Zimin and Sokolov, 2013).

Present Research

Previous writers pondering the correlation between the Great Mughal and Orlov diamonds did not analyse court texts from the Mughal Empire in the Persian language or sources available in the Russian language. The present author's research has been largely based on such material.

A matter of key significance is to determine the Western weight conversions that Tavernier used for the Indian units of the Great Mughal—*rattis*, also known as *surkhs* (Halhed, 1776). Weight units for gems (as weights and measures in general) were quite varied in Asia, Africa and Europe depending on the epoch and geographical location. Normally, the Eastern authors did not specify the local units for the weights of gems they were describing. The weight of identically named units could also differ in reference to gems vs. metals (Lockyer, 1711; Kelly, 1832; Hinz, 1955).

When describing Aurangzeb's diamond, Tavernier's weight conversion was that 1 ratti corresponded to 0.875 of 'our carats' (Tavernier, 1692). Valentine Ball (1889) maintained that the Frenchman converted Eastern weight units for gems into Florentine carats, which were equivalent to about 0.196 g. Ball based his argument on information contained in Tavernier's work pertaining to a diamond weighing 139.5 Florentine carats—the largest diamond in Europe at that time—seen by him in the collection of the Great Prince of Tuscany and known later as the Florentine diamond. The weight of this stone, cited by Tavernier and lost since the times of World War I, was very close to the 137.27 metric carats of The Great Diamond of Tuscany, as it is known from later sources (Ball, 1889; Balfour, 2009).

In fact, it is probable that the weight of the Florentine diamond was reported by Tavernier in local (Florentine) units, as he did sometimes in the case of gems that he saw or heard about during his Eastern voyages (see below; Tavernier, 1692). The present author did not, however, find any information suggesting that the Florentine carat was used universally by Western gem traders at that time. Therefore, one may wonder if this conversion was applied by Tavernier consistently in reference to the various gems mentioned by him. In this author's view, it is more probable that in writing

Figure 6: Various views of the Orlov diamond are shown in this 1767 drawing that was made in Amsterdam by Frans de Bakker. If the Orlov was in fact the same as the Great Mughal diamond, then the image of the rough stone in the upper left must have been conjectural, since the diamond was previously cut in the 17th century. Source: Rijksmuseum, Amsterdam, The Netherlands, www.rijksmuseum.nl/nl/collectie/RP-P-1911-2912.

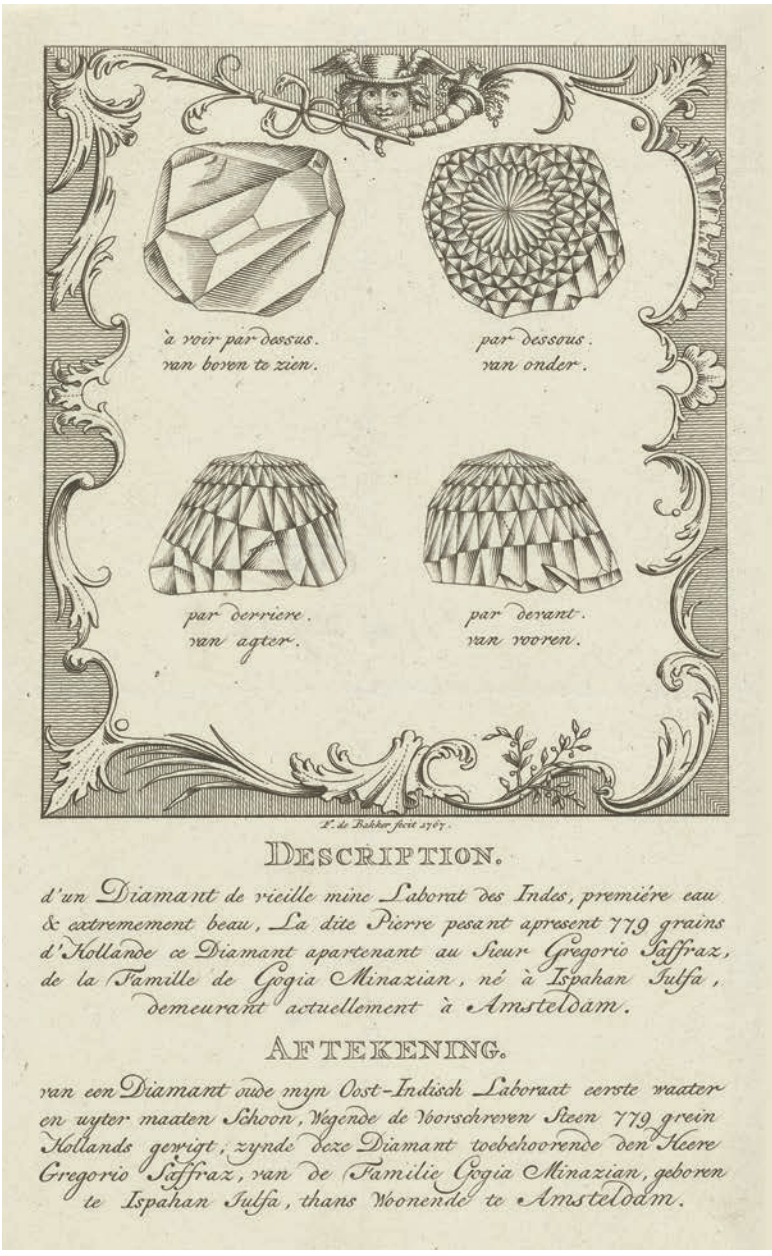

'our carats'—similarly as for French livres, which he described as 'our money'—the famous diamantaire had in mind the French carat commonly used in his home country, the weight of which was about 0.205 g (Tavernier, 1692). In that case, 1 ratti would correspond to about 0.179 g or about 0.896 metric carats, and the 319.5 rattis reported for the Great Mughal Diamond would thus correspond to ~286 ct.

However, according to 17th century Mughal and Deccani chronicles, and most importantly a letter from Shah Jahan (the owner of the stone) to the king of Golconda, the weight of the Great Mughal diamond was 9 *tanks*, which some of these sources indicate is equivalent to 216 rattis or surkhs (e.g. Mīr 'Ālam, AH[1] 1266; Khāfī Khān, 1869; Kanbūh and Yazdani, 1939; Aziz, 1942; Sarkar, 1951; Awranghābādī et al., 1999), rather than the 319.5 rattis reported by Tavernier. A weight of 216 rattis corresponds to ~193.5 ct, if the metric carat conversion suggested above is used. Again, the current weight of the Orlov diamond is 189.62 ct.

Tavernier and the Great Mughal Diamond

If in fact the Great Mughal was actually somewhat over 190 ct, why did Tavernier overstate the weight? For this we are left with conjectures. To the best of this author's knowledge, there are three possible explanations: (1) a mistake in estimating its weight, (2) purposeful deceit or (3) his knowledge of the diamond was gained indirectly, for example, on the basis of accounts given by others.

The possibility that Tavernier made a mistake in estimating the weight of the diamond by nearly 90 ct seems impossible for such an experienced diamantaire (Paxton, 1856). Therefore one might consider that Tavernier deliberately overstated the weight of the diamond, perhaps intending to evoke a stronger impression on those readers who were told since the 16th century about the fabulous riches of the Mughal Empire (Foster, 1921; Keene and Kaoukji, 2001). However, this author feels that the most probable explanation is that Tavernier possessed only indirect knowledge of the Great Mughal diamond. It is known that the Frenchman did in fact include in his work drawings and detailed descriptions of gems that he did not examine personally. Among this group were, for example, gems of the ruler of Bijapur and the Shah of Persia; he most probably gained the information about these during his travels from royal gem keepers or merchants.[2] It is also probable that he obtained knowledge about one of the most famous diamonds of the Muslim world—the Great Table, from which were cut the Nur al-Ayn and Darya-ye Nur stones now found in the treasury of Iran—not by analysing the original gem, as he claims, but by examining a model of the stone (Malecka, 2014a; Malecka, in prep.-a).

The possibility that Tavernier gained information about the Great Mughal diamond from third parties is supported by his drawing of this stone (again, see Figure 3), which was described by one 19th century scholar as 'rough' or 'rude' (Maskelyne, 1860a,b). His drawing could easily have been made on the basis of a description, and therefore not all the details depicted in it should be assumed credible.[3] Indirect knowledge may account for the fact that depictions of other historical diamonds may differ significantly from one another (I'timād al-Salṭanah, AH 1349; Tavakkulī Bazzāz, AH 1380; Diba et al., 1998; Raby, 1999).

If indeed Tavernier obtained information indirectly about the Great Mughal diamond, this certainly does not preclude that the presentation of Aurangzeb's jewels, which he mentioned, actually took place. The showing of valuables from the treasury was often practised in the Muslim world (al-Tanūkhī, AH 1393). It should be underscored, however, that during Tavernier's visit, the most valuable jewels of the Mughal court were not in the possession of Aurangzeb, but rather were kept by his jailed father Shah Jahan, who refused to give them up despite requests from his son (Manucci, 1907; Begley and Desai, 1990). As a connoisseur of gems, Shah Jahan most certainly was attached to his collection of precious objects. It should be emphasized as well that in the Islamic world, the

[1] In reporting the year of ancient scripts, 'AH' means *Anno Hegirae*, or 'in the year of the Hijra'.

[2] Another potential source of Tavernier's information—court inventories—should be excluded, in this author's opinion. First, there is no evidence that the Frenchman had any access to them. Second, a survey of equivalent surviving material from the Islamic world shows that the weight and/or drawings of even large stones was never or rarely noted (Topkapı Sarayı Müzesi Arşivi, AH 1091).

[3] It has also been suggested that the drawings contained in Tavernier's work of the stones he most certainly saw and handled may not be fully credible (Sucher, 2009).

involuntary transfer of valuable stones to another ruler indicated the giver's subservient status; this was particularly the case for diamonds in Mughal India, as their possession was an imperial monopoly (Ferishta, 1829; de Coutre, 1991; Boym, 2009; Malecka, in prep.-b).

It is well worth adding that the most important gems, functioning as regalia, were often worn by the rulers personally. It is also known that Shah Jahan would display a diamond given to him by Mir Jumla by placing it on his turban (Valentijn, 1726; Malecka, in prep.-b). This author finds it doubtful that Shah Jahan would have given a stone of this importance to his son prior to being incarcerated. Such an event would have undoubtedly been noted by court chroniclers scrupulously registering movements of large gems. In view of the above considerations, this author suspects, as did some 19th–20th century authorities, that during Tavernier's visit to the Mughal court, the Great Mughal diamond in fact was in the possession of Shah Jahan, and this excluded the possibility of it being examined by the Frenchman (Maskelyne, 1860a; Aziz, 1942).

Due to large discrepancies regarding the weight of the diamond from Persian-language sources of the epoch as compared to Tavernier's work, the present author deduces that Tavernier did not actually see the Great Mughal diamond. The presumed weight of the Great Mughal, however, both before (~790 ct) and after fashioning (~286 ct), probably was not invented by the Frenchman himself.[4] Tavernier reported the mass of imperial gems by using various units popular in India, which he recalculated into carats only in the case of the diamond in question. It may therefore be supposed that the presumed weights of the Great Mughal both prior to and after polishing were obtained from the imperial treasure keeper, who could have demonstrated the tendency—not at all alien to his profession—to overstate the weight of gems possessed by his master (Brydges Jones, 1833; Meen and Tushingham, 1968; Malecka, in prep.-b). Most likely, this same source also provided Tavernier with information pertaining to the polished stone's appearance.

[4] According to eminent Russian mineralogist Alexander Fersman, one of the few experts who has studied the Orlov, this stone was cut probably from a rough stone weighing ~400 ct (Fersman, 1955). Assuming that the Great Mughal diamond is identical to the Orlov, this provides an additional argument for negating Tavernier's statement that the rough stone from which the Great Mughal was cut weighed ~790 ct.

Conclusions

According to Persian-language sources from the epoch, in 1656 the Great Mughal diamond weighed about 193.5 ct. This is quite close to the 189.62 ct of the Orlov diamond at the Kremlin. The weight difference of ~3.8 ct is very small compared to the sizes of these stones. In fact, various sources from the Great Mughal's time period and cultural circle have indicated that the weight of an important gem could differ by more than a dozen carats (Sāravī Fatḥ Allāh, AH 1371; Sālūr et al., AH 1374; Riḍā' Qulī Khān Hidāyat, AH 1380; Fasā'ī Ḥusainī and Fasā'ī Rastgār, 1988). In this author's opinion, due to similarities in weight, shape, type of cut and flaws, the stone given in 1656 by Mir Jumla to Shah Jahan was in fact the same as the diamond presently known as the Orlov. Since it must have been presented to Shah Jahan in polished form, the abovementioned account by Tavernier about it being cut by Hortensio Borgio cannot be true.

This article provides strong evidence that Tavernier did not see the diamond he described, since during his visit at the Mughal court the stone most probably was in the possession of Shah Jahan. The scene of examination of this stone was then contrived by the Frenchman in order to make the text more attractive and was incorporated into the chapter containing descriptions of Aurangzeb's valuables shown to him.

References

Anonymous, 1853. History of the diamond. *The Eclectic Magazine of Foreign Literature, Science, and Art*, January, 12–13.

Anonymous, 1866. O bolshom imperatorskom almaze. *Russkiy Arkhiv,* Vypusk 4 [see p. 644].

Awrangābādī S.K., Shāhnavāz ʿA.a-H.i. and Prashad B., 1999. *The Maāthir-ul-Umarā: Being Biographies of the Muhammādan and Hindu Officers of the Timurid Sovereigns of India from 1500 to about 1780 A.D.*, Vol. 2. Low Price Publications, Delhi, India [see p. 191].

Aziz A., 1942. *The Imperial Treasury of the Indian Mughuls*. Idarah-i-Adabiyāt-i-Delli, Delhi, India [see pp. 190, 220, 242].

Balfour I., 2009. *Famous Diamonds*, 5th edn. Antique Collectors' Club, Woodbridge, Suffolk, 335 pp. http://dx.doi.org/10.1108/09504121011012094, [see pp. 112, 118, 211].

Ball V., 1889. Appendix I: I. The Great Mogul's diamond and the true history of the Koh-i-Nur. In J.-B. Tavernier, *Travels in India*, Vol. 2, Cambridge University Press, Cambridge, 2012, 431–449, http://dx.doi.org/10.1017/CBO9781139192125.

Begley W.E. and Desai Z.A., 1990. *The Shah Jahan Nama of 'Inayat Khan: An Abridged History of the Mughal Emperor Shah Jahan (...)*. Oxford University Press, Delhi, India, 624 pp. [see p. 564].

Boym M., 2009. *Michała Boyma Opisanie Świata*. Ed. and transl. by E. Kajdański, Oficyna Wydawnicza Volumen, Warsaw, Poland, 325 pp. [see pp. 299–300].

Bruton E., 1970. *Diamonds*. N.A.G. Press, London, 372 pp. [see Fig. 10.1, p. 160].

Brydges Jones H., 1833. *The Dynasty of the Kajars*. J. Bohn, London [see p. cxxxviii].

de Coutre J., 1991. *Andanzas Asiáticas*. Ed. by E. Stols, B. Teensma and J. Verberckmoes, Historia 16, Madrid, Spain, 494 pp. [see pp. 254–267].

Diba L., Ekhtiar M. and Robinson B.W., Eds., 1998. *Royal Persian Paintings: The Qajar Epoch 1785–1925*. Brooklyn Museum of Art in association with I.B. Tauris Publishers, Brooklyn, New York, USA, 296 pp. [see nos. 40, 76].

Dutens L., 1783. *Des Pierres Précieuses et des Pierres Fines avec les Moyens de les Connaître & de les Évaluer*. Joseph Molini, Florence, Italy, 151 pp. [see p. 33].

Fasā'ī Ḥusainī Ḥ. and Fasā'ī Rastgār M., 1988. *Fārsnāmah-'i Nāṣirī*, Vol. 1. Mu'assasah-i Intishārāt-i Amīr Kabīr, Tehran, Iran, 866 pp. [see p. 659].

Ferishta M.K., 1829. *History of the Rise of the Mahomedan Power in India, till the Year AD 1612*, Vol. 3. Transl. by J. Briggs, Cambridge University Press, Cambridge, 2013, 544 pp., http://dx.doi.org/10.1017/CBO9781139506670 [see p. 84].

Fersman A., 1922. Almaz Shah. *Izvestiya Rossiiskoi Akademii Nauk*, Seriia 6, **16**(1–18), 451–462.

Fersman A., 1924–25. *Almaznyi Fond SSSR*. Narodnoy Kommissariat Finansov, Moscow, Russia, Vypusk IV [see pp. 10–11].

Fersman A., 1955. *Kristallografiia Almaza*. Izd-vo Akademii Nauk SSSR, Moscow, Russia, 566 pp. (republished in 2013 by Book on Demand Ltd.) [see p. 482].

Foster W., 1921. *Early Travels in India, 1583–1619*. S. Chand, Delhi, India, https://archive.org/details/earlytravelsinin00fostuoft [see pp. 101–102, 112].

Gemelli Careri G.F., 1700. *Giro del Mondo del Dottor D. Gio. Francesco Gemelli Careri*, Vol. 3. Giuseppe Roselli, Naples, Italy, https://archive.org/details/girodelmondodeld03geme [see pp. 264-265].

Halhed N.B., 1776. *A Code of Gentoo Laws, or, Ordinations of the Pundits (...),* London, 396 pp., https://archive.org/details/codeofgentoolaws00halh [see p. 11].

Harlow G.E., 1998. *The Nature of Diamonds*. Cambridge University Press in association with the American Museum of Natural History, Cambridge and New York, New York, USA, 278 pp. [see p. 110].

Hinz W., 1955. *Islamische Masse und Gewichte; Umgerechnet ins metrische System*. E.J. Brill, Leiden, The Netherlands, 66 pp.

Howard H., 1677. A description of the diamond-mines, as it was presented by the Right Honourable, the Earl Marshal of England, to the Royal Society. *Philosophical Transactions of the Royal Society*, **12**, 907–917, http://dx.doi.org/10.1098/rstl.1677.0028.

I'timād al-Salṭanah, AH 1349. *Sadr al-tawārīkh: Sharh-i ḥāl-i ṣadr a'ẓamhā-i pādshāhān-i qājār; az Hājj Ibrāhīm Kalāntar ta Mīrzā 'Alī Aṣgar Khān Amīn as-Sulṭān*. Ed. by M. Ḥ Khān, Waḥīd, Tihrān [see p. 91].

Jagnaux R., 1885. *Traité de Minéralogie Appliquée aux Arts, a l'Industrie, au Commerce et a l'Agriculture*. Octave Doin, Paris, France, 883 pp. [see p. 171].

Kanbūh M.S. and Yazdani G. 1939. *'Amal-i Ṣāliḥ: al-mawsūm bih Shāh'jahān'nāmah*, Vol. 3. Asiatic Society, Calcutta, India [see p. 235].

Keene M. and Kaoukji S., 2001. *Treasury of the World: Jewelled Arts of India in the Age of the Mughals*. Thames & Hudson in association with the al-Sabah Collection, Dar al-Athar al-Islamiyyah and Kuwait National Museum, London, 160 pp. [see p. 6].

Kelly P., 1832. *Oriental Metrology; Comprising the Monies, Weights, and Measures of the East Indies, and other Trading Places in Asia, Reduced to the English Standard by Verified Operations*. Longman, Rees, Orme, & Co., London, 178 pp. [see pp. 30, 36, 48, 91].

Khāfī Khān M.H., 1869. *The Muntakhab al-lubāb of Khāfī Khān*, Part 1. Ed. by Ahmad Kabīr al-Dīn, College Press, Calcutta, India [see p. 753].

King C.W., 1867. *The Natural History, Ancient and Modern, of Precious Stones and Gems, and of Precious Metals*, Vol. 1. Bell & Daldy, London [see pp. 82–83].

Kuznetsova L.K., 2009. *Peterburgskie Iuveliry: Vek Vosemnadtsatyĭ, Brilliantovyĭ*. Tsentrpoligraf, Moscow, Russia, 542 pp. [see p. 174].

Lockyer C., 1711. *An Account of the Trade in India (...)*. Samuel Crouch, London, 352 pp. [see p. 263].

Malecka A., 2014a. The mystery of the Nur al-'Ayn diamond. *Gems&Jewellery*, **23**(7), 20–22.

Malecka A., 2014b. Did Orlov buy the Orlov? *Gems&Jewellery*, **23**(6), 10–12.

Malecka A., in prep.-a. Was the Great Table a Safavid stone? On the origin of the most important crown jewel of Iran.

Malecka A., in prep.-b. *Amulets, Poisons and Royal Splendor: Diamonds in the Islamic World*, Part II: Diamond Biographies.

Manucci N., 1907. *Storia do Mogor: Or Mogul India, 1653–1708*, Vol. II. Ed. and transl. by W. Irvine, John Murray, London, 482 pp. [see p. 20].

Maskelyne N.S., 1860a. On diamonds. *The Chemical News*, **1**, 208–213.

Maskelyne N.S., 1860b. On diamonds. *The Engineer*, **9**, 25 May, 329.

Master S., 1911. *The Diaries of Streynsham Master, 1675–1680, and Other Contemporary Papers Relating Thereto*. Ed. by R.C. Temple, John Murray, London, 512 pp., https://archive.org/details/diaries16751680o02mastuoft [see pp. 172–174].

Meen V.B. and Tushingham A.D., 1968. *Crown Jewels of Iran*. University of Toronto Press, Toronto, Canada, 159 pp. [see p. 53.].

Mīr 'Ālam, Abū al-Qāsim, AH 1266. *Ḥadīqat al-'ālam*, Vol. 1. Hyderabad, India [see, p. 357].

Moneta Cavenago-Bignami S., 1980. *Gemmologia*. Hoepli, Milan, Italy, 1,734 pp. [see pp. 282–283].

Moreland W.A., 1931. *Relations of Golconda in the Early Seventeenth Century*. Hakluyt Society, London, 109 pp. [see pp. 31–33].

Pallas (P.S.), 1805. Istoricheskoie izvestie o bolshom almaze, nakhodiashchemsa nynie v rossiisko-imperatorskom skipetre. *Vestnik Evropy*, **12**, June [see p. 291].

Paxton J.R., 1856. *Jewelry and the Precious Stones: With a History, and Description from Models, of the Largest Individual Diamonds Known: Including, Particularly, a Consideration of the Koh-i-Noor's Claim to Notoriety*. John Penington & Son, Philadelphia, USA, 40 pp., https://archive.org/details/jewelrypreciouss00paxt [see p. 20].

Polynina I., 2012. *Sokrovishcha Almaznogo Fonda Rossii*. Slovo, Moscow, Russia [see p. 190].

Raby J., 1999. *Qajar Portraits*. Azimuth Editions in association with the Iran Heritage Foundation, London, 104 pp. [see no. 110].

Riḍā' Qulī Khān Hidāyat, AH 1380. *Tārīkh-i rawḍat aṣ-ṣafā fī sīrat al-anbiyā' wa al-mulūk wa al ḫulafā'*, Vol. XIII. Aṣāṭīr, Tihrān [see p. 7,098].

Rybakov B.A., 1975. *Sokrovishcha Almaznogo Fonda SSSR* [*Treasures of the USSR Diamond Fund*]. Izobrazitelnoe Iskusstvo, Moscow, Russia [see Skipetr Imperatorskii entry].

Sālūr Q.M., Sīstānī Ī.A., Afshār Ī. and Sālūr M., AH 1374. *Rūznāmah-'i khāṭirāt-i 'Ayn al-Salṭanah*, Vol. 2. Asāṭīr, Tihrān [see p. 1,014].

Sāravī Fatḥ Allāh M., AH 1371. *Tārīkh-i Muḥammadī: Aḥsan al-Tavārīkh*. Mu'assasah-i Intishārāt-i Amīr Kabīr, Tehran, 403 pp. [see p. 255].

Sarkar J.N., 1951. *The Life of Mir Jumla, the General of Aurangzab*. Thacker, Spink, Calcutta, India, 362 pp. [see p. 106].

Schrauf A., 1869. *Handbuch der Edelsteinkunde*. Druck und Verlag von C. Gerold's Sohn, Vienna, Austria, 252 pp. [see pp. 103–104].

Shcherbina E., 2014. *Indiia: Dragotsennosti, Pokorivshie Mir*. Gosudarstvennye Muzei Moskovskogo Kremlia, Moscow, Russia, 427 pp. [see p. 15].

Shipley R.M., 1955. *Famous Diamonds of the World*. Gemological Institute of America, Los Angeles, California, USA, 62 pp. [see pp. 13–15].

Streeter E.W., 1882. *The Great Diamonds of the World. Their History and Romance*. Ed. by J. Hatton and A.H. Keane, George Bell & Sons, London, 346 pp., https://archive.org/details/greatdiamondsofw00stre [see p. 69].

Sucher S., 2009. A crystallographic analysis of the Tavernier Blue diamond. *Gems & Gemology*, **45**(3), 178–185, http://dx.doi.org/10.5741/gems.45.3.178.

al-Tanūkhī, Muḥsin ibn 'Alī, AH 1393. *Mukhtaṣar Nishwār al-muḥāḍarah wa-akhbār al-mudhākarah*, Vol. 8. Dār Ṣādr, Beirut, Lebanon [see pp. 243–245].

Tavakkulī Bazzāz M., AH 1380. *Gawhar-i Īrān*. Mu'assasah-i Farhangī Hunarī-i Āryan, Tihrān, 159 pp. [see p. 118].

Tavernier J.-B., 1676. *Les Six Voyages de Jean Baptiste Tavernier (…) en Turquie, en Perse, et aux Indes (…)*. Paris, France, 604 pp.

Tavernier J.-B., 1692. *Les Six Voyages de Jean Baptiste Tavernier (…) en Turquie, en Perse, et aux Indes (…)*, Vol. 2. Paris, France, 782 pp. [see pp. 278–279, 294, 549].

Topkapı Sarayı Müzesi Arşivi, AH 1091. *Manuscript D*. 12/1–2.

Valentijn F., 1726. *Oud en nieuw Oost-Indiën (…)*, Vol. 4, Part 2. Joannes van Braam, Dordrecht, The Netherlands, 151 pp.

Zimin I.V. and Sokolov A.R., 2013. *Iuvelirnye Sokrovishcha Rossiiskogo Imperatorskogo Dvora* [*The Jewelry Treasure of the Russian Imperial Court*]. Tsentrpoligraf, Moscow, Russia, 766 pp. [see table 25].

The Author

Anna Malecka
Kalima Project, Abu Dhabi Authority for Culture and Heritage, United Arab Emirates
Email: diamonds.malecka@gmail.com

Acknowledgement

The author wishes to thank three anonymous reviewers for their useful comments and assistance in the preparation of this paper.

A Lead-Glass-Filled Corundum Doublet

Supparat Promwongnan, Thanong Leelawatanasuk and Saengthip Saengbuangamlam

In September 2015, a 1.75 ct pink sapphire was submitted to the Gem and Jewelry Institute of Thailand's Gem Testing Laboratory (GIT-GTL). The stone showed internal features (e.g. flash effects and trapped gas bubbles) that are commonly seen in lead-glass-filled rubies and sapphires. In addition, the sample turned out to be an assembled stone, consisting of a pink sapphire crown and a near-colourless sapphire pavilion. These two portions were joined along a lead-glass-filled contact layer slightly below the girdle that locally contained areas of corundum fragments. We concluded that this stone was a lead-glass-filled corundum doublet.

The Journal of Gemmology, **35**(1), 2016, pp. 64–68, http://dx.doi.org/10.15506/JoG.2016.35.1.64

Introduction

Lead-glass-filled corundum was first encountered over a decade ago, and has continued to appear in the gem market in various forms (see, e.g., Kitawaki, 2004; Smith et al., 2005; McClure et al., 2006; Milisenda et al., 2006; SSEF, 2009; Henn et al., 2014, Leelawatanasuk et al., 2015; Ounorn and Leelawatanasuk, 2015; Panjikar, 2015). Nowadays such treated stones are widely available, mostly in the low-end jewellery market. The starting material typically consists of low-quality corundum, although a variety of colours and transparencies have been treated by this method (see references above). In September 2015, the GIT-GTL received an unusual lead-glass-filled sapphire that was characterized for this report.

Sample and Methods

The 1.75 ct sample consisted of a pear-shaped modified brilliant measuring 8.32 × 7.21 × 3.81 mm (Figure 1). We used standard gemmological instruments to measure the stone's properties, and its internal features were observed with both a gemmological microscope and an immersion microscope using methylene iodide. In addition, the gem was viewed with a DiamondView instrument. We used a Thermo Nicolet 6700 Fourier-transform infrared (FTIR) spectrometer

Figure 1: This 1.75 ct pear-shaped stone proved to consist of a sapphire doublet containing fissures and cavities filled with lead glass. Photo by S. Saengbuangamlam.

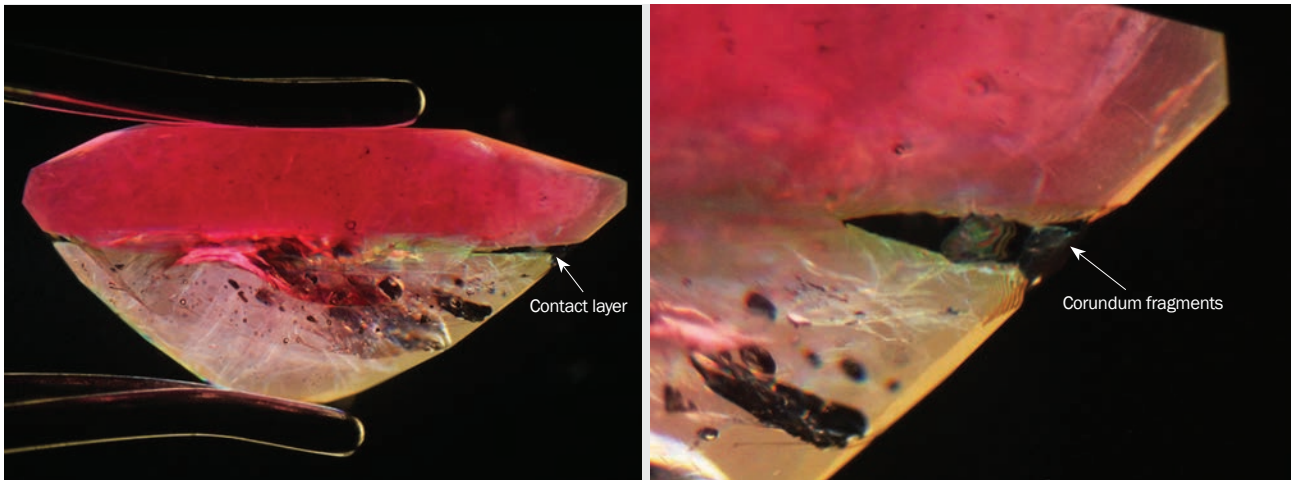

Figure 2: The doublet consists of a pink sapphire crown and a near-colourless sapphire pavilion that are joined along a contact layer located slightly below the girdle (left, image width 6.5 mm). Viewed with higher magnification, the contact layer is seen to locally consist of dark (isotropic) glassy material containing some anisotropic angular fragments of corundum (right, image width 2.2 mm). Photomicrographs by S. Promwongnan, in immersion with cross-polarized light.

to obtain IR transmittance spectra in the range of 4000–400 cm^{-1}. X-radiography was performed with a Softex SFX-100 instrument. Chemical analysis was carried out by energy-dispersive X-ray fluorescence (EDXRF) spectroscopy using an Eagle III system.

Results

Basic Properties

The gemmological properties of this stone were consistent with natural corundum. It had RIs of 1.770–1.761 (measured on the table facet) and a hydrostatic SG of 3.98. The polariscope gave a doubly refractive, uniaxial negative reaction. The stone fluoresced moderate red to long-wave UV radiation, with somewhat weaker luminescence to short-wave UV.

Microscopic Features

When the sample was examined using an immersion microscope between crossed polarizers, it was obvious that it was actually a composite stone (Figure 2, left). It consisted of a doublet formed of two distinctly different pieces: pink sapphire for the crown and near-colourless sapphire for the pavilion. These two pieces were joined together along a contact layer located slightly below the stone's girdle. Higher magnification (Figure 2, right) revealed that the contact layer was filled with glassy material that locally contained randomly oriented fragments of corundum.

Further examination with a standard gemmological microscope at high magnification showed internal features indicative of lead-glass-filled corundum. A blue flash effect associated with filled fractures/fissures was the most prominent characteristic, and was seen in both the pink and near-colourless portions (Figure 3a). Several trapped gas bubbles also were clearly seen in the filled fissures (Figure 3b). Additional inclusions consisted of minute particulates (Figure 3c) and planar 'fingerprints' (Figure 3d), which suggested that the corundum pieces forming both parts of this stone were of natural origin.

In the DiamondView, the relatively low lustre of the glass-filled cavities could be seen easily with reflected light using the instrument's sample chamber illuminator (Figure 4a). When exposed to the DiamondView's deep-UV excitation, the glassy material was inert and appeared as dark areas along the contact layer and in fissures and cavities, in contrast to the strong red fluorescence of the host corundum (Figure 4b,c). In places, the contact layer contained some bright-luminescing angular fragments of corundum embedded in the dark-appearing glassy material.

Mid-Infrared Spectroscopy

The mid-IR spectrum of the sample showed broad absorption features at approximately 3500, 2597 and 2256 cm^{-1} that are commonly present in lead-glass-filled corundum (Figure 5).

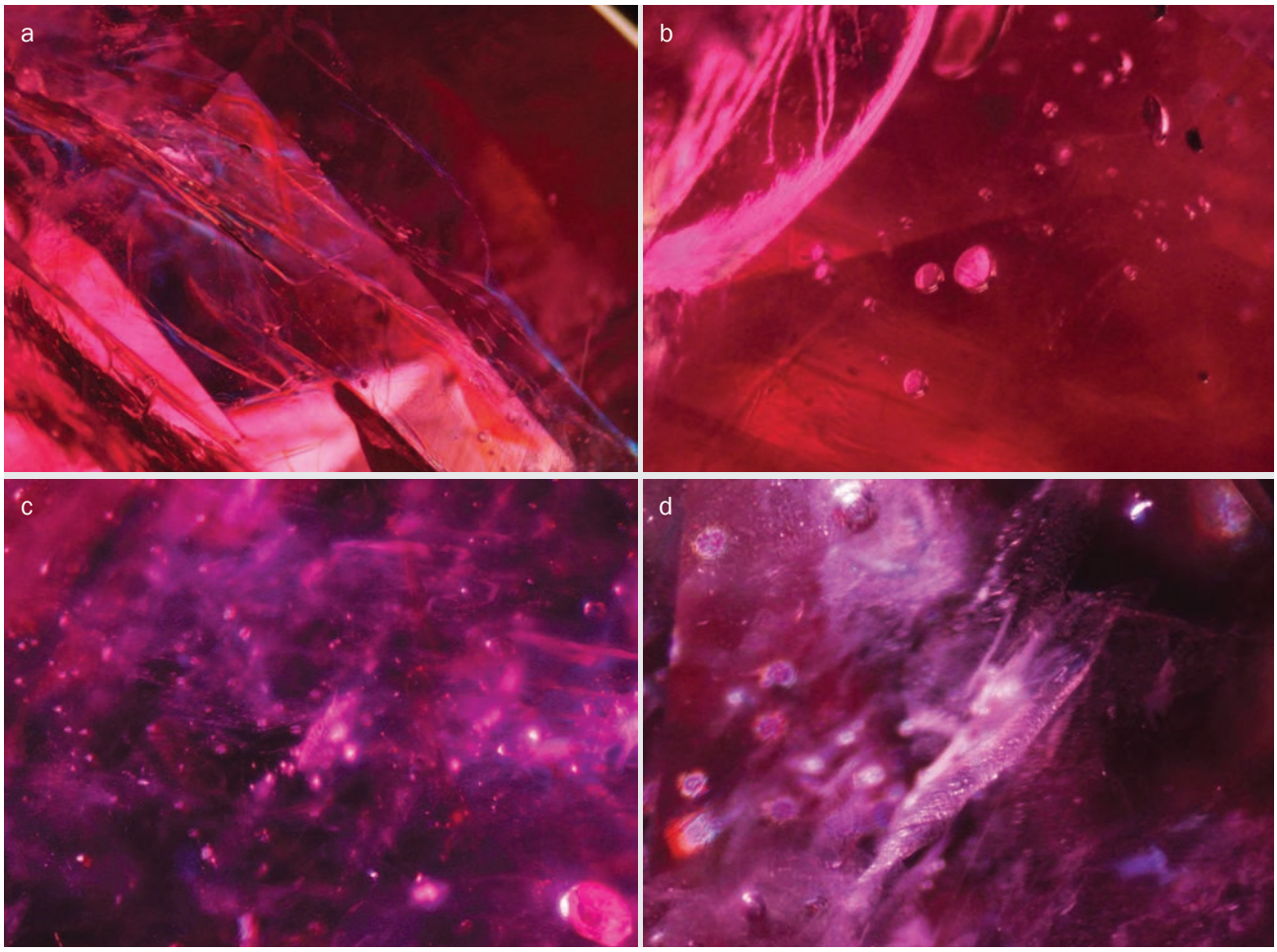

Figure 3: Internal features seen in the lead-glass-filled corundum doublet consist of (a) several filled fractures showing blue flash effects, (b) gas bubbles trapped inside the filler, (c) minute particulates and (d) planar fingerprints. Photomicrographs by S. Promwongnan; image widths 2.1, 1.5, 1.6 and 1.1 mm for photos a–d, respectively.

X-radiography

The X-ray image of the stone (Figure 6, left) revealed that the contact layer consisted of a high-density (dark-appearing) material. Furthermore, high-density material also was present along many fractures inside the host corundum and in cavities on the stone's surface. These results are consistent with the presence of a lead-containing glass filler in fissures and cavities, as well as within the contact layer of this doublet.

Figure 4: These DiamondView images of the 1.75 ct lead-glass-filled corundum doublet show the sample in reflected light from the sample chamber illuminator (a), and exposed to ultra-short-wave UV radiation (b and c). The glass filler has a low lustre in reflected light, and is inert to UV radiation—in contrast to the strong red fluorescence of the host corundum. Note also the presence of some angular fragments of corundum in the glassy material along the contact layer between the crown and pavilion (particularly in image c). Photos by S. Promwongnan.

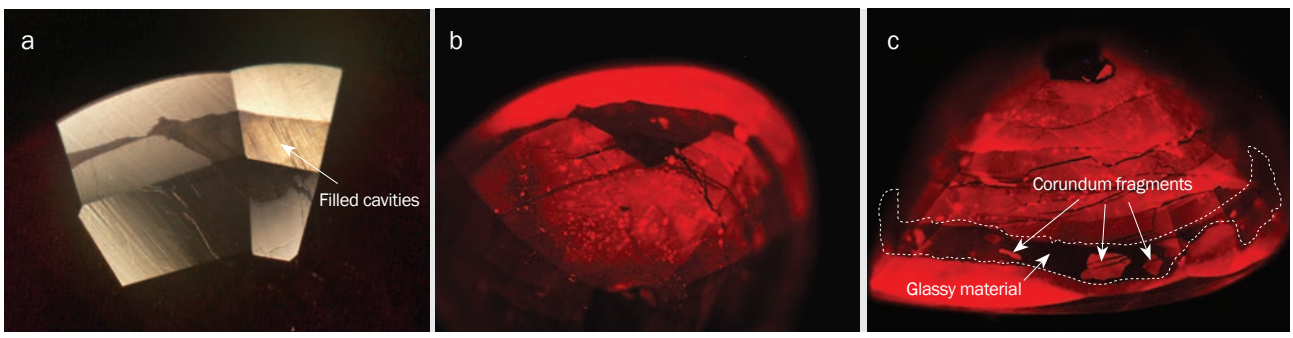

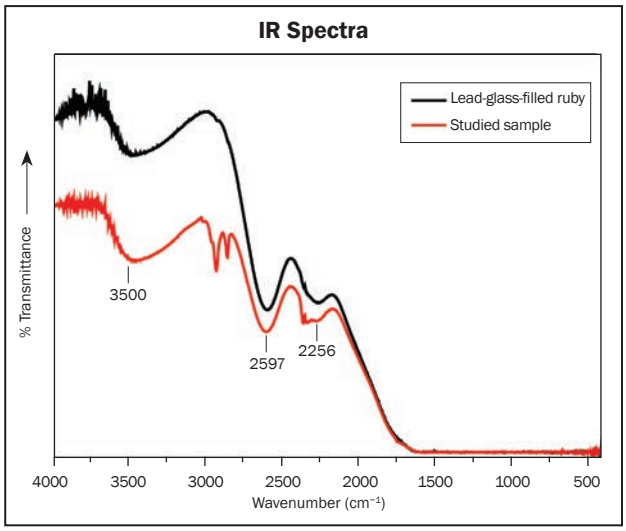

Figure 5: FTIR transmittance spectra are shown here for the tested corundum doublet as compared with a lead-glass-filled ruby reference sample. Both spectra display similar broad bands at approximately 3500, 2597 and 2256 cm^{-1} that are commonly seen in lead-glass filled materials. The bands at approximately 3000–2900 cm^{-1} in the doublet may be due to sample contamination (finger oils, etc.).

Chemical Analysis

EDXRF spectroscopy of the crown and pavilion sides of the corundum doublet showed traces of Ti, V, Cr, and Fe (and Ga in the crown); as expected, the Cr content of the pink sapphire forming the crown side was much higher than that of the near-colourless pavilion (Table I). Also detected were significant amounts of Pb and Si in both portions of the stone, which confirmed that it was lead-glass filled. Much greater quantities of these elements were detected in the pavilion than in the crown, apparently due to a larger amount of glass filling encountered by the beam in that area (i.e. within fractures and/or in the contact layer of the doublet).

Table I: Trace-element contents by EDXRF of the corundum doublet.

Area	TiO_2	V_2O_5	Cr_2O_3	Fe_2O_3	Ga_2O_3	SiO_2	PbO_2
Crown	0.03	0.02	0.57	0.19	0.01	0.36	0.39
Pavilion	0.02	0.02	0.11	0.19	nd*	1.63	7.11

* Abbreviation: nd = not detected.

Discussion and Conclusions

Based on the above evidence, it is clear that this stone was a lead-glass-filled doublet composed of pink and near-colourless sapphire. The presence of small, angular corundum fragments within the glass-filled contact layer suggests that these two pieces could have been accidentally or intentionally brought together during the lead-glass treatment process. Bonding together of their flat surfaces enabled this composite material to be cut into an attractive but deceiving gemstone. Thus, this sample should be referred to as a lead-glass-filled corundum doublet.

References

Henn U., Schollenbruch K. and Koch S., 2014. Gem Notes: Corundum with colored lead-glass fillings. *Journal of Gemmology*, **34**(2), 111–112.

Figure 6: An X-ray image (left) of the lead-glass-filled corundum doublet is shown with a corresponding view taken in immersion with cross-polarized light (right). The X-rays reveal a high-density material that appears as dark areas in fractures and fissures, and along the contact layer between the crown and pavilion. Photos by S. Promwongnan; image width 6.4 mm.

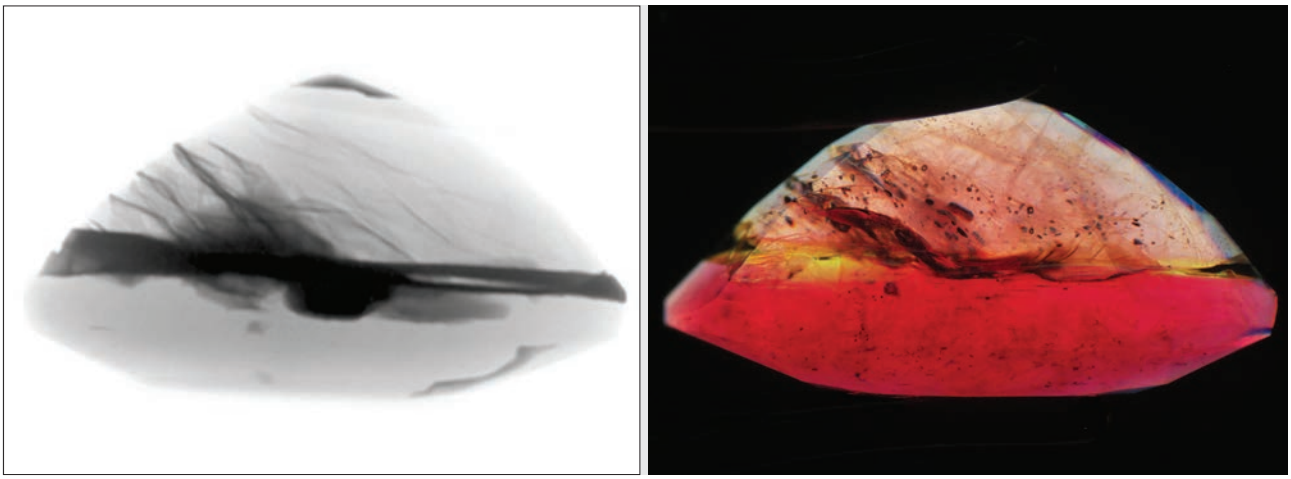

Kitawaki H., 2004. Lead-glass impregnated ruby. *Gemmology*, **45**(416), May, 18 (in Japanese with English translation).

Leelawatanasuk T., Susawee S., Promwongnan S. and Atsawatanapirom N., 2015. Green lead-glass-filled sapphires. *Journal of Gemmology*, **34**(5), 420–427, http://dx.doi.org/10.15506/jog.2015.34.5.420.

McClure S.F., Smith C.P., Wang W. and Hall M., 2006. Identification and durability of lead glass–filled rubies. *Gems & Gemology*, **42**(1), 22–34, http://dx.doi.org/10.5741/gems.42.1.22.

Milisenda C.C., Horikawa Y., Manaka Y. and Henn U., 2006. Rubies with lead glass fracture fillings. *Journal of Gemmology*, **30**(1–2), 37–42, http://dx.doi.org/10.15506/jog.2006.30.1.37.

Ounorn P. and Leelawatanasuk T., 2015. GIT Lab Update: Yellow lead-glass-filled sapphire. The Gem and Jewelry Institute of Thailand, Bangkok, 16 July, www.git.or.th/2014/eng/testing_center_en/lab_notes_en/glab_en/2015/07/16/Yellow_Lead-glass_filled_sapphire.pdf.

Panjikar J., 2015. Gem Notes: Lead-glass-filled yellow sapphires. *Journal of Gemmology*, **34**(6), 488–489.

Smith C.P., McClure S.F., Wang W. and Hall M., 2005. Some characteristics of lead-glass-filled corundum. *Jewellery News Asia*, **255**, November, 79–84.

SSEF, 2009. How much glass is in the ruby? *SSEF Facette*, **19**, 8–9, www.ssef.ch/fileadmin/Documents/PDF/facette16.pdf.

The Authors

Supparat Promwongnan, Thanong Leelawatanasuk and Saengthip Saengbuangamlam
The Gem and Jewelry Institute of Thailand
4th Floor, ITF Tower, Silom Road, Bangrak
Bangkok 10500, Thailand
Email: lthanong@git.or.th

Acknowledgements

The authors thank Dr Pornsawat Wathanakul, Dr Visut Pisutha-Anond, Wilawan Atichat and Boontawee Sriprasert for their valuable suggestions and their extensive reviews of this article.

A. Kleiman & Co.

Simply...
Pure...
Quality

Natural and Untreated +1-415-982-3500

Tucson AGTA GemFair

Hong Kong March Gem Show at the Asia World Expo

BASELWORLD

Las Vegas AGTA GemFair

Hong Kong September Gem Fair at the Asia World Expo

Conferences

AGA Tucson Conference

The 2016 Accredited Gemologists Association Conference in Tucson, Arizona, USA, took place 3 February, with the theme 'Where in the World?—Origin of Gem Species & More'. Attended by 132 people, the event was moderated by AGA president Stuart Robertson, and featured six speakers.

Andrew Cody (Cody Opal, Melbourne, Australia) began the conference with a presentation on the various types of opal, their attributes and where they have been mined, as well as current pricing trends for fine Australian opal.

Dr Daniel Nyfeler (Gübelin Gem Lab, Lucerne, Switzerland) reviewed 10 years of using laser ablation–inductively coupled plasma–mass spectrometry (LA-ICP-MS) in his gemmological laboratory. The trace-element data provided by this technique is useful for the detection of treatments and synthetics, and also for determining a gem's geographic origin. To obtain meaningful data, it is necessary to employ a highly trained and knowledgeable operator, to have a comprehensive collection of reference samples, and to use appropriate data reduction and processing procedures.

Claire Mitchell (Gem-A, London) described the use of the spectroscope in gemmology. After reviewing the history and development of studying absorption bands in gems and minerals, she explained the differences between prism and diffraction-grating spectroscopes, and gave several tips on how to obtain good spectra (e.g. the use of strong lighting; see Figure 1). She then described the various types and applications of advanced spectroscopic instrumentation.

Richard Hughes (Lotus Gemology, Bangkok, Thailand) gave a presentation called 'Forests and Trees—Ten Lessons in Gemology' that conveyed some of his experience and research gleaned from decades of working with gems. An overall principle that he emphasized was to beware when things do not make sense and to get more information before making a decision.

Shawn O'Sullivan gave a presentation for **Arthur Groom** (Eternity Natural Emerald, Ridgewood, New Jersey, USA) on the clarity enhancement of emerald. He indicated that it is difficult for gem laboratories to accurately assess the amount or effect of fracture filling because the stones are not seen by the labs before treatment (and after cleaning of the fissures). His company no longer cleans emeralds unless they also perform the enhancement, since some unscrupulous dealers were obtaining laboratory reports on cleaned stones and then having them treated.

Figure 1: Gem-A's Claire Mitchell demonstrates the use of strong fibre-optic lighting to obtain a good spectrum of a transparent gemstone with a handheld spectroscope. Photo by Henry Mesa.

Marc Beverly (University of New Mexico, USA) described his experience visiting an enormous cavern containing giant selenite crystals in Naica, Chihuahua State, Mexico. The hot and humid conditions in the cave, combined with the sharp and slippery crystals, created hazardous conditions, but the selenites were awe-inspiring. The expedition has been documented in a National Geographic video that is accessible at www.youtube.com/watch?v=0OLdSJmvcUs.

The conference was followed by the AGA Gala, where The Antonio C. Bonanno Award for Excellence in Gemology was presented to Dr Cigdem Lule (Gemworld International Inc., Glenview, Illinois, USA).

Brendan M. Laurs

GILC Tucson Conference

The Gemstone Industry & Laboratory Conference took place on 1 February 2016 in Tucson, Arizona, USA (Figure 2). The event was moderated by GILC chairman Edward Boehm, and was attended by approximately 80 invitees.

Dr Lore Kiefert (Gübelin Gem Lab, Lucerne, Switzerland) gave a presentation for **Dr Daniel Nyfeler** on the radiogenic age dating of gems. The ages of many gem deposits worldwide are well constrained, particularly for corundum and emerald. At the Gübelin Gem Lab, surface-reaching zircon inclusions in selected client stones are now being analysed by LA-ICP-MS to determine the age of the host sapphire or ruby (for more information, see *The Journal* article by K. Link, 'Age determination of zircon inclusions in faceted sapphires', **34**(8), 2015, 692–700). Combined with other methods, the resulting age information provides a useful piece of data to aid geographic origin determination.

Dr James Shigley (Gemological Institute of America, Carlsbad, California, USA) reviewed GIA's research on the observation and measurement of colour in gems. Faceted gemstones display a complex face-up appearance that is influenced by several factors, including the light source, faceting style, colour (and colour distribution), visual effects (windowing, extinction, etc.), pleochroism and reflections from the observer or viewing environment. To accurately calculate colour coordinates of a gem, these factors must be taken into account, as well as the colour sensitivity of the human eye.

Bruce Bridges (Bridges Tsavorite, Tucson, Arizona, USA) examined the traceability of a gem from the source to the end consumer. He gave examples of some stones that are vertically integrated through some or all stages of mining, processing, cutting and marketing, such as tsavorite from his operation in Kenya, demantoid from the Green Dragon mine in Namibia, emerald from the Belmont mine in Brazil and ruby from True North's project in Greenland. At the end of his presentation, he posed the question, "At what level does traceability start?"

These talks were followed by a general discussion session that provided a lively debate on laboratory terminology for describing colour on reports. The conference concluded with a special announcement by **Ruben Bindra** (president of the American Gem Trade Association) that AGTA had revised its 'Code of Ethics and Principles of Fair Business Practice' to include mine-to-market traceability and transparency source disclosure protocols; the International Colored Gemstone Association adopted the revised code at the ICA Board of Directors meeting on 31 January in Tucson.

Brendan M. Laurs

Figure 2: Attendees of the GILC Conference in Tucson listen to one of the presentations. The topics at this year's event included the age dating of gems, colour measurement and observation, and traceability from the source to the end consumer. Photo by Sherri Graves.

Jewelry Industry Summit

The first Jewelry Industry Summit for Responsible Sourcing was held at the Fashion Institute of Technology in New York, New York, USA, on 10–13 March 2016. The 160 attendees represented all sectors of the industry from mining to retail, including manufacturers, designers and educators, as well as NGOs and personnel from the U.S. Department of State.

The five primary objectives of the summit were as follows:

Figure 3: Participants of the Jewelry Industry Summit joined focus groups to discuss various topics related to socially and environmentally responsible practices in the gem and jewellery industry. Photo by Peggy Jo Donahue.

1. Generate a broad-based awareness of facts related to the jewellery industry supply chain and responsible sourcing, and explore what works and what does not.
2. Create a shared vision that ensures viability of the supply chain and all jewellery businesses as they evolve to meet changing expectations from industry members and the consuming public.
3. Explore the possibility of generating industry-wide goals that all members of the supply chain can reasonably work toward.
4. Begin to develop guiding principles that will help any sector make progress through continuous improvement.
5. Decide if and how to implement and measure the success of any plan resulting from these discussions.

Administration of the summit was coordinated by **Suzan Flamm**, **Cecilia Gardner** and **Sara Yood**, all of the Jewelers Vigilance Committee (New York City). **Cheri Torres** and **Mike Feinson** of Innovation Partners International were hired to facilitate the summit, and they kept ideas flowing by creating focus groups to brainstorm on various topics (e.g. Figure 3) and report back to the larger group. This invited every attendee to be engaged and feel part of the discussion process.

Formal presentations were made by various companies within and outside the jewellery industry to share inspirational stories of success, as well as challenges they faced along the way. The format included a panel of presenters from the jewellery industry that consisted of Eric Braunwart (Columbia Gem House, Vancouver, Washington, USA) on small-scale and artisanal mining, **Jamie McGlinchey** (Melissa Joy Manning, Brooklyn, New York) on socially responsible jewellery creation, **Marcelo Ribeiro** (Belmont, Minas Gerais, Brazil) on socially and environmentally responsible emerald mining in Brazil, and **Stewart Grice** (Hoover & Strong, North Chesterfield, Virginia, USA) on socially and environmentally responsible precious metals refining.

Following the panel discussion, **Eric Jens** (ABN AMRO Bank, Amsterdam, The Netherlands) presented his company's strategy to help its clients generate business opportunities. He also handed out an attractive brochure ('Sustainable Diamond Jewellery Guide') outlining the details of their strategy. Though it was written with diamonds in mind, many of the practices could theoretically be applied to the coloured stone industry as well.

There were two presenters from outside industries. **Maria Gorsuch-Kennedy** (EMC Corp., Boston, Massachusetts, USA) discussed supply-chain sustainability and how EMC applies its environmental and conflict minerals program throughout its computer hardware product lifecycle. **Margo Sfeir** (Elevate Global Ltd., New York City) described the responsible-sourcing management tools that her company has developed to help private-label product companies identify management practices to improve responsible sourcing.

Responsible-sourcing protocols were addressed by **David Bouffard** (Signet Jewelers, Akron, Ohio, USA) and **Andrew Bone** (Responsible Jewellery Council [RJC], London). Bouffard detailed Signet's commitment to maintaining and improving consumer confidence in jewellery products by addressing the social, ethical and environmental risks facing the industry at large. He outlined their recently launched responsible-sourcing protocol for diamonds, which was built on the United Nations' Guiding Principles on Business and Human Rights and the Due Diligence Guidance for Responsible Supply Chains developed by the Organisation for Economic Co-operation and Development (OECD). Bone focused on RJC's independently audited Code of Practices and Chain-of-Custody Certification and how they relate to diamonds, gold and platinum-group

metals. RJC, a not-for-profit organization, currently has over 700 stakeholders.

Inspiring stories were presented by **Anna Bario** (Bario Neal, Philadelphia, Pennsylvania, USA) and **Eduardo Escobedo** (Responsible Ecosystems Sourcing Platform [RESP], Troinex, Switzerland). Bario described the rapid success her company has achieved while focusing on handcrafted jewellery made with reclaimed precious metals, fair-mined gold, ethically sourced gemstones and low-impact environmentally conscious practices. Escobedo explained RESP's mission to create positive environmental, social and economic impacts by fostering change toward the sustainable use of natural resources. A relative newcomer, RESP works with the cosmetics, fashion and jewellery industries; it recently published a report titled 'Challenges to Advancing Environmental and Social Responsibility in the Coloured Gems Industry' (see What's New entry on page 2 of this issue).

Dorothée Gizenga (Diamond Development Initiative [DDI], Ottawa, Ontario, Canada) gave a fascinating presentation on her organization's activities to transform artisanal mining into a source for sustainable development (Figure 4). Through collective small-scale mining groups who meet certain fair-trade protocols, DDI helps the miners sell their rough diamonds to selected buyers. DDI also provides assistance to these miners with housing, education and safer working conditions.

Figure 4: Dorothée Gizenga spoke at the Jewelry Industry Summit about Diamond Development Initiative's efforts to transform artisanal mining into a source for sustainable development for small-scale miners. Photo by Peggy Jo Donahue.

Lynsey Cesca Jones (VF Corp., Greensboro, North Carolina, USA) explained how her company has addressed supply-chain sourcing issues. VF is a lifestyle, footwear and accessories company that owns brands such as North Face, Timberland, Wrangler, Nautica and JanSport. Jones presented real-world scenarios and how her company addressed these challenges through improved responsible sourcing practices.

Hannah Koep-Andrieu (OECD) discussed the OECD Due Diligence Guide for Responsible Supply Chains of Minerals from Conflict-Affected and High-Risk Areas. These guidelines recommend a five-step framework for risk-based due diligence in the mineral supply chain: (1) Establish strong company management systems, (2) identify and assess risk in the supply chain, (3) design and implement a strategy to respond to identified risks, (4) carry out independent third-party audits and (5) report on supply-chain due diligence.

Ideas resulting from the brainstorming sessions that were held during the summit were posted on the walls of the two main meeting rooms. As the days progressed, the ideas were refined to possible goals and initiatives. Attendees were then encouraged to come up with a number of action plans and select those that each wanted to support. Examples included helping miners and gem cutters in developing countries with safety education and using better equipment to avoid health-related issues, educating and conveying responsible-sourcing information to jewellery sales associates, researching consumer attitudes about responsible sourcing and sustainability, and communicating through various media the accomplishments of the industry in these areas.

Finally, volunteers were solicited to steward the summit into its next steps and future meetings. Many industry leaders stepped up to join the new committee.

Interested readers are encouraged to visit the summit's website (www.jewelryindustrysummit.com/new-page-3) to download information sheets related to the responsible sourcing of diamonds, coloured stones, and gold and precious metals, as well as a list of useful links regarding legal requirements, voluntary standards, association and company practices, and sourcing activities by other industries outside the gem and jewellery sector.

Edward Boehm (edward@raresource.com)
RareSource, Chattanooga, Tennessee, USA

Gem-A

THE GEMMOLOGICAL ASSOCIATION
OF GREAT BRITAIN

Communicate colour with confidence

Sign up for our **Coloured Stones Grading Course**, in association with GemeWizard® — the leader in gem digital colour communication. At just £795, this course will provide you with a grounding in colour grading, an essential skill required for a successful career in appraisal, retail, auctioning and trading.

For more information or to sign up contact **education@gem-a.com**.

Creating gemmologists since 1908

Join us.

The Gemmological Association of Great Britain, 21 Ely Place, London, EC1N 6TD, UK. T: +44 (0)20 7404 3334 F: +44 (0)20 7404 8843.

Gem-A Notices

CEO APPOINTED

Alan Hart FGA DGA has been appointed Chief Executive Officer of Gem-A. A former member of the Gem-A Council, Hart is currently Head of Earth Sciences Collections at the Natural History Museum, London. With a wealth of experience in the gem and mineral trade, Hart started his career at the Natural History Museum in 1981 as Assistant Minerals Scientific Officer, and gained a BSc in geology from Birkbeck College, University of London, in 1994. He progressed to his current position of Principle Curator of Gems and Minerals and Head of Earth Sciences Collections in 2012.

Hart will assume his new position at Gem-A on 1 June 2016, and he will remain affiliated with the Museum as Associate Scientist with access to the collections.

GIFTS TO THE ASSOCIATION

The Association is most grateful to the following for their gifts for research and teaching purposes:

Eric Braunwart, Columbia Gem House, Vancouver, Washington, USA, for five pieces of rough hyalite (Guanajuato, Mexico), four faceted iolites (Wyoming, USA) and seven pieces of ruby in mica schist (Wyoming, USA).

Tom Chatham, Chatham Created Gems, San Francisco, California, USA, for a flux-grown synthetic sapphire crystal containing a platinum inclusion.

Anzor Douman, Arzawa Mineralogical Inc., Winchester, Virginia, USA, for specimens of rough sodalite (Afghanistan), turquoise (Iran), demantoid (Iran), a sapphire crystal (Pakistan), and rough and cut Mali garnets.

Zena Haddad for a square plate of Kenyan soapstone called a 'Kisii stone' after the Kisii tribe that lives in the Tabaka Hills in western Kenya; the plate features a giraffe image.

Craig Hazelton, Lafayette, Colorado, USA, for a phenakite crystal (Aquatera claim, Mt. Antero, Colorado, USA).

Dr Jaroslav Hyršl, Prague, Czech Republic, for a rough piece of sekaninaite (Dolní Bory, Moravia, Czech Republic).

Dr Michele Macrì, Rome, Italy, for four faceted chrome diopsides (Brazil).

Marcus McCallum FGA, Hatton Garden, London, for a copy of *Gems&Jewellery*, **1**(4), 1992 (following a Gem-A appeal for that issue).

Mauro Pantò, The Beauty in the Rocks, Laigueglia, Savona, Italy, for faceted specimens of ceruleite (Peru), hyalite (Hungary), agatized coprolite (Utah, USA), stichtite (South Africa), sunstone (Norway) and neptunite (Benitoite Gem mine, California, USA).

Helen Serras-Herman FGA, Gem Art Center, Rio Rico, Arizona, USA, for a slab of 'bumble bee jasper' from Indonesia.

Ashish Sogani, Rakhi Inc., New York, New York, USA, for a mother-of-pearl bead and a glass-filled sapphire, and faceted samples of amethyst, green crackled quartz, rock crystal (faceted bead), tourmalinated quartz, labradorite and 'tiger iron' quartz.

Dr Thet Tin Nyunt, Gemological Science Centre, Yangon, Myanmar, for two rough pieces of colourless beryl (Kuaukse, Mandalay, Myanmar).

Sid Tucker, Homedale, Idaho, USA, for pyrope gem gravel concentrated by ants (Navajo Nation, Arizona, USA).

Dr Marco Campos Venuti, Seville, Spain, for a rough piece of polyhedral agate (Rio Grande do Sul, Brazil) and a cabochon reportedly cut from thomsonite (Portugal).

Bear Williams FGA and **Cara Williams FGA**, Stone Group Labs, Jefferson City, Missouri, USA, for six simulated turquoise beads (dyed and stabilized magnesite) showing various colours and markings.

MEMBERSHIP

At a meeting of the Council held on 11 March 2016, Miranda Wells was appointed as Chair of the Gem-A Council. Wells, Head of Gemmology at Birmingham City University and Course Director of the BSc (Hons) Gemmology & Jewellery Studies degree, has been a member of the Council for four years. The Council also appointed Paul Greer DGA and Kerry Gregory FGA DGA as Vice Chairs. Wells succeeds Nigel Israel FGA DGA, who remains a member of the Council.

The Council of the Association have elected the following to membership:

Fellowship (FGA)

Baptiste, Karen Anne, Panadura, Sri Lanka
Chan Wai Keung, Kowloon, Hong Kong
Davison, Alexander, Southend-on-Sea, Essex
Ji Kaijie, Shanghai, P.R. China
Saksirisamphan Rimml, Phornthip, Näfels, Switzerland
Slootweg, Peter, Nootdorp, Zuid-Holland, The Netherlands
Wang Siyu, Beijing, P.R. China

Diamond Membership (DGA)

Belsham, Lesley, Great Dunmow, Essex
Imre, Alexandra Terez Jenssen, Sevenoaks, Kent

Associate Membership

Armstong, Ceri Louise, Clapham, London
Armstrong, Richard, Flint, Texas, USA
Corkum, John, Niagara Falls, Ontario, Canada
Golden, Scott, Houston, Texas, USA
Hamadi, Sam, Newcastle-upon-Tyne, Tyne & Wear
Kearns, Bobbi, Knoxville, Tennessee, USA
Oakley, Sally, Wombourne, Staffordshire
Van Leeuwen, Suzanne, Amsterdam, The Netherlands
Wheat, Barbara, Astoria, New York, USA

OBITUARY

Leonard Baker
1921–2016

Leonard Alfred Baker FGA (D. 1948), of Ferndown, Dorset, passed away on 21 March 2016. At Gem-A's centenary celebration in 2013, Leonard was honoured with a Lifetime Membership as the longest-standing Fellow of the Association.

Leonard was born in Barnsbury, North London, in March 1921. He entered the Royal Air Force in September 1940 as a mechanic working on Hampden bombers and volunteered on a number of occasions to fly as aircrew (gunner), during one of which he was shot down on a return trip from Hanover, Germany. He was discharged from the RAF in August 1946 with an unblemished record.

He joined his father, George Baker, to be trained as a jeweller before taking a jewellery manufacturing apprenticeship with master craftsman E. A. Wallace (formerly of English Art Works, who supplied Cartier). After attending night school to study gems, in 1948 he qualified in the Gemmology Diploma examination and became a Fellow of the Gemmological Association of Great Britain.

He then formed a manufacturing jewellery company, Leonard A. Baker Ltd. A facsimile of the jewelled peacock inspired by the throne of Titania's Palace earned his company recognition from the Arts Council, and he was awarded a Fellowship of the Royal Society of Arts (FRSA).

After 38 years of manufacturing jewellery for celebrities from around the world, his company gained the distinction of a unique official Post Office address: Messrs Leonard A. Baker Ltd, Oxford Circus, London, England. This was an achievement of which he was justly proud.

Although Leonard retired in 1984, he continued lecturing worldwide on gems and gemmology until 1997.

Leonard leaves his grandson Lee Baker (the author of this obituary), Lee's wife Caroline and great-grandson Luke. He will be sadly missed by close family and friends.

Lee Baker

Learning Opportunities

CONFERENCES AND SEMINARS

ASJRA's Weekend in Washington: Great Estates, Historic Jewelry, and Decorative Arts
13–14 May 2016
Washington DC, USA
www.jewelryconference.com/sched.html

30th Annual Santa Fe Symposium
15–18 May 2016
Albuquerque, New Mexico, USA
www.santafesymposium.org

37th World Diamond Congress
16–19 May 2016
Dubai, United Arab Emirates
http://diamondcongress2016.com

8th International Conference on Mineralogy and Museums
17–19 May 2016
Changsha, Hunan, China
www.mm8-2016.cn

SNAG^{neXt}
18–21 May 2016
Asheville, North Carolina, USA
www.snagmetalsmith.org/events/snagnext

China (Changsha) Mineral & Gem Show
19–23 May 2016
Changsha, China
www.changsha-show.com/enindex.html
Note: Includes a seminar programme.

10th International Conference on New Diamond and Nano Carbons
22–26 May 2016
Xi'an, China
http://ndnc2016.xjtu.edu.cn

JCK Talks 2016
2–6 June 2016
Las Vegas, Nevada, USA
http://lasvegas.jckonline.com/Education

Maine Pegmatite Workshop 2016
27 May–4 June 2016
Poland, Maine, USA
http://pegworkshop.com

12th International GeoRaman Conference
9–15 June 2016
Novosibirsk, Russia
http://georaman2016.igm.nsc.ru

Compiled by Georgina Brown and Brendan Laurs

15th Rendez-Vous Gemmologiques de Paris
13 June 2016
Paris, France
www.facebook.com/pages/Association-Française-de-Gemmologie

Scandinavian Gem Symposium
18 June 2016
Kisa, Sweden
http://sgs.gemology.se

Sainte-Marie-aux-Mines 53rd Mineral & Gem Show
23–26 June 2016
Sainte-Marie-aux-Mines, France
www.sainte-marie-mineral.com/english/modules/cultural-activities
Note: Includes a seminar programme.

2nd Eugene E. Foord Symposium on Pegmatites
15–19 July 2016
Golden, Colorado, USA
www.colorado.edu/symposium/pegmatite

Northwest Jewelry Conference
12–14 August 2016
Seattle, Washington, USA
www.northwestjewelryconference.com

46th ACE IT Annual Mid-Year Education Conference
13–16 August 2016
Newport Beach, California, USA
www.najaappraisers.com/html/conferences.html

Dallas Mineral Collecting Symposium
19–21 August 2016
Dallas, Texas, USA
www.dallassymposium.org

35th International Geological Congress
27 August–4 September 2016
Cape Town, South Africa
www.35igc.org
Sessions of Interest: Gems: Bringing the World Together; The Dynamic Earth and Its Kimberlite, Cratonic Mantle and Diamond Record Through Time; Diamonds and Crustal Recycling into Deep Mantle

Internationrence on Diamond and Carbon Materials
4–8 September 2016
Le Corum, Montpellier, France
www.diamond-conference.elsevier.com

ASA 2016 International Appraisers Conference
11–14 September 2016
Boca Raton, Florida, USA
www.appraisers.org/Education/conferences/ASA-Conference

2nd European Mineralogical Conference (emc2016)
11–15 September 2016
Rimini, Italy
http://emc2016.socminpet.it
Sessions of Interest: Gem Materials; Inclusions in Minerals as a Record of Geological Processes; New Analysis Methods and Application

IRV Loughborough Conference
17–19 September 2016
Loughborough
www.jewelleryvaluers.org/Loughborough-Conference

49th Annual Denver Gem & Mineral Show
16–18 September 2016
Denver, Colorado, USA
www.denvermineralshow.com
Note: Includes a seminar programme.

42nd Pacific Northwest Chapter Friends of Mineralogy Symposium
14–16 October 2016
Longview, Washington, USA
www.friendsofmineralogy.org/symposia.html

Gem-A Conference
5–8 November 2016
London
www.gem-a.com/news–events/gem-a-conference-2016.aspx

Gem and Jewelry Institute of Thailand Conference (GIT 2016)
14–15 November 2016
Pattaya, Thailand
www.git.or.th/2014/index_en.html

EXHIBITS

Europe

Fabergé – The Tsar's Jeweller and the Connections to the Danish Royal Family
12 May–25 September 2016
Museet på Koldinghus, Kolding, Denmark
www.koldinghus.dk/uk/exhibitions/exhibitions-2016/faberge.html

Open Space—Mind Maps. Positions in Contemporary Jewellery
Until 15 May 2016
Nationalmuseum Design, Stockholm, Sweden
www.nationalmuseum.se/English-startpage/Exhibitions/Open-Space--Mind-Maps

Take it Personally [jewellery and adornment]
Until 1 June 2016
Museum of Cultural History, Oslo, Norway
www.khm.uio.no/english/visit-us/historical-museum/temporary-exhibitions/2015/this-is-personal.html

A Motley Crew—New Pieces from the Collection
Until 12 June 2016
Schmuckmuseum, Pforzheim, Germany
www.schmuckmuseum.de/flash/SMP_en.html

Heavenly Bodies—The Sun, Moon and Stars in Jewellery
8 July–30 October 2016
Schmuckmuseum, Pforzheim, Germany
www.schmuckmuseum.de/flash/SMP_en.html

Elements: From Actinium to Zirconium
Until 26 February 2017
Ulster Museum, Belfast, Northern Ireland
http://nmni.com/um/What-s-on/Elements

Smycken: Jewellery. From Decorative to Practical
Ongoing
Nordiska Museet, Stockholm, Sweden
www.nordiskamuseet.se/en/utstallningar/jewellery

North America

A Passion for Jade: The Heber Bishop Collection
Until 19 June 2016
The Metropolitan Museum of Art, New York, New York, USA
www.metmuseum.org/exhibitions/listings/2015/passion-for-jade

Variations on a Theme: 25 Years of Design from the AJDC
Until July 2016
Gemological Institute of America, Carlsbad, California, USA
www.gia.edu/gia-museum-variations-theme-25-years-design-AJDC

Thunderbirds: Jewelry of the Santo Domingo Pueblo
Until 5 September 2016
Abby Aldrich Rockefeller Folk Art Museum, Williamsburg, Virginia, USA
http://tinyurl.com/zgyd54k

Fabergé from the Matilda Geddings Gray Foundation Collection
Until 27 November 2016
The Metropolitan Museum of Art, New York, New York, USA
www.metmuseum.org/exhibitions/listings/2011/faberge

Glitterati: Portraits & Jewelry from Colonial Latin America
Until 27 November 2016
Denver Art Museum, Denver, Colorado, USA
www.denverartmuseum.org/exhibitions/glitterati

Arts of Islamic Lands: Selections from The al-Sabah Collection, Kuwait
Until 29 January 2017
Museum of Fine Arts, Houston, Texas, USA
www.mfah.org/exhibitions/arts-islamic-lands-selections-al-sabah-collection-

American Mineral Heritage: Harvard Collection
Until February 2017
Flandrau Science Center & Planetarium, Tucson, Arizona, USA
http://flandrau.org/exhibits/harvard

Gold and the Gods: Jewels of Ancient Nubia
Until 14 May 2017
Museum of Fine Arts, Boston, Massachusetts, USA
www.mfa.org/exhibitions/gold-and-gods

Amber Secrets: Feathers from the Age of Dinosaurs
Ongoing
Houston Museum of Natural Science, Texas, USA
www.hmns.org/exhibits/special-exhibitions/amber-secrets-feathers-from-the-age-of-dinosaurs

City of Silver and Gold: From Tiffany to Cartier
Ongoing
Newark Museum, New Jersey, USA
www.newarkmuseum.org/SilverAndGold.html

Fabergé: From a Snowflake to an Iceberg
Ongoing
Houston Museum of Natural Science, Texas, USA
www.hmns.org/exhibits/special-exhibitions/faberge-a-brilliant-vision/

Gemstone Carvings
Ongoing
Houston Museum of Natural Science, Texas, USA
www.hmns.org/exhibits/special-exhibitions/gemstone-carvings

Gilded New York
Ongoing
Museum of the City of New York, New York, USA
www.mcny.org/content/gilded-new-york

Jewelry, from Pearls to Platinum to Plastic
Ongoing
Newark Museum, New Jersey, USA
www.newarkmuseum.org/jewelry

Mightier than the Sword: The Allure, Beauty and Enduring Power of Beads
Ongoing
Yale Peabody Museum of Natural History, Yale University, New Haven, Connecticut, USA
http://peabody.yale.edu/exhibits/mightier-sword-allure-beauty-and-enduring-power-beads

Australia

A Fine Possession: Jewellery & Identity
Until 22 May 2016
Powerhouse Museum, Sydney, New South Wales, Australia
www.powerhousemuseum.com/exhibitions/jewellery

OTHER EDUCATIONAL OPPORTUNITIES

Gem-A Workshops and Courses
Gem-A, London
www.gem-a.com/education/course-prices-and-dates.aspx

Advanced Diamond Program
16 or 17 May 2016
Birmingham
www.naj.co.uk/en/news/events-conferences.cfm/seminar-for-valuers-identifying-synthetic-and-treated-diamonds

Minerals and Gems: Unlocking the Earth's Treasure Chest
21 June–9 August 2016
Harvard University Summer School, Cambridge, Massachusetts, USA
www.summer.harvard.edu/courses/minerals-gems-unlocking-earths-treasure-chest/33384

Gemstone Safari to Tanzania
11–28 July 2016
Morogoro, Umba, Arusha, Longido, Merelani and Lake Manyara, Tanzania
www.free-form.ch/tanzania/gemstonesafari.html

Lectures with The Society of Jewellery Historians
Burlington House, London, UK
www.societyofjewelleryhistorians.ac.uk/current_lectures

28 June 2016
Neil Wilkin—Bronze Age Bodily Adornment: How was It Made and Worn?

27 September 2016
Galina Korneva—The Grand Duchess Maria Pavlovna's Contacts with Paris Jewellers and Her Collection of Treasures

25 October 2016
Robert Baines—Bogus or Real: Jewellery and the Capture of Human Drama

22 November 2016
Kieran McCarthy—Fabergé and London

Mayer & Watt

Want an *Ace* up your sleeve?

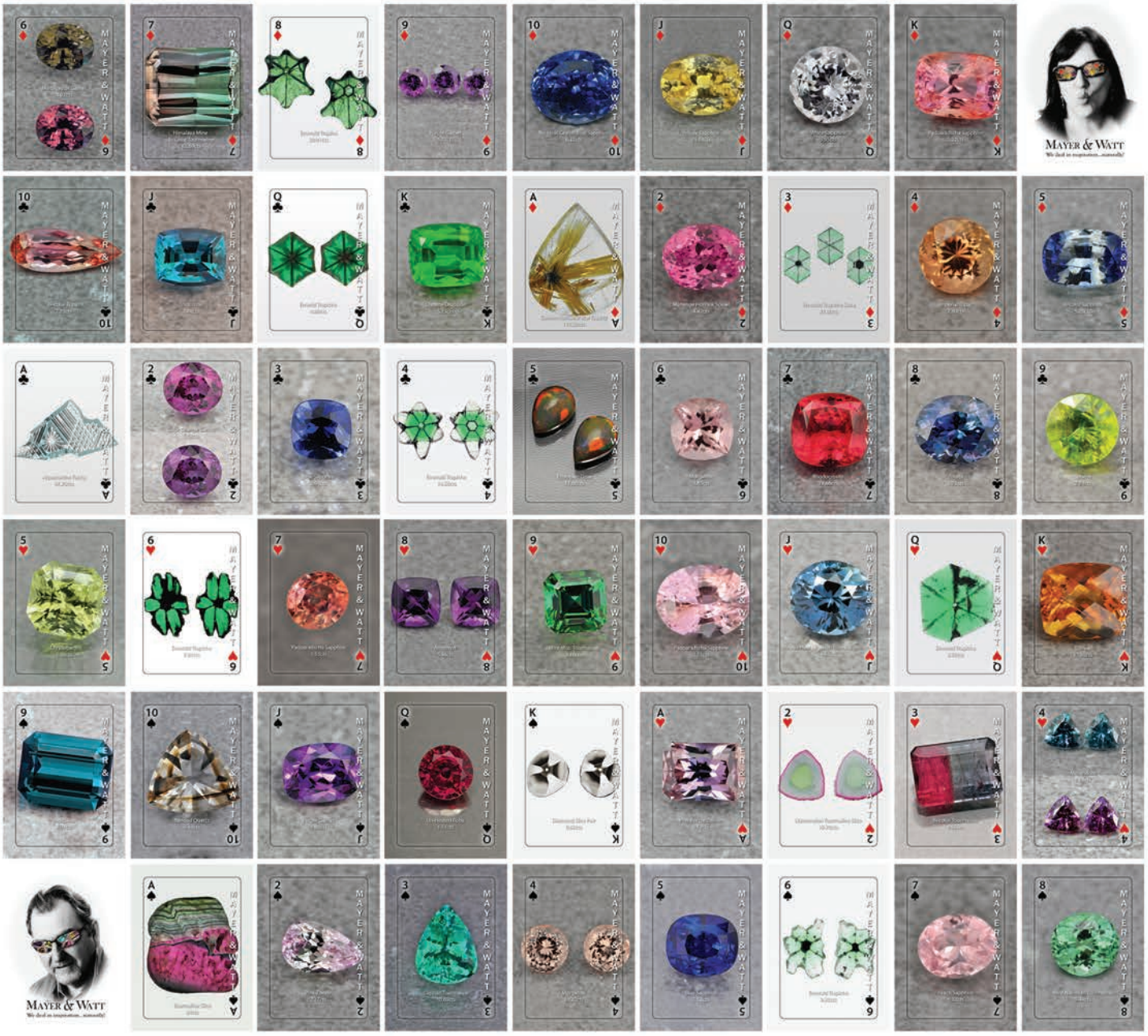

JCK Las Vegas AGTA
Booth #1005

Download the Mayer and Watt App for iOS/Droid.

We *Deal* in inspiration...Naturally.

www.mayerandwatt.com

New Media

Exotic Gems, Vol. 4: How to Identify, Evaluate & Select Jade & Abalone Pearls

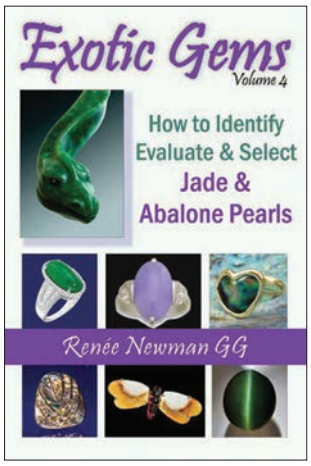

By Renée Newman, 2016. International Jewelry Publications, Los Angeles, California, USA, 136 pages, ISBN 978-0929975504. US$19.95 softcover.

This book is the fourth in a series covering exotic and unusual gems by Renee Newman that explores their history, lore, evaluation, geographic sources and identifying properties. I find these books very readable and highly recommend all of them.

In this Volume 4, *Jade & Abalone Pearls*, a quick perusal of the table of contents shows 12 chapters (116 pages) that are devoted to jade. The final, 13th, chapter dedicates 13 pages to understanding abalone pearls.

Well-written books on jade in the English language are rare. The advantages of this book are that it is inexpensive, understandable and extensively researched. Newman provides answers to most questions that a person with curiosity about gemstones might have. All of the chapters are well illustrated with numerous photographs depicting the corresponding content. Newman also uses tables effectively to illustrate various gemmological points.

The first chapter, 'Why Is Jade so Prized?', briefly covers what makes jade special, with sections titled Durability, Carvability, Color Palette, Auditive Quality, Luster, Rarity, Status Symbol, Therapeutic Virtues, Historical Significance, Investment Appreciation Potential and Spiritual & Mystical Significance. Newman covers these attributes in just four pages, but the reader can find more detailed explanations of some of them in the following chapters. Chapter 2 answers the question 'What Is Jade?' and is followed by Chapter 3, 'Jadeite or Nephrite Jade?' The latter includes a useful table, 'Characteristics of Jadeite Jade Versus Nephrite Jade', which compares and contrasts their various properties (e.g. chemical formulas, RIs, reaction to heat, etc.) according to 19 categories.

Chapters 4 and 5 cover imitations and treatments. Minerals and rocks that look like jade include more than a dozen varieties (e.g. chrysoprase, aventurine, etc.). Many treatments are performed on jade, including waxing, heating, coating and polymer impregnation, among others. These chapters provide a well-researched discussion of these aspects.

Chapter 6 offers a discussion of price factors for jadeite and nephrite, including colour, clarity, cutting style/shape, cut quality, carat weight or stone size, transparency, treatment status and texture. Figure 6.1 shows a magnificent jadeite ring that sold for US$101,400 at Sotheby's in 2004. (*Reviewer's note*: Today it could be valued at perhaps more than 10 times this amount.) Newman mentions that the highest auction price for a piece of jadeite jewellery was attained in 2014 (US$27,440,000 for a necklace sold by Sotheby's Hong Kong); China was the driving force. Several other notable auction pieces are described and pictured in detail. In this chapter Newman includes the Mason-Kay 'Colors of Jade' chart (Figure 6.8), which is one of my personal favourites and was nice to see reproduced here.

Chapters 7 through 12 cover various sources of jade—both nephrite and jadeite—including China, Myanmar (Burma), Guatemala, Canada, USA and other sources. All of these chapters provide interesting reading and anecdotes relating to these various jade localities.

Chapter 13 on abalone pearls gives a brief history of various localities, especially concentrating on North America, including Baja California (Mexico), and California and Oregon (USA). *Pāua* abalone mabe pearl cultivation is briefly mentioned. Identification, pricing and care are also discussed. Numerous photographs accompany the abalone pearl chapter.

The book ends with a bibliography and an index.

William F. Larson
Palagems.com, Fallbrook, California, USA

Gems & Crystals: From One of the World's Great Collections

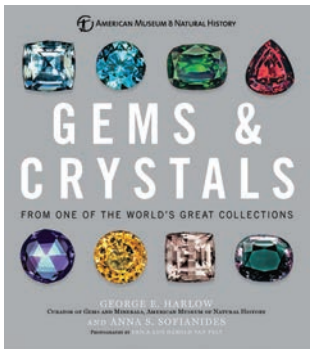

By George E. Harlow and Anna S. Sofianides, 2015. Sterling, New York, New York, USA, 232 pages, ISBN 978-1454917113. US$27.95 hardcover.

The first edition of this lovely picture book was published in 1990. The 2015 edition has been updated in several, but alas not all, subjects.

From One of the World's Great Collections in the title refers to the American Museum of Natural History (AMNH) in New York City, USA, which indeed has a great collection with a storied history. Names such as Dr G. F. Kunz, J. P. Morgan and Tiffany & Co. are associated with its early development; later mineral and gem curators included Herbert Whitlock, Dr Vincent Manson and Dr George Harlow, the present curator and an author of this book. Thus the history given in the book is rather parochial to the AMNH.

Part One describes what a gem is, first from a historical basis and then in terms of its mineralogy and desirable properties. The 'meat' of the book is found in Part Two, titled 'Gallery of Gems and Crystals', in which each important gem material is discussed either alone (e.g. diamond, topaz, opal) or in combination with similar materials (e.g. chrysoberyl with spinel, feldspar group minerals and garnet group minerals).

For each gem material, the description is subdivided into data, properties, historical notes, legends and lore, occurrences, materials that could be confused for the gem, evaluation criteria and, of course, is accompanied by beautiful pictures. The emphasis on history and especially lore is traditional for the AMNH, hearkening back to Kunz's interests. Although the scientific data are generally error-free, it would have been helpful if the authors had included a separate section on synthesis and gem treatments for each material, as this information is often critical in determining a gem's value.

Unfortunately, the information in this book is dated with regard to recent finds and changes in the availability of some gem materials. The section on garnets, for instance, treats 'malaia' as the latest variety, although since then spessartine from Namibia, grandite garnets from Mali and mint-green grossular from Tanzania have been discovered. The garnet section also starts with the old adage that garnets "come in every colour except blue", ignoring the relatively recent production of colour-change garnets that can vary with different illumination from purplish red to violetish blue, blue and greenish blue.

A second example of outdated information is the pearl section's omission of the tremendous availability of Chinese freshwater tissue-nucleated cultured pearls, which are now ubiquitous. Also, the range of colour-treated cultured pearls is much larger than before, and the flamboyantly iridescent abalone pearls are not mentioned. Perhaps the AMNH does not yet have excellent yet representative examples of these missing gem materials.

The authors also indicate that tanzanite is extremely rare, although in the past few decades, fine and commercial tanzanites have been about as available in jewellery stores as rubies, emeralds and sapphires. (Admittedly, this trend may not be permanent, as commercially important deposits of tanzanite are known from only a single source.)

Another problem with this book concerns the colour reproduction of some of the photographs. This is particularly the case for some green gems (e.g. amazonite, serpentine imitation of jade) and for the carved rose quartz *Fu* dog on page 134. Also in some figure captions for images containing more than one gem variety, it is not clear which stone is which material (e.g. the chalcedonies and other gems on page 145).

A last (mineralogical) criticism of this book is that the title is perhaps misleading. The AMNH has many excellent crystals, but with a few exceptions (e.g. amazonite), the only crystals shown are gemmy transparent examples of gem mineral crystals. Should the book instead be titled *Gems & Gemmy Gem Mineral Crystals*?

These issues aside, this is a very good book for understanding the stories and science behind gems, and for appreciating their incredible beauty. It is especially recommended for anyone who does not have the 1990 edition.

Dr Mary L. Johnson
Mary Johnson Consulting
San Diego, California, USA

OTHER BOOK TITLES*

Diamonds

***The Global Diamond Industry: Economics and Development,* Vol. I**
Ed. by Roman Grynberg and Letsema Mbayi, 2015. Palgrave Macmillan, Hampshire, 288 pages, ISBN 978-1137537577. £75.00 hardcover or £75.00 Kindle edition.

***The Global Diamond Industry: Economics and Development,* Vol. II**
Ed. by Roman Grynberg and Letsema Mbayi, 2015. Palgrave Macmillan, Hampshire, 320 pages, ISBN 978-1137537607. £75.00 hardcover or £75.00 Kindle edition.

***Rough Diamonds, a Practical Guide,* 2nd edn.**
By Nizam Peters, 2015. American Institute of Diamond Cutting, Deerfield Beach, Florida, USA, 274 pages, ISBN 978-0966585490. US$165.00 hardcover.

Gem Localities

***Minerals of Ohio*, 2nd edn.**
By Ernest H. Carlson, 2015. Ohio Department of Natural Resources Division of Geological Survey Bulletin 69, Columbus, Ohio, USA, 290 pages. US$30 hardcover.

Minerals of Georgia: Their Properties and Occurrences
By Julian Gray and Robert Cook, 2016. University of Georgia Press, Athens, Georgia, USA, 344 pages, ISBN 978-0820345581. US$32.95 flexibound.

New York Rocks & Minerals: A Field Guide to the Empire State
By Dan R. Lynch and Bob Lynch, 2016. Adventure Publications, Cambridge, Minnesota, USA, 264 pages, ISBN 978-1591935247. US$14.95 softcover.

General Reference

The Collector and His Legacy: Irénée du Pont and the Mineralogical Collection of the University of Delaware
By Sharon Fitzgerald, 2015. Mineralogical Record Inc., Tucson, Arizona, USA, 96 pages. US$15.00 softcover.

Gold: Nature and Culture
By Rebecca Zorach and Michael W. Phillips Jr., 2016. Reaktion Books, Edinburgh, Scotland, 224 pages, ISBN 978-1780235776. £14.95 softcover.

* Compiled by Georgina Brown and Brendan Laurs

Medieval Jewelry and Burial Assemblages in Croatia (East Central and Eastern Europe in the Middle Ages, 450–1450)
By Vladimir Sokol, 2015. Brill, Leiden, The Netherlands, 268 pages, ISBN 978-900418553. £92.00 softcover.

Mineral Collections in Austria
By Thomas Weiland, 2015. Mineralogical Record Inc., Tucson, Arizona, USA, 96 pages. US$15.00 softcover.

***Minerals: Their Constitution and Origin,* 2nd edn.**
By Hans-Rudolf Wenk and Andrey Bulakh, 2016. Cambridge University Press, Cambridge, 620 pages, ISBN 978-1107514041. £49.99 softcover, £95.00 hardcover or £47.49 Kindle edition.

***Moore's Compendium of Mineral Discoveries 1960–2015,* Vols. I and II**
By Thomas P. Moore, 2016. Mineralogical Record Inc., Tucson, Arizona, USA, 1,644 pages. US$399.00 hardcover.

The Munich Show/Mineralientage München: Theme Book Precious Stones
Ed. by The Munich Show, 2016. Wachholtz Verlag GmbH, 216 pages, ISBN 978-3529054617. €28.00 hardcover.

Jewellery and *Objets d'Art*

Art as Adornment: The Life and Work of Arthur George Smith
By Charles L. Russell, 2015. Outskirts Press, Parker, Colorado, USA, 264 pages, ISBN 978-1478744788. US$64.95 hardcover or US$56.95 softcover.

Asia Imagined: In the Baur and Cartier Collections
By Estelle Niklès van Osselt, 2016. Yale University Press, New Haven, Connecticut, USA, 368 pages, ISBN 978-8874397228. US$90.00 hardcover.

Cartier Dazzling: High Jewelry and Precious Objects
By François Chaille, 2016. Flammarion, Paris, France, 272 pages, ISBN 978-2080202604. €95.00 hardcover.

Pamela Love: Muses and Manifestations
By Pamela Love and Francesco Clemente, 2016. Rizzoli, New York, New York, USA, 176 pages, ISBN 978-0847848195. US$45.00 hardcover.

The Fire Within

"For in them you shall see the living fire of the ruby, the glorious purple of the amethyst, the sea-green of the emerald, all glittering together in an incredible mixture of light."

– Roman Elder Pliny, 1st Century AD

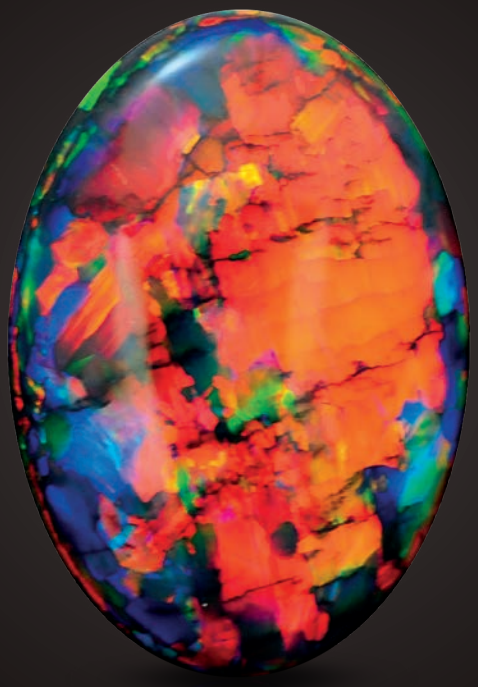

Black Opal 15.7 Carats

Suppliers of Australia's finest opals to the world's gem trade.

CODY OPAL

Level 1 - 119 Swanston Street Melbourne Australia

T. +61 3 9654 5533 E. info@codyopal.com

www.codyopal.com

INTERNATIONAL COLORED GEMSTONE ASSOCIATION MEMBER

JOG

Literature of Interest

Coloured Stones

Blue minerals: Exploring cause & effect. E.A. Skalwold and W.A. Bassett, *Rocks & Minerals,* **91**(1), 2016, 61–77, http://dx.doi.org/10.1080/00357529.2016.1099136.

Bumble bee 'jasper'. H. Serras-Herman, *Gems&Jewellery,* **24**(6), 2015, 26–28.

Chemistry of opal from Ethiopia. H. Ren and L. Li, *Journal of Gems & Gemmology,* **17**(4), 2015, 23–28 (in Chinese with English abstract).

Colorimetric analysis of green jadeite. D.J. Nie, Y. Zou and X.K. Zhu, in P. Chen (Ed.), *Material Science and Engineering,* Proceedings of the 3rd Annual 2015 International Conference on Material Science and Engineering, CRC Press/Balkema, Leiden, The Netherlands, 2016, 411–414, http://dx.doi.org/10.1201/b21118-87.

Fire obsidian. T. Dodge, *Gems&Jewellery,* **25**(1), 2016, 19–21.

Gemmological characteristic [*sic*] of peridot from Jiaohe, Jilin Province. J. Gu, Q. Zhao, J. Lai, C. Wang and Z. Yin, *Journal of Gems & Gemmology,* **17**(5), 2015, 24–31 (in Chinese with English abstract).

Gemmological characteristic [*sic*] of ruby and sapphire from Muling, Heilongjiang Province. Y. Liu and T. Chen, *Journal of Gems & Gemmology,* **17**(4), 2015, 1–7 (in Chinese with English abstract).

The history and occurrence of 'Buxton diamonds'. R. Starkey and J. Faithfull, *Journal of the Russell Society,* **18**, 2015, 24–45.

The Hope Chrysoberyl. A. Hart, *Gems&Jewellery,* **25**(1), 2016, 22.

Hope, Hertz and a red spinel. J. Ogden, *Gems&Jewellery,* **24**(6), 2015, 20–21.

Influence of impurities on Cr^{3+} luminescence properties in Brazilian emerald and alexandrite. N. Ollier, Y. Fuchs, O. Cavani, A.H. Horn and S. Rossano, *European Journal of Mineralogy,* **27**(6), 2015, 783–792, http://dx.doi.org/10.1127/ejm/2015/0027-2484.

Les jades, lapidaireries comparatives [The jades, lapidary comparisons]. E. Gonthier and I.-A. Gonthier, *Revue de Gemmologie A.F.G.,* **194**, 2015, 17–28.

Long-range and short-range order in gem pargasite from Myanmar: Crystal-structure refinement and infrared spectroscopy. D. Heaveysege, Y.A. Abdu and F.C. Hawthorne, *Canadian Mineralogist,* **53**(3), 2015, 497–510, http://dx.doi.org/10.3749/canmin.1400107.

Nano-structure of the cristobalite and tridymite stacking sequences in the common purple opal from the Gevrekseydi deposit, Seyitömer-Kütahya, Turkey. M. Hatipoğlu, Y. Kibici, G. Yanık, C. Özkul and Y. Yardımcı, *Oriental Journal of Chemistry,* **31**(1), 2015, 35–49, http://dx.doi.org/10.13005/ojc/310104.*

Oxygen isotopic composition as an indicator of ruby and sapphire origin: A review of Russian occurrences. S.V. Vysotskiy, V.P. Nechaev, A.Yu. Kissin, V.V. Yakovenko, A.V. Ignat'ev, T.A. Velivetskaya, F.L. Sutherland and A.I. Agoshkov, *Ore Geology Reviews,* **68**, 2015, 164–170, http://dx.doi.org/10.1016/j.oregeorev.2015.01.018.

Quartz: A bull's eye on optical activity. E.A. Skalwold and W.A. Bassett, 2015, 16 pages, www.minsocam.org/msa/OpenAccess_publications/Skalwold/Quartz_Bullseye_on_Optical_Activity.*

Pretty padparadscha. R.W. Hughes, *InColor*, **30**, 2016, 30-40.

Raman spectra, morphology and color of beryl. S. Dencheva and K. Bogdanov, *Geosciences 2015*, 10–11 December 2015, Sofia, Bulgaria, 15–16, http://tinyurl.com/jzwk8df.*

Source constraints on turquoise of the Erlitou site by infrared spectra. J. Ren, X. Ye, Y. Wang, S. Luo and G. Shi, *Spectroscopy and Spectral Analysis,* **35**(10), 2015, 2627–2772 (in Chinese with English abstract).

Tsavorite: Discovery of green vanadium-chrome grossular and its market situation analysis. Z. Li, S. Zhao, Z. Qiu, L. Li and X. Jin, *Journal of Gems & Gemmology,* **17**(4), 2015, 37–48 (in Chinese with English abstract).

U.S. state gemstones that are blue. M.I. Jacobson, *Rocks & Minerals,* **91**(1), 2016, 36–47, http://dx.doi.org/10.1080/00357529.2016.1099132.

Value factors, design, and cut quality of colored gemstones (non-diamond) [Parts 1 and 2]. A. Gilbertson, *GemGuide,* **35**(1), 2016, 2–13.

Value factors, design, and cut quality of colored gemstones (non-diamond) [Parts 3 and 4]. A. Gilbertson, *GemGuide,* **35**(2), 2016, 2–11.

Vanadium- and chromium-bearing pink pyrope garnet: Characterization and quantitative colorimetric analysis. Z. Sun, A.C. Palke and N. Renfro, *Gems & Gemology,* **51**(4), 2015, 348–369, http://dx.doi.org/10.5741/GemS.51.4.348.*

* Article freely available for download, as of press time

Cultural Heritage

The coral network: The trade of red coral to the Qing imperial court in the eighteenth century. P. Lacey, in A. Gerritsen and G. Riello (Eds.), *The Global Lives of Things—The Material Culture of Connections in the Early Modern World,* Routledge, New York, New York, USA, 2015, 81–102.

Exploitation of mother of pearl in the Middle Ages, Clos d'Ugnac archaeological site (Pennautier, Aude, France): Malacological study, consumption, exploitation and utilization of the nacre. L. Bertin, *Quaternary International,* **375**, 2015, 145–152, http://dx.doi.org/10.1016/j.quaint.2015.04.042.

The Grand Sapphire of Louis XIV and the "Ruspoli" sapphire: Historical and gemological discoveries. F. Farges, G. Panczer, N. Benbalagh and G. Riondet, *Gems & Gemology,* **51**(4), 2015, 392–409, http://dx.doi.org/10.5741/GEMS.51.4.392.*

Diamonds

The age of predictable primary diamond sources in the northeastern Siberian Platform. S.A. Grakhanov, N.N. Zinchuk and N.V. Sobolev, *Doklady Earth Sciences,* **465**(2), 2015, 1297–1301, http://dx.doi.org/10.1134/s1028334x15120193.

The characteristic photoluminescence and EPR features of superdeep diamonds (São-Luis, Brazil). O.P. Yuryeva, M.I. Rakhmanova, V.A. Nadolinny, D.A. Zedgenizov, V.S. Shatsky, H. Kagi and A.Yu. Komarovskikh, *Physics and Chemistry of Minerals,* **42**(9), 2015, 707–722, http://dx.doi.org/10.1007/s00269-015-0756-7.

The crucial role of crystallography in diamond research. F. Nestola, *Rendiconti Lincei,* **26**(2), 2015, 225–233, http://dx.doi.org/10.1007/s12210-015-0398-1.

Detection of diamonds in kimberlite by the tagged neutron method. V.Yu. Alexakhin, V.M. Bystritsky, N.I. Zamyatin, E.V. Zubarev, A.V. Krasnoperov, V.L. Rapatsky, Yu.N. Rogov, A.B. Sadovsky, A.V. Salamatin, R.A. Salmin, M.G. Sapozhnikov, V.M. Slepnev, S.V. Khabarov, E.A. Razinkov, O.G. Tarasov and G.M. Nikitin, *Nuclear Instruments and Methods in Physics Research Section A: Accelerators, Spectrometers, Detectors and Associated Equipment,* **785**, 2015, 9–13, http://dx.doi.org/10.1016/j.nima.2015.02.049.

Diamond formation due to a pH drop during fluid–rock interactions. D.A. Sverjensky and F. Huang, *Nature Communications*, **6**, 2015, article 8702, 7 pages, http://dx.doi.org/10.1038/ncomms9702.*

Diamondiferous subcontinental lithospheric mantle of the northeastern Siberian craton: Evidence from mineral inclusions in alluvial diamonds. V.S. Shatsky, D.A. Zedgenizov, A.L. Ragozin and V.V. Kalinina, *Gondwana Research,* **28**(1), 2015, 106–120, http://dx.doi.org/10.1016/j.gr.2014.03.018.

Diamonds and water in the deep Earth: A new scenario. F. Nestola and J.R. Smyth, *International Geology Review,* **58**(3), 2015, 263–276, http://dx.doi.org/10.1080/00206814.2015.1056758.

Highly saline fluids from a subducting slab as the source for fluid-rich diamonds. Y. Weiss, J. McNeill, D.G. Pearson, G.M. Nowell and C.J. Ottley, *Nature,* **524**(7565), 2015, 339–342, http://dx.doi.org/10.1038/nature14857.

The ins and outs of polished diamonds: Cleavage. G. Millington, *Gems&Jewellery,* **24**(3), 2015, 8–12.

The ins and outs of polished diamonds: Fluorescence. G. Millington, *Gems&Jewellery,* **25**(1), 2016, 10–15.

The ins and outs of polished diamonds: Mystery holes. G. Millington, *Gems&Jewellery,* **24**(4), 2015, 30–33.

The ins and outs of polished diamonds: Oddities. G. Millington, *Gems&Jewellery,* **25**(2), 2016, 20–23.

The ins and outs of polished diamonds: Surface damage. G. Millington, *Gems&Jewellery,* **24**(6), 2015, 8–10.

The ins and outs of polished diamonds: Take the strain. G. Millington, *Gems&Jewellery,* **24**(7), 2015, 12–16.

The ins and outs of polished diamonds: Thick and thin. G. Millington, *Gems&Jewellery,* **24**(5), 2015, 8–10.

Kimberlite-hosted diamonds in Finland. H. O'Brien, in W.D. Maier, R. Lahtinen and H. O'Brien (Eds.), *Mineral Deposits of Finland,* Elsevier, Amsterdam, The Netherlands, Chapter 4.4, 2015, 345–375, http://dx.doi.org/10.1016/b978-0-12-410438-9.00014-5.

Luminescence in diamonds of the Sao Luiz placer (Brazil). V.P. Mironov, A.L. Rakevich, F.A. Stepanov, A.S. Emel'yanova, D.A. Zedgenizov, V.S. Shatsky, H. Kagi and E.F. Martynovich, *Russian Geology and Geophysics,* **56**(5), 2015, 729–736, http://dx.doi.org/10.1016/j.rgg.2015.04.004.

Out of the blue: From Agra to Totnes. J. Ogden, *Gems&Jewellery,* **25**(1), 2016, 37.

Partnerships for 21st century development in Africa. R.M. O'Ferrall, *World Diamond Magazine,*

6, 2016, 66–68, www.worlddiamondmark.org/sites/default/files/wdmagazine_vol_6.pdf.*

Preliminary study on the unique spectroscopic characteristics of natural and synthetic diamonds. J. Yan, X. Wang, J. Tao, J. Zhang and X. Hu, *Spectroscopy and Spectral Analysis,* **35**(10), 2015, 2723–2729 (in Chinese with English abstract).

Surface source of Coromandel diamonds (Minas Gerais State, Brazil) and their possible origin from the Serra Negra/Salitre supervolcano. J. Karfunkel, D.B. Hoover, A.F. Fernandes, G.N.C. Sgarbi, K. Kambrock, D. Walde and G. Michel-felder, *Neues Jahrbuch für Geologie und Paläontologie – Abhandlungen,* **277**(2), 2015, 237–250, http://dx.doi.org/10.1127/njgpa/2015/0499.

Gem Localities

^{40}Ar/^{39}Ar ages and trace element variations in Colombian emeralds. E. Svadlenak, B.S. Hons. thesis, Oregon State University, Corvallis, Oregon, USA, 2015, http://ir.library.oregonstate.edu/xmlui/bitstream/handle/1957/55954/SvadlenakEllenE2015.pdf?sequence=4.*

Alluvial sapphires from Montana: Inclusions, geochemistry, and indications of a metasomatic origin. J.C. Zwaan, E. Buter, R. Mertz-Kraus and R.E. Kane, *Gems & Gemology,* **51**(4), 2015, 370–391, http://dx.doi.org/10.5741/GEMS.51.4.370.*

Aquamarine from Stoneham and vicinity, Oxford County, Maine. C.A. Francis, M. Felch, A.U. Falster and D.A. Bailey, *Rocks & Minerals,* **91**(1), 2016, 28–35, http://dx.doi.org/10.1080/00357529.2016.1099131.

Bahia golden rutilated quartz. B. Cook, *Gems&Jewellery,* **24**(4), 2015, 8–10.

Charakteristik des Purschensteiner Amethysts aus dem sächsischen Erzgebirge und seine Verwendung im 18. Jahrhundert [Characteristics of the 'Purschenstein amethyst' found in the Saxon Erzgebirge and its application in reference to the 18th century]. G. Holzhey, *Gemmologie: Zeitschrift der Deutschen Gemmologischen Gesellschaft,* **64**(3/4), 2015, 53–72.

Cornish serpentine. S. Steele, *Gems&Jewellery,* **25**(1), 2015, 10–15.

Finding flint in Kefalonia [Greece]. H. Serras-Herman, *Gems&Jewellery,* **24**(3), 2015, 20–21.

Maya jade: The revival of a gem revered by royalty. H. Serras-Herman, *Gems&Jewellery,* **24**(5), 2015, 20–23.

Petrogenetic evolution of pegmatites of the Shigar Valley, Skardu, Gilgit-Baltistan, Pakistan. M.H. Agheem, M.T. Shah, T. Khan, M. Murata, H. Dars and M. Zafar, *Arabian Journal of Geosciences*, **8**(11), 2015, 9877–9886, http://dx.doi.org/10.1007/s12517-015-1900-x.

Sapphire within zircon-rich gem deposits, Bo Loei, Ratanakiri Province, Cambodia: Trace elements, inclusions, U–Pb dating and genesis. F.L. Sutherland, P.C. Piilonen, K. Zaw, S. Meffre and J. Thompson, *Australian Journal of Earth Sciences*, **62**(6), 2015, 761–773, www.tandfonline.com/doi/abs/10.1080/08120099.2015.1101015.

Splendor in the outback: A visit to Australia's opal fields. T. Hsu, A. Lucas and V. Pardieu, *Gems & Gemology,* **51**(4), 2015, 418–427, http://dx.doi.org/10.5741/GEMS.51.4.418.*

Tourmaline d'Afghanistan [Tourmaline from Afghanistan]. J. Panjikar, *Revue de Gemmologie A.F.G.,* **194**, 2015, 9–12.

Instruments and Techniques

Analysis of impurity effects on the coloration of corundum by laser-induced breakdown spectroscopy (LIBS). S.K. Ho, *Applied Spectroscopy,* **69**(2), 2015, 269–276, http://dx.doi.org/10.1366/13-07304.

Analysis of trace elements in opal using PIXE. R. Hinrichs, A.P.L. Bertol and M.A.Z. Vasconcellos, *Nuclear Instruments and Methods in Physics Research Section B: Beam Interactions with Materials and Atoms,* **363**, 2015, 75–78, http://dx.doi.org/10.1016/j.nimb.2015.08.008.

Double trouble: Navigating birefringence. E.A. Skalwold and W.A. Bassett, 2015, 20 pages, www.minsocam.org/msa/OpenAccess_publications/Skalwold/Double_Trouble_Navigating_Birefringence.pdf.*

Nondestructive investigation on the 17-18th centuries Sicilian jewelry collection at the Messina regional museum using mobile Raman equipment. G. Barone, D. Bersani, J. Jehlička, P.P. Lottici, P. Mazzoleni, S. Raneri, P. Vandenabeele, C. Di Giacomo and G. Larinà, *Journal of Raman Spectroscopy,* **46**(10), 2015, 989–995, http://dx.doi.org/10.1002/jrs.4649.

Miscellaneous

Cameos of the rainforest. H. Serras-Herman, *Gems&Jewellery,* **24**(7), 2015, 28–31.

Characterization of tarnish spots in Chinese high-purity gold jewelry. T. Lu, J. Zhang, Y. Lan, Y. Ma, H. Chen, J. Ke, Z. Wu and M. Tang, *Gems & Gemology,* **51**(4), 2015, 410–417, http://dx.doi.org/10.5741/GEMS.51.4.410.*

Export competitiveness of the small and medium scale enterprises in Sri Lanka: A case study based on the gem and jewellery

sector. N.N.W. Dollawatta and S.W.S.B. Dasanayaka, *Journal of Social Sciences – Sri Lanka*, **7**(1), 2015, 13 pages, http://repository.kln.ac.lk/bitstream/handle/123456789/11040/39.pdf?sequence=1&isAllowed=y.*

Identification and study of the origin of gemstone [*sic*]. W. Huang, D. Chao, R. Fu and W. Cai, *Superhard Material Engineering,* **27**(5), 2015, 53–57 (in Chinese with English abstract).

News Press

12 most expensive gemstones in the world. T. Nace, *Forbes*, 2 November 2015, www.forbes.com/sites/trevornace/2015/11/02/12-most-expensive-gemstones-world.*

Borrowing from solar and chip tech to make diamonds faster and cheaper. J. Markoff, *New York Times*, 11 November 2015, www.nytimes.com/2015/11/12/science/borrowing-from-solar-and-chip-tech-to-make-diamonds-faster-and-cheaper.html.*

Conservationists welcome Hong Kong move to ban ivory trade. C. Torchia, *Associated Press,* 14 January 2016, http://bigstory.ap.org/article/92fa0e5faed44c74ab639cccb4666098/conservationists-welcome-hong-kong-move-ban-ivory-trade.*

Excavated warrior-priest tomb with unparalleled riches prompts new consideration of ancient Greek history. Y. Wang, *Washington Post*, 27 October 2015, www.washingtonpost.com/news/morning-mix/wp/2015/10/27/excavated-warrior-tomb-with-unparalleled-riches-prompts-new-consideration-of-ancient-greek-history.*

Freshwater pearl mussels, the jewel in Scotland's crown, extinct in 11 rivers. C. Green, *Independent,* 28 December 2015, www.independent.co.uk/environment/freshwater-pearl-mussels-the-jewel-in-scotlands-crown-extinct-in-11-rivers-a6788691.html.*

Internet giants struggle to keep ivory off the market. R. Bale and J. Actman, *National Geographic,* 29 January 2016, http://news.nationalgeographic.com/2016/01/160129-Yahoo-ivory-online-sales-Google-eBay-Amazon-Craigslist.*

Myanmar continues search after deadly landslide at jade mine. T. Fuller, *New York Times*, 23 November 2015, www.nytimes.com/2015/11/24/world/asia/myanmar-landslide-jade-mine.html.*

The secret life of gemstones. J.M. Crow, *Cosmos*, 2 November 2015, https://cosmosmagazine.com/earth-sciences/secret-life-gemstones.*

The stories behind the biggest jewelry sales of 2015. J. Tarmy, *Bloomberg Business*, 18 December 2015, www.bloomberg.com/news/articles/2015-12-18/the-most-expensive-jewelry-sold-at-auction-in-2015-photos.*

Why it's so hard to put a price on the world's biggest diamonds. T. Biesheuvel, *Bloomberg Business,* 21 December 2015, www.bloomberg.com/news/articles/2015-12-22/why-it-s-so-hard-to-put-a-price-on-the-world-s-biggest-diamonds.*

Treasure trove of warrior jewellery unearthed in Russia: Ancient grave belongs to woman who worshipped fire 2,000 years ago. W. Stewart, *Daily Mail*, 13 August 2015, www.dailymail.co.uk/sciencetech/article-3196696/Treasure-trove-warrior-jewellery-unearthed-Russia-Ancient-grave-belongs-woman-worshipped-fire-2-000-years-ago.html.*

Organic Gems

The lure of ivory. M. Campbell Pedersen, *Gems&Jewellery,* **24**(5), 2015, 26–27.

Origin of nacre's iridescence in abalone shell. L. Tang and G. Zhang, *Journal of Gems & Gemmology,* **17**(5), 2015, 18–23 (in Chinese with English abstract).

Pearls

Coloring factors of natural and dyed golden pearls and research progress on their identification methods. Q. Guo and Z. Xu, *Rock and Mineral Analysis,* **34**(5), 2015, 512–519 (in Chinese with English abstract).

The effect of different culture methods on the quality of round pearls produced by the black-lip pearl oyster *Pinctada margaritifera* (Linnaeus, 1758). P. Kishore and P.C. Southgate, *Aquaculture,* **451**, 2016, 65–71, http://dx.doi.org/10.1016/j.aquaculture.2015.08.031.

Gemmological characteristic of the northern pearl of China. S. Chu and Y. Luo, *Journal of Gems & Gemmology,* **17**(4), 2015, 29–35 (in Chinese with English abstract).

Natural pearls. A. Vasiliu, in F. Marin, F. Brümmer, A. Checa, G. Furtos and I.G. Lesci (Eds.), *Key Engineering Materials,* Vol. 672, Biomineralization: From Fundamentals to Biomaterials & Environmental Issues, 2015, 80–102, http://dx.doi.org/10.4028/www.scientific.net/KEM.672.80.*

Rares perles cerclées à double axe de rotation [Rare circled pearls with a double axis of rotation]. J.-P. Gauthier, G. Gutierrez, M. Serrar and T.N. Bui, *Revue de Gemmologie A.F.G.,* **194**, 2015, 4–7.

Thermal stability of nacre proteins of the Polynesian pearl oyster: A proteomic study. A. Parker, F. Immel, N. Guichard, C. Broussard and F. Marin, in F. Marin, F. Brümmer, A. Checa, G. Furtos and I.G. Lesci (Eds.), *Key Engineering Materials,* Vol. 672, Biomineralization: From Fundamentals to

Biomaterials & Environmental Issues, 2015, 222–234, http://dx.doi.org/10.4028/www.scientific.net/KEM.672.222.*

Social Studies

The art of governing contingency: Rethinking the colonial history of diamond mining in Sierra Leone. L. D'Angelo, *Historical Research,* **89**(243), 2015, 136–157, http://dx.doi.org/10.1111/1468-2281.12103.

A diamantine struggle: Redefining conflict diamonds in the Kimberley Process. L. Bruffaerts, *International Affairs,* **91**(5), 2015, 1085–1101, http://dx.doi.org/10.1111/1468-2346.12399.

Synthetics and Simulants

Composite opal rough. C. Williams, *Gems&Jewellery,* **24**(4), 2015, 12–13.

The end of an era [history of synthetic diamond production in Sweden]. J. Asplund, *Gems&Jewellery,* **24**(3), 2015, 24–27.

Gemmological characteristics of an azure synthetic spinel. N. Chen, R. Li and Z. Xu, *Superhard Material Engineering,* **27**(6), 2015, 56–59 (in Chinese with English abstract).

A historic synthetic diamond. G. Roskin and C. Mitchell, *Gems&Jewellery,* **24**(4), 2015, 14–15.

Identification characteristic of near-colourless melee-sized HPHT synthetic diamond in Chinese jewelry market. Y. Lan, R. Liang, T. Lu, T. Zhang, Z. Song, H. Ma and Y. Ma, *Journal of Gems & Gemmology,* **17**(5), 2015, 12–17 (in Chinese with English abstract).

Intrinsic and extrinsic absorption of chemical vapor deposition single-crystal diamond from the middle ultraviolet to the far infrared. S. Webster, Y. Chen, G. Turri, A. Bennett, B. Wickham and M. Bass, *Journal of the Optical Society of America B,* **32**(3), 2015, 479–484, http://dx.doi.org/10.1364/josab.32.000479.

MPCVD growth of ^{13}C-enriched diamond single crystals with nitrogen addition. C.M. Yap, A. Tarun, S. Xiao and D.S. Misra, *Diamond and Related Materials,* **63**, 2015, 2–11, http://dx.doi.org/10.1016/j.diamond.2015.10.004.*

Perles en ambre traité [Treated amber beads]. T.T. Sun and L.H. Ying, *Revue de Gemmologie A.F.G.,* **194**, 2015, 15–16.

Study of gemmological characteristics of a type of imitated chicken-blood stone. Y. Xiong, C. Chen, N. Chen and Y. Wang, *Superhard Material Engineering,* **27**(6), 2015, 51–55 (in Chinese with English abstract).

Treatments

Characteristic of sapphire by filling treatment. L. Feng, Q. Zhang and X. Yang, *Journal of Gems & Gemmology,* **17**(4), 2015, 16–22 (in Chinese with English abstract).

Introduction and identification of optimizing processed jadeite and jade imitation. T. Pang, F. Deng and J. Lin, *Superhard Material Engineering,* **27**(4), 2015, 53–57 (in Chinese with English abstract).

Microwave heat treatment of natural ruby and its characterization. S. Swain, S.K. Pradhan, M. Jeevitha, P. Acharya, M. Debata, T. Dash, B.B. Nayak and B. K. Mishra, *Applied Physics A,* **122**(3), 2016, article 224, 7 pages, http://dx.doi.org/10.1007/s00339-016-9703-9.

Process exploration of heat treatment on ruby and sapphire from Madagascar. M. Ye, J. Di and X. Xie, *Journal of Gems & Gemmology,* **17**(4), 2015, 8–15 (in Chinese with English abstract).

Compilations

***G&G* Micro-World.** 'Dragon's eye' fire agate • Red heart inclusion in diamond • Trapiche muscovite • Parisite in Colombian quartz • Violetish blue spinel in yellow sapphire • Four-ray stars in Paraíba tourmaline. *Gems & Gemology,* **51**(4), 2015, 441–445, www.gia.edu/gems-gemology.*

Gem News International. Demantoid with large fluid inclusion • Demantoid from Veracruz, Mexico • Grandidierite from Madagascar • Bluish green chalcedony marketed as 'Aquaprase' • Ruby from Zahamena, Madagascar • Plastic imitation of golden coral • Conference reports. *Gems & Gemology,* **51**(4), 2015, 446–462, www.gia.edu/gems-gemology.*

Gemmologie aktuell. Suolunite from Canada • Daylight-fluorescent opal from Mexico • 'Strawberry feldspar' • Buchite from the Eifel, Germany • Purple garnet from Mozambique and Malawi. *Gemmologie: Zeitschrift der Deutschen Gemmologischen Gesellschaft,* **64**(3/4), 2015, 45–52.

Lab Notes. Octahedral pattern of graphite inclusions in diamond • Treated pink diamond with synthetic-appearing growth structure • 13.09 ct type Ib rough diamond • Uranium in hyalite • Fossil *Tridacna* blister pearls • Unusual internal structure in a natural pearl • Pearls reportedly from *Spondylus* and *Trochoidea* species • 3.23 and 2.51 ct CVD-grown synthetic diamonds • Synthetic quartz bangle. *Gems & Gemology,* **51**(4), 2015, 428–440, www.gia.edu/gems-gemology.*

Conference Proceedings

2015 China Gems & Jewelry Academic Conference. Beijing, China, 30 November 2015, *China Gems*, November–December 2015, 460 pages.

Gem-A
INSTRUMENTS

Getting confusing results with your Chelsea Colour Filter™?

Inferior copies are being found more and more on the market — the accuracy of these filters is inconsistent with that of a true Gem-A Chelsea Colour Filter™ and may give you incorrect results. We hold the original master filters worked on by Basil Anderson and C.J. Payne in 1934, upon which all of our subsequent filters are based.

Make sure you buy your Chelsea Colour Filter™ only from Gem-A Instruments.

Only £25 + VAT*

To place an order contact instruments@gem-a.com or call +44 (0)207 404 3334.

* Postage and packing fee applies. 20% VAT applies to UK and European countries, except companies with a valid VAT registration number.

Creating gemmologists since 1908

Join us.

Pala International

Palagems.com / Palaminerals.com

+1 800 854 1598 / +1 760 728 9121

Natural Emerald, Zambia • 3.25 ct • 11.66 x 8.60 x 5.39 mm • GIA cert

Photo: Mia Dixon